AD-A062 291 OHIO STATE UNIV COLUMBUS DEPT OF AERONAUTICAL AND AS--ETC F/G 7/4
IGNITION, COMBUSTION, DETONATION, AND QUENCHING OF REACTIVE MIX--ETC(U)
JUN 78 R EDSE, O P DHIMAN AFOSR-73-2511

UNCLASSIFIED AFOSR-TR-78-1483 NL

1 OF 2
ADA
062291

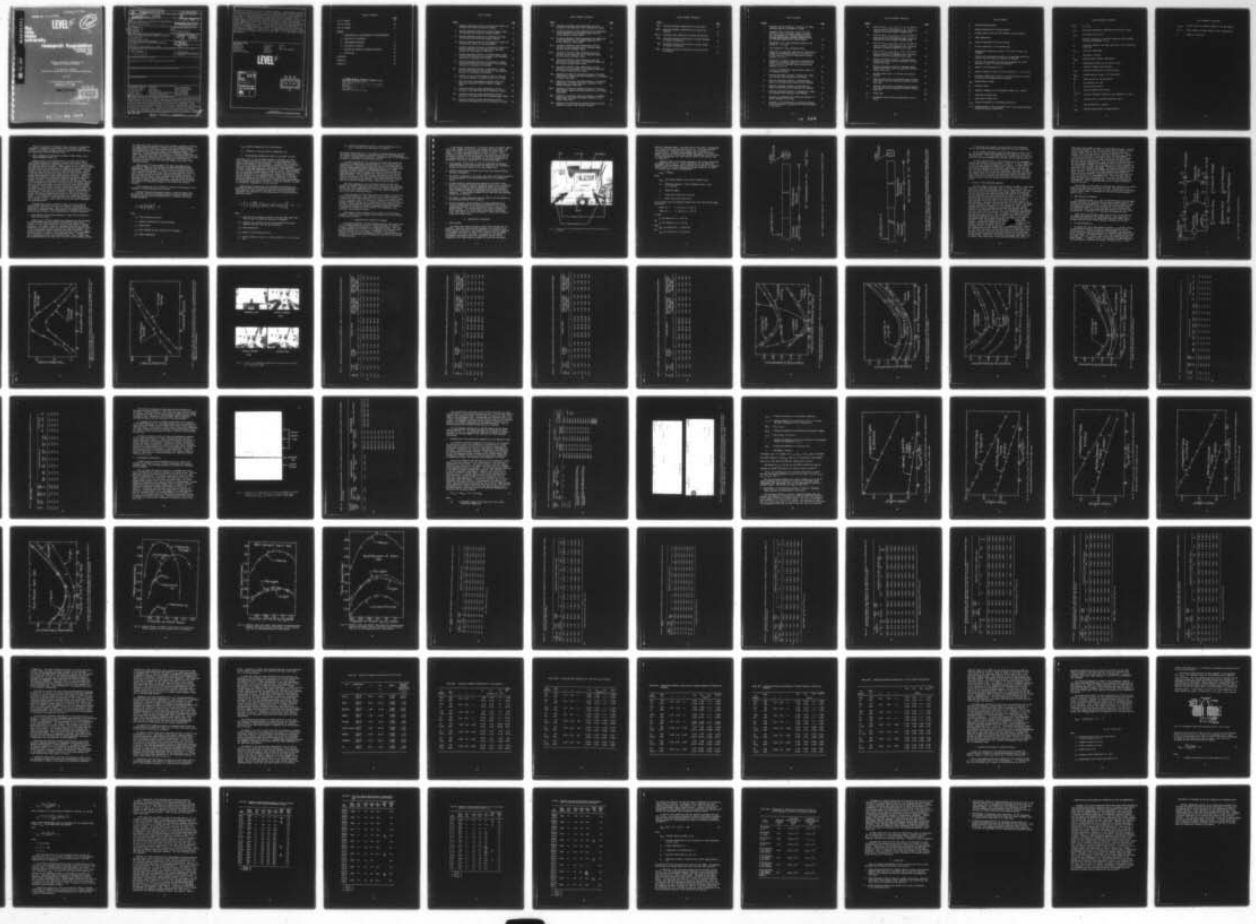

RF Project 760100/783641
FINAL REPORT

AFOSR-TR- 78-1483

LEVEL II

the ohio state university
research foundation
1314 kinnear road
columbus, ohio
43212

IGNITION, COMBUSTION, DETONATION, AND QUENCHING OF REACTIVE MIXTURES

R. Edse and O. Dhiman
Department of Aeronautical and Astronautical Engineering

June 1978

AIR FORCE OFFICE OF SCIENTIFIC RESEARCH
Bolling Air Force Base
Washington, D.C. 20332

AFOSR 73-2511

UNCLASSIFIED

SECURITY CLASSIFICATION OF THIS PAGE (When Data Entered)

REPORT DOCUMENTATION PAGE	READ INSTRUCTIONS BEFORE COMPLETING FORM
1. REPORT NUMBER: AFOSR-TR-78-1483	2. GOVT ACCESSION NO.
3. RECIPIENT'S CATALOG NUMBER	
4. TITLE (and Subtitle): IGNITION, COMBUSTION, DETONATION, AND QUENCHING OF REACTIVE MIXTURES	5. TYPE OF REPORT & PERIOD COVERED: FINAL Rept. 1 Apr 73 — 31 Mar 78
6. PERFORMING ORG. REPORT NUMBER: RF 760100/783641	
7. AUTHOR(s): RUDOLPH EDSE, OM P. DHIMAN	8. CONTRACT OR GRANT NUMBER(s): AFOSR-73-2511
9. PERFORMING ORGANIZATION NAME AND ADDRESS: THE OHIO STATE UNIVERSITY RESEARCH FOUNDATION, 1314 KINNEAR RD, COLUMBUS, OHIO 43212	10. PROGRAM ELEMENT, PROJECT, TASK AREA & WORK UNIT NUMBERS: 2308A2, 61102F, A2
11. CONTROLLING OFFICE NAME AND ADDRESS: AIR FORCE OFFICE OF SCIENTIFIC RESEARCH/NA, BLDG 410, BOLLING AIR FORCE BASE, D C 20332	12. REPORT DATE: June 1978
	13. NUMBER OF PAGES: 102
14. MONITORING AGENCY NAME & ADDRESS (if different from Controlling Office): 105 p.	15. SECURITY CLASS. (of this report): UNCLASSIFIED
	15a. DECLASSIFICATION/DOWNGRADING SCHEDULE

16. DISTRIBUTION STATEMENT (of this Report)

Approved for public release; distribution unlimited.

17. DISTRIBUTION STATEMENT (of the abstract entered in Block 20, if different from Report)

18. SUPPLEMENTARY NOTES

19. KEY WORDS (Continue on reverse side if necessary and identify by block number)

QUENCHING DISTANCE	CATALYSIS	FLAME PROPAGATION
QUENCHING SURFACE	DIFFUSION	IGNITION TEMPERATURE
FLAME ARRESTOR	HEAT TRANSFER	FLAME THICKNESS
BURNER TUBE	ADIABATIC FLAME TEMPERATURE	BAND SPECTROGRAM
CHAIN REACTION	ROTATIONAL TEMPERATURE	NON-EQUILIBRIUM

20. ABSTRACT (Continue on reverse side if necessary and identify by block number)

A burner tube having a rectangular cross-section with a width-to-length ratio of approximately 200 has been used for measuring the quenching distances of various fuel oxidizer mixtures by squeezing the flames between two movable plates. For laminar flames the quenching distances were found to be independent of the initial gas speed, the Reynolds number of the flow of unburned gas, and the geometry of the burner port. However, they depend on the material and structure of the quenching surface; the composition of the unburned gas, its thermal conductivity, diffusion coefficient, and specific heats; the adiabatic flame/

DD FORM 1 JAN 73 1473

400 015

UNCLASSIFIED

SECURITY CLASSIFICATION OF THIS PAGE (When Data Entered)

temperature, and the linear rate of flame propagation. Spectrographic studies revealed that quenching greatly reduces the concentrations of active species in the flame and that the populations of the rotational levels of the CH radical correspond to temperatures which are much higher than the adiabatic flame temperature. A simple mathematical model has been used to develop a theoretical equation for the prediction of quenching distances of various fuel-oxidizer mixtures. For the study of the effect of turbulence on the transition from deflagration to detonation, a new tube with open end for flowing gas mixtures has been constructed and assembled. To gain a better insight into the effect of extremely low temperatures several series of experiments have been carried out with hydrogen-oxygen-third gas mixtures. No simple relationship between initial gas density and detonation induction distance seems to exist according to these measurements.

KEY WORDS (cont)

TURBULENCE
LAMINAR FLOW
DETONATION
DEFLAGRATION
INDUCTION DISTANCE
FLASH-BACK
BLOW-OFF
METHANE
ACETYLENE
HYDROGEN
OXYGEN
AIR
INERT GAS ADDITIVE

LEVEL II

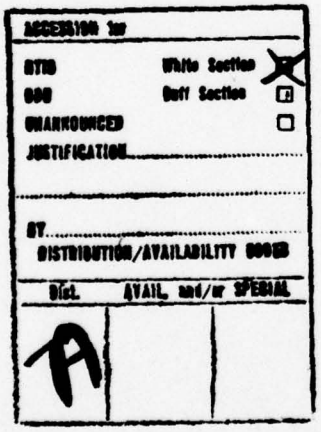

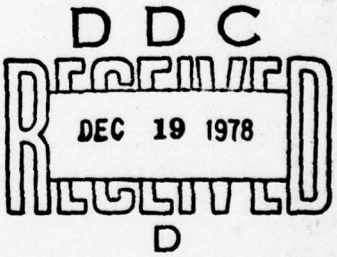

TABLE OF CONTENTS

LIST OF TABLES

LIST OF TABLES (Continued)

LIST OF TABLES (Continued)

LIST OF FIGURES

LIST OF FIGURES (Continued)

LIST OF SYMBOLS

d_Q	flame quenching distance
λ	thermal conductivity of the gas mixture
c_p	average specific heat per unit volume of the gas mixture
T_F	flame temperature
T_{ig}	ignition temperature of the gas mixture
T_O	initial temperature of the unburned gas
f	dimensionless geometrical factor of the order of unity (by Friedman)
A	fraction of the molecules present in the gas phase which must react so that the flame can continue to propagate
k_i	specific rate constant for the reaction between the active particles of kind i and the fuel molecules
N_f	number of fuel molecules per cc
p_i	partial pressure of kind i of active particles i = H, O, or OH
D_i	diffusion coefficient of kind i of active particles in the gas at reaction zone temperature and pressure
L_{min}	minimum burner length
R_e	Reynolds number
d_h	hydraulic diameter of the rectangular burner, $d_h = 2ab/a+b$
a	long side of burner slot
b	short side of burner slot
$I_{n'n''}$	relative intensity of a rotational transition
n', n''	quantum numbers of the rotational levels in the upper and lower electronic states, respectively

LIST OF SYMBOLS (Continued)

$A^*_{n'n''}$	$A_{n'n''}\nu^4_{n'n''}$
$A_{n'n''}$	transition probability including the statistical weight
$\nu_{n'n''}$	wave number of the line
F	constant depending on electronic transition and instrument factors but independent of $E_{n'}$
$E_{n'}$	rotational energy of the upper state for a fixed vibrational transition
T_{rot}	rotational temperature
k	Boltzmann's constant
T_{wall}	quenching plate surface temperature
α	dimensionless factor of the order of unity
δ	adiabatic laminar flame thickness
D_{mix}	diffusion coefficient of the gas mixture
H_{min}	minimum ignition energy of the gas mixture
$\mathcal{M}$	molecular mass of the gas mixture
R	gas constant for a gas
$\mathcal{R}$	universal gas constant
σ_i	collison diameter for the gas i
$\Omega_i^{(2,2)*}$	collision integral dependent on the parameter $T^* = kT_i/\epsilon$
c_{v_i}	specific heat at constant volume for a gas i
η_i	mole fraction for a species i
λ_{mix}	thermal conductivity of the gas mixture

$c_{\rho\ mix}$	specific heat at constant pressure of the gas mixture
V_A, V_B	molal volumes of liquid species A and B respectively
ϵ	energy of a particle

IGNITION, COMBUSTION, DETONATION, and QUENCHING OF REACTIVE MIXTURES

Three different topics of the research program have been investigated during this report period

1 APRIL 1977 to 31 MARCH 1978

I. INVESTIGATION OF THE MECHANISM OF FLAME QUENCHING

A. INTRODUCTION

Although many studies[1-9] on the determination of quenching distances of flames of gaseous pre-mixed fuel-oxidizer mixtures have been reported in the literature, an adequate theory for predicting flame quenching has not been published. It is not known whether quenching is accomplished primarily by energy losses from the flame by means of thermal conduction or by destruction of active radicals by means of diffusion and/or inhibitors. The following study was undertaken to elucidate the mechanism of quenching by means of a novel quenching device which permits a detailed experimental examination of the quenching process.

Much experimental as well as theoretical work has been done on the topic of flame quenching notably in the four areas reported below.

1. Use of Halogenated Compounds for Flame Inhibition or Flame Quenching

Burdon et al.[1] studied the chemical nature of the combustion products resulting from the addition of methyl bromide to hydrogen-air and carbon monoxide-air mixtures. It was found that the limit flame temperature (close to either fuel-lean or fuel-rich limit) of these mixtures was substantially and progressively raised by the increasing additions of methyl bromide both on the lower- and upper- limit sides. This increase in limit flame temperature was attributed to the chemical intervention of methyl bromide in the flame reactions. Belles and O'Neal[2] studied the efficiency of the various halogenated flame-extinguishing agents by adding these to propane-air mixtures. It was concluded that a halogenated extinguishing agent which results in higher values of average rate constants for fuel-air-agent reactions, in general, was more effective in flame quenching, when comparison was based on the same volume of the agent added. Rosser et al.[3] measured the flame speeds of methane-air mixtures containing various halogenated extinguishing agents and found that halogenated compounds which reduce the flame speeds of methane-air-agent gas mixtures are better extinguishing agents. Wilson et al.[4] studied the structure of methane-oxygen flames inhibited by hydrogen chloride, hydrogen bromide, and chlorine. From a comparison of the composition and reaction rate profiles of the unquenched methane-oxygen flames with those of methane-oxygen-agent flames it was concluded that fire extinguishers should

add the halogenated extinguishing agent when the mixing of the oxidizer and fuel is taking place rather than when the combustion is nearly complete and that the extinguishing agent should be stable enough so that it can react with the active species before undergoing decomposition. Larsen[5] studied the effect of a very large number of halogenated extinguishing agents on hydrocarbon fuel-oxidizer flames and compared their extinguishing characteristics with those of inert gases. It was concluded that halogenated compounds are effective as flame suppressants in direct proportion to their molecular weights. Halogenated agents play a dual role in the suppression of flames. Their primary role is similar to that of inert gases; i.e., they act as heat sinks. In addition to this primary mechanism they appear to act as fuels once they are heated to high enough temperatures and this is where these agents enter into the reaction mechanism of the flames. In this role the halogenated agents would be flame suppressants only within the context that the addition of excess fuel to a flammable mixture produces a nonflammable mixture.

For all of these halogenated extinguishing agents the flame-extinguishing property is attributed to the destruction of active chain carriers generated in the combustion zone. These radicals greatly affect the reaction mechanism of the fuel-oxidizer flames. Because of this behavior the halogenated extinguishing agents are of considerable importance to the physical chemist but their role in flame quenching is limited to some very special cases.

2. Attenuation or Quenching of Flames by the Addition of Powdered Salts

Dolan[6] studied the effect of fine powders of sodium bicarbonate and alkali halides on the ignition of methane air mixtures. These powders were introduced in the form of a suspension into methane-air gas mixtures and the mixture was then ignited by a spark. He concluded that inorganic dust suspensions inhibit the explosion of a methane-air mixture because the large surface area of the dust cools the advancing flame. Laffite and Bouchet[7] observed the suppression of explosion waves in methane-oxygen, propane-oxygen, isobutane-oxygen, and hydrogen-oxygen mixtures to which fine powders of various salts have been added. It was found that both deflagrations and detonations (in the pre-detonation stage) can be suppressed by the addition of powdered salts. Iya et al.[8] studied the mechanism of attenuation of methane-air flames to which powdered sodium bicarbonate and sodium tartrate had been added. It was found that flame inhibition through the addition of these salts is a homogeneous process. These inhibitors reduce the peak OH concentrations in the flame and promote the recombination of free radicals. McHale[9] studied the mechanism of flame quenching of the after-burning plume of a rocket motor to which various potassium compounds were added. It was concluded that these compounds, when introduced in powdered form into the exhaust gas, are vaporized in the combustion zone to produce gaseous products that react with the active species via homogeneous gas reactions.

Whereas the addition of powdered salts, like that of halogenated compounds, to combustible gas mixtures affect primarily chemical kinetics of the flame, for many practical applications, flame arrestors are needed which utilize mechanical means.

3. Flame Quenching and Attenuation by Means of Metal Chokes, Wire Gauzes, Synthetic Foams, etc

Egerton et al.[10] used sintered metals to quench the flames of stoichiometric mixtures of hydrogen or methane with oxygen. These investigators found that sintered bronze can be used as a flame arrestor even when the gases are flowing. There appeared to be no relation between the efficiency of the arrestor and its porosity but an increase in the thickness of the arrestor improved its quenching efficiency. Sintered stainless steel was found to be less effective than sintered bronze. It was also found that sintered metals are less effective in arresting methane-oxygen explosions that hydrogen-oxygen explosions. Palmer[11] studied the quenching of propane-air flames by wire gauzes made from a variety of metals. Using wire gauze arrestors mounted in a short vertical tube and with explosions initiated at the open end of the tube it was concluded that there was a critical velocity of approach below which the flame was quenched and above which the flame passed through the arrestor. Dixon[12] made a detailed experimental study of propane-air flames which he arrested by metal screens and synthetic foams. He concluded that flame speed is an important parameter in evaluating the effectiveness of various arrestor materials. Metal screens were effective when flame propagation rates were low but did not stop fast flames. On the other hand, foams arrested fast flames and allowed slow flames to pass through. It was found that the type of material, pore size, thickness, and the flame speed at the time of arrest influenced the quenching process.

Although metal screens, synthetic foams, etc. can be used to quench flames effectively, they are not suitable for studying the mechanism of flame quenching. Their use for this purpose involves a great deal of parametric data gathering which ultimately may not provide helpful design criteria for the construction of effective arrestors.

4. Investigation of Quenching Mechanism of Flames and the Design of a Flame Arrestor Model

Blanc et al.[13,14] while studying the mechanism of flame quenching in different fuel-oxidizer mixtures, initiated the flames with a powerful electric spark between two parallel glass plates of variable separation. The flames continued to propagate only when the distance between the two parallel plates was greater than the quenching distance of the fuel-oxidizer mixture; otherwise the flame was quenched. The distance between the plates at which the flame just failed to propagate was considered to be equal to the quenching distance. Friedman[15,16] used a rectangular burner with adjustable width. Once a steady flame was established above the burner port, the gas flow was suddenly stopped.

The flame then either flashed back or was quenched, depending on whether the burner width was greater or smaller than the quenching distance. The maximum width of the burner at which the flame no longer entered upon flow reduction was taken to be equal to the quenching distance. Nair and Gupta[17] measured quenching distances for commercial butane-air flames with a variable-width slot provided in a constant-volume spherical bomb. Ionization probes were used to indicate the quenching of the flame. The slot width was adjusted until no signal was obtained from the ionization probes and this slot width was assumed to be equal to the quenching distance.

Blanc et al.[13,14] and Friedman,[15,16] while investigating the quenching of flames by solid surfaces and making quenching distance measurements, concluded that the nature of the solid surface does not affect the quenching distance. It was found that quenching distances were virtually the same for copper, mica, or glass surfaces as well as glass surfaces coated with salts of high chain-breaking efficiency. It has been inferred that all types of surfaces are equally effective in promoting the free radical recombinations. Thus the various materials with widely different thermal conductivities apparently did not produce any change in the quenching distance of the various fuel-oxidizer mixtures.

A brief discussion of the theories of previous investigators on the mechanism of flame quenching is given below.

Friedman[15] measured quenching distances of hydrogen-oxygen-inert gas flames and derived the following equation, which is based on the assumption that the flame quenching process is primarily controlled by heat conduction:

$$d_Q = \frac{2\lambda}{u_F c_p} \left(\frac{1}{f} \frac{T_F - T_{ig}}{T_{ig} - T_O} \right)^{1/2} \quad \text{cm}, \tag{1}$$

where

d_Q = flame quenching distance,

λ = thermal conductivity of the gas mixture,

u_F = flame speed,

c_p = heat capacity per unit volume of the cold gas,

T_F = flame temperature,

T_{ig} = ignition temperature of the gas mixture,

T_o = unburned or cold gas mixture temperature, and

f = dimensionless geometrical factor of the order of unity.

According to Eq. (1) the quenching distance is dependent on flame speed, thermal conductivity, heat capacity, flame temperature, and ignition temperature of the gas mixture. He showed that an equation based on the assumption that quenching is primarily controlled by diffusion of active species does not produce the measured quenching distances of hydrogen-oxygen-inert gas mixtures. Friedman and Johnston[16] have also studied the quenching of propane-air flames. They concluded that the quenching distance depends on the initial gas pressure and the initial temperature of the quenching plate surface; the quenching distance decreases as the quenching surface temperature is increased. They investigated also the effect of initial temperature of the gas mixture and observed that for propane-air flames the quenching distance is proportional to the minus 0.91 power of pressure and minus 0.5 power of the absolute temperature of the gas mixture.

Simon et al.[18] studied some lean hydrocarbon-air mixtures and developed an equation for predicting the flame quenching distances of these mixtures. They assumed that diffusion of active species was predominent and formulated the following equation for calculating the quenching distance:

$$d_Q = \left[\frac{A}{k_i} \left(\frac{12T_F^2}{(298)^2 N_f} \right) \left(\frac{1}{p_H/D_H + p_O/D_O + p_{OH}/D_{OH}} \right) \right]^{1/2} \text{ cm}, \qquad (2)$$

where

A = fraction of the molecules present in the gas phase which must react so that the flame can continue to propagate,

k_i = specific rate constant for the reaction between the active particles of kind i and the fuel molecules,

T_F = flame temperature,

N_f = number of fuel molecules per cc,

p_i = partial pressure of kind i of active particles i = H, O, or OH, and

D_i = diffusion coefficient of kind i of active particles in the gas at reaction zone temperature and pressure.

The authors showed that Eq. (2) is capable of giving quenching distances which agree with the measured quenching distances for lean hydrocarbon-air flames at subatmospheric pressures. According to Eq. (2) the quenching distance is a function of initial gas pressure.

A similar equation was also proposed by Berlad[19] who studied the quenching of propane-oxygen-nitrogen mixtures. He concluded that an equation based on diffusion processes only can be used successfully to predict propane-oxygen-nitrogen quenching distances. His studies were also made on flames burning at subatmospheric pressures. Flame quenching studies of Simon et al.[18] and Berlad[19] have shown that the flame-quenching distance is definitely a function of the initial gas mixture pressure. It was shown by these investigators that for the same fuel-to-oxidizer ratio the quenching distance decreases with the increase in the initial gas pressure. This effect was to be expected since the diffusion coefficient varies inversly with pressure.

Since the equations for the quenching distance by both Simon et al.[18] and Berlad[19] have been based on the assumption that diffusion controls the flame propagation exclusively, the theories indicate that the destruction of chain carriers at the surface plays an important role in the flame quenching process.

Berlad and Potter,[20] while working with slot burners of three different surface geometries, have shown that the quenching distance is a function of the surface geometry of the burner. They showed, through a set of equations, that it is possible to formulate a relationship between quenching distance and the dimensions of the burners at a given pressure. These equations were tested by determining experimentally the quenching distances of downward propagating propane-air flames as a function of fuel-air ratio and pressure, for rectangular slots, cylinders, and cylindrical annuli.

Relationships between combustion wave parameters and quenching distances, based purely on thermal considerations, have been tabulated by Lewis and von Elbe.[21]

FORMULATION AND OBJECTIVE OF PROBLEM

An adequate mechanism for flame quenching has not been established. It is not known whether the process of flame quenching is primarily thermal or primarily diffusional or a combination of both. This lack of understanding exists in spite of the numerous investigations which have been carried out on this topic. Furthermore, all previous studies dealt only with the fundamental problem of flame quenching and, therefore, no efforts were made to develop any criteria for the design of flame arrestors.

In the present investigation, a fixed-slot copper rectangular burner, with a high length-to-width ratio, was designed and constructed. The flames were quenched by squeezing them between two movable parallel plates. The flame quenching apparatus is shown in Fig. 1. This technique of flame quenching is free from trial and error; in addition the errors introduced in the measurement of quenching distance due to the downward movement of the gas mixture at the time of quenching are eliminated. This burner design has the following advantages:

1. Spectrographic observations of both the unquenched and partially quenched flames can be made because the flame cone of a rectangular burner can be easily focused on the spectrograph slit.

2. Different fuel-oxidizer mixtures can be used for making quenching distance measurements.

3. The effect of geometry of the burner, gas speed, and Reynolds number of of the gas mixture on the quenching distance can be ascertained easily.

4. By using different quenching plate materials, the effect of the nature of the material upon the quenching distance can be determined. The effect of various catalytic compounds, which may contribute to flame quenching through the destruction of active chain carriers, can be studied by coating the quenching plate surfaces with these compounds. A long duration contract of the flame with the quenching surface can be achieved.

5. The effect of plate temperature and also that of the gas mixture on the quenching distance can be studied.

6. The role played by radical diffusion in flame quenching can be studied by making both qualitative and quantitative use of the spectrograms obtained for the unquenched as well as the partially quenched flames. The understanding of the radical diffusion in flame quenching can be further aided through mass spectrometry since flame samples for mass spectrometric studies can be readily drawn from steady flames.

II. DESCRIPTION OF APPARATUS

1. Burner Design

Two Bunsen-type copper rectangular burners were designed and constructed. Copper was preferred over stainless steel because of its higher thermal conductivity, easy machineability, and ease of handling. A rectangular slot burner is better than a circular type for taking spectroscopic pictures of the flame. As pointed out by Gaydon,[22] a rectangular type burner produces an appreciable increase in the brightness of the flame image and weighs the inner cone more highly

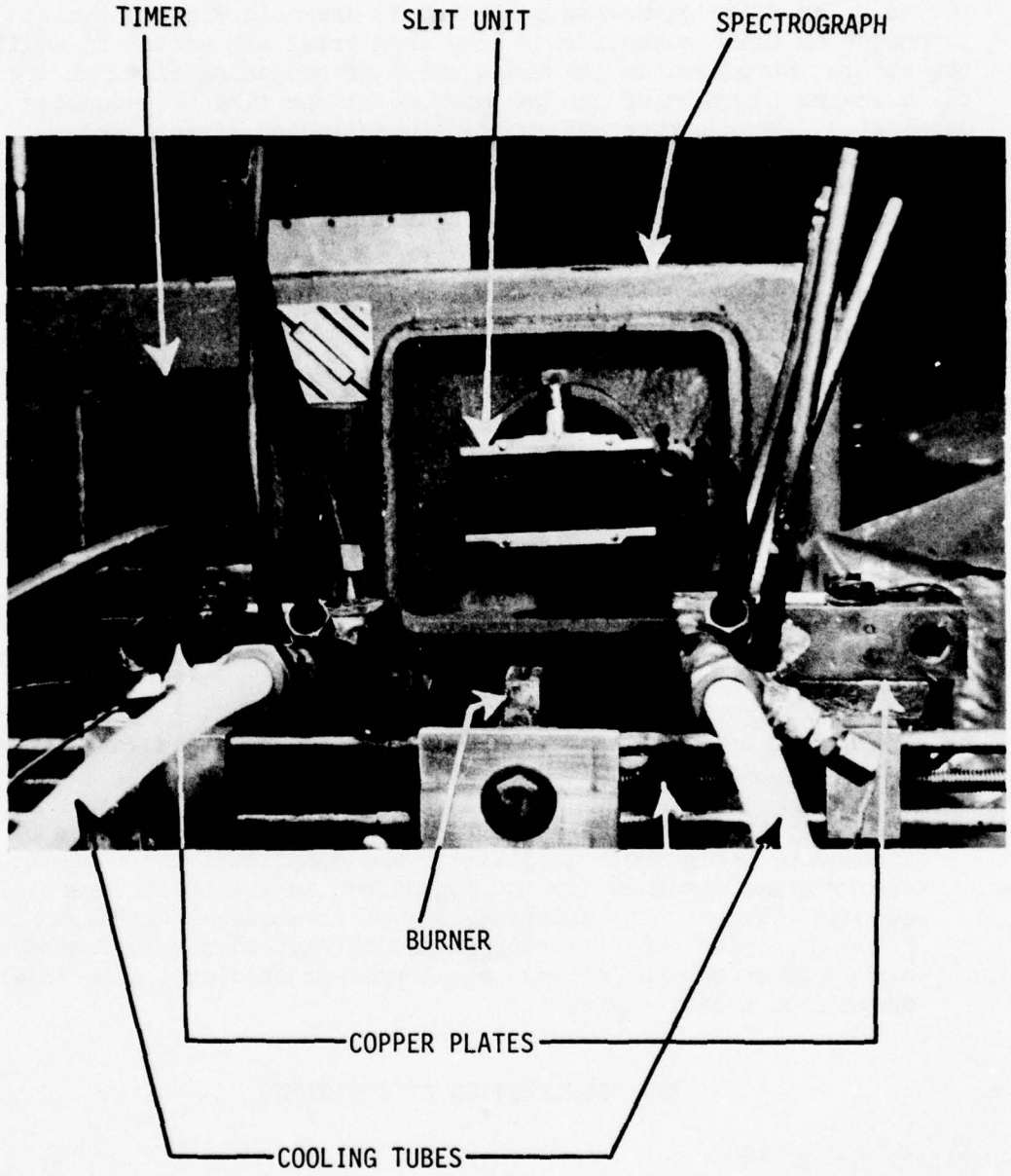

Fig. 1 Photograph of the Flame-Quenching Apparatus with Burner No. 1 in place.

than the interconal gases. The inner cone of the flame is photographed in the direction of the long side of the slot. This type of burner also produces a relatively thick reaction zone as compared to a circular burner. Ordinary conical Bunsen-type flames on circular burner tubes are not suitable for detailed examination of the structure of flame front because the light from all parts of the reaction zone is superposed.[22]

Schematic views of two burners employed in the present experiments are shown in Fig. 2 and 3. It has been pointed out by Gaydon and Wolfhard[23] that for laminar flow to prevail in the burner, the Reynolds number should be less than 2300 and the minimum length of the burner to establish such a flow is approximately

$$L_{min} = 0.05 R_e d_h \ ,$$

where

L_{min} = the minimum length of the burner required in cm,

d_h = hydraulic diameter of the rectangular burner in cm; $d_h = 2ab/a+b$,

R_e = Reynolds number,

a = long side of the slot in cm, and

b = short side of the slot in cm.

In the present case two different burners were used with the following dimensions:

Burner No. 1 a = 2.54 cm, b = 0.32 cm

Burner No. 2 a = 0.64 cm, b = 0.17 cm

so that

d_h (for Burner No. 1) = 0.57 cm

and

d_h (for Burner No. 2) = 0.17 cm,

hence

L_{min} (for Burner No. 1) = 65.55 cm

and

L_{min} (for Burner No. 2) = 31.05 cm.

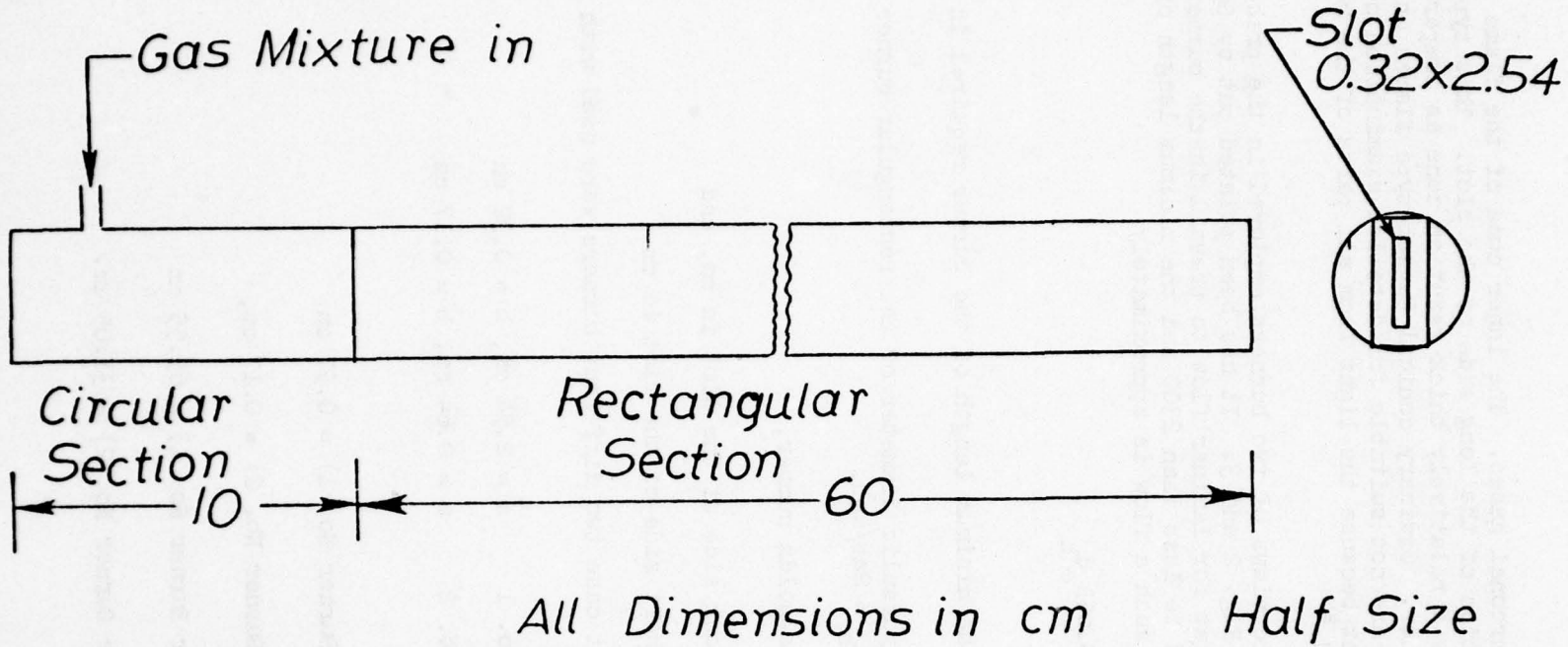

Fig. 2 Schematic View of Burner No. 1 Used for Flame-Quenching Studies of Methane-Air Flames

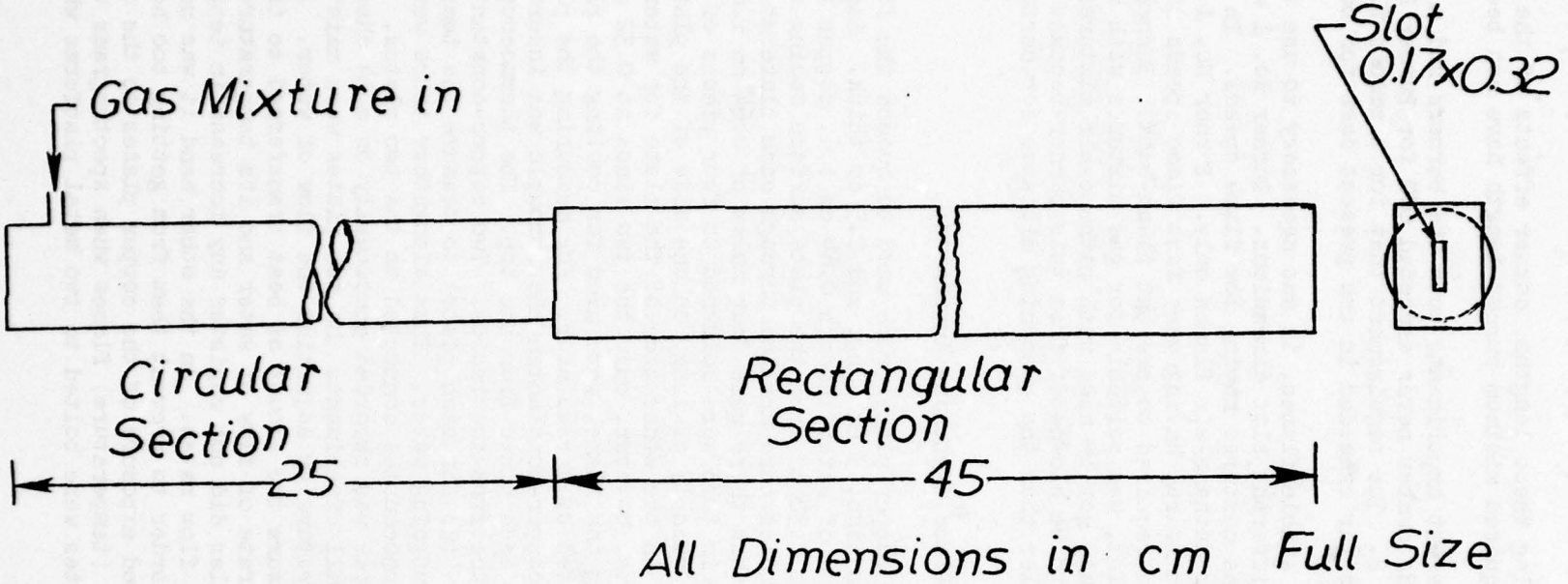

Fig. 3 Schematic View of Burner No. 2 Used for Flame-Quenching Studies of Methane-Oxygen, Acetylene-Air, Hydrogen-Air, Hydrogen-Oxygen-Helium, Hydrogen-Oxygen-Nitrogen, Hydrogen-Oxygen-Argon, and Hydrogen-Oxygen-Carbon Dioxide Flames

In computing these lengths, corner effects of the rectangular slot on the required minimum burner length have not been considered.

In the present experiments both the burners had a length of 70 cm and the Reynolds number never exceeded 600 for Burner No. 1 nor 2000 for Burner No. 2. The requirement that for a smooth flow L/d be of the order of 50 was far exceeded in the present case for both the burners.

To obtain stable flames, it was necessary to use two rectangular burners with different slot dimensions. Burner No. 1 with a bigger slot was used for gas mixtures having low flame speeds. In these studies, it was used for methane-air flames only. Burner No. 1 could not be used with gas mixtures having very fast flame speeds since very high flow rates were required to prevent flash-back. Burner No. 2, which had a narrow slot, was suitable for gas mixtures with high flame speeds This burner could not be used with methane-air mixtures because these flames tended to be blown-off from this burner because the burner slot width was smaller than the quenching distance for certain methane-air ratios.

2. Design of Flame Quenching Apparatus

Two solid copper plates were used to quench the flames. Each copper plate was 10 cm high, 5 cm long, and 2.5 cm thick. Each plate was cooled by a flow of water through 0.64 cm i.d. copper tubes. Two holes were drilled at 0.32 cm from the plate surface facing the burner and then two more holes were drilled through each plate at 0.64 cm apart so that altogether there were four holes of 0.64 cm i.d. in each plate. The four holes in turn were soldered to four pieces of 0.64 cm i.d. copper tubing, each 15 cm long, on one side of the plate for water inlet and four on the other side of the plate for water outlet. In most experiments, however, only the two lines at 0.32 cm from the plate surface, facing the flame, were used for cooling the plates. The water flow was adjusted by a regulator. For measuring the plate surface temperature a copper-constantan thermocouple was inserted into the surface of the each plate from the top. The thermocouple just touched the plate surface from the inside. Two copper-constantan thermocouples were also used (two for each plate) to measure the temperature of the incoming and outgoing water. Thus altogether there were six copper-constantan thermocouples connected to the two plates. The output of each thermocouple was recorded continually on a 12 channel Brown recorder. In all experiments the two plates were maintained at a constant temperature by adjusting the flow rate. Initially it was planned to measure the amount of heat transferred to the water by measuring the rate of flow of water and its temperature rise. However, the thermocouples did not register any increase in temperature, even for very small flow rates. On the other hand it was necessary to cool the plates in order to prevent them from getting too hot, especially during prolonged exposure of the copper plates to the combustion gas of high-energy (temperature) flames when spectrograms were taken. The two copper plates were bolted to two metal platforms which could be

moved inward and outward by means of a hand-operated spindle. The two plates were arranged so that they were flush with the burner top and could be moved over the top of the burner to obtain the desired distance between the two plates. The entire assembly (i.e., plates, spindle, etc.) was bolted to the optical bar of a spectrograph. A 1.3 cm slot was drilled in the optical bar so that the burner could be moved inside the bar for a proper focusing of the burner flame onto the slit of a spectrograph. After the flame was focused properly, the plate-spindle assembly was permanently bolted at that position. The plate-spindle assembly was so designed that it could be mounted on the optical bars of either the Hilger & Watts prism spectrograph or the Jarrel-Ash 21 ft grating spectrograph. The burner was held in place with a set screw, which in turn allowed for vertical adjustment of the burner position. The burner was placed symmetrically between the plates in the slot provided in the optical bar so that the flame cone could be focused on the spectrograph slit. When the Hilger & Watts large aperture prism spectrograph was used, it was not necessary to focus the flame with a condensing lens. With the Jarrel-Ash grating spectrograph, a quartz condensing lens had to be used to focus the flame on its slit.

The distances of the plates at quenching were measured with a feeler gauge which permitted an accuracy of 0.01 mm. The surfaces of the copper plates were polished so that the exact distance could be measured with the feeler gauge. A photograph of the entire burner assembly is shown in Fig. 1.

3. Spectroscopic Measurements

For qualitative work (i.e., for the identification of various bands obtained from both the unquenched and partially quenched flames of the various fuel-oxidizer mixtures) a Hilger & Watts large aperature prism spectrograph was employed because it permitted short exposure times. For quantitative work (i.e., for measuring the relative intensities and rotational flame temperatures were high dispersion was the primary consideration) a Jarrel-Ash 21 ft grating spectrograph was used.

Kodak 103a-F spectroscopic plates were used for all measurements for taking spectrograms of the various flames, These plates are sensitive from about 2500 Å to about 6800 Å and have rather uniform response over the entire visible spectrum, especially in the red.

4. Gas Flow Measurements

All gases were taken from standard cylinders. A constant pressure of each gas was maintained by means of reducing regulators in the metering section. Before entering the mixing chamber, the gases were passed through back pressure regulators to eliminate mutual interference of the gas flows. The metered flows of fuel and oxidizer were fed into the burner inlet via a solenoid valve after being thoroughly mixed in a mixing chamber. A schematic view of the apparatus used for making gas flow measurements, along with the burner, is shown in Fig. 4. All

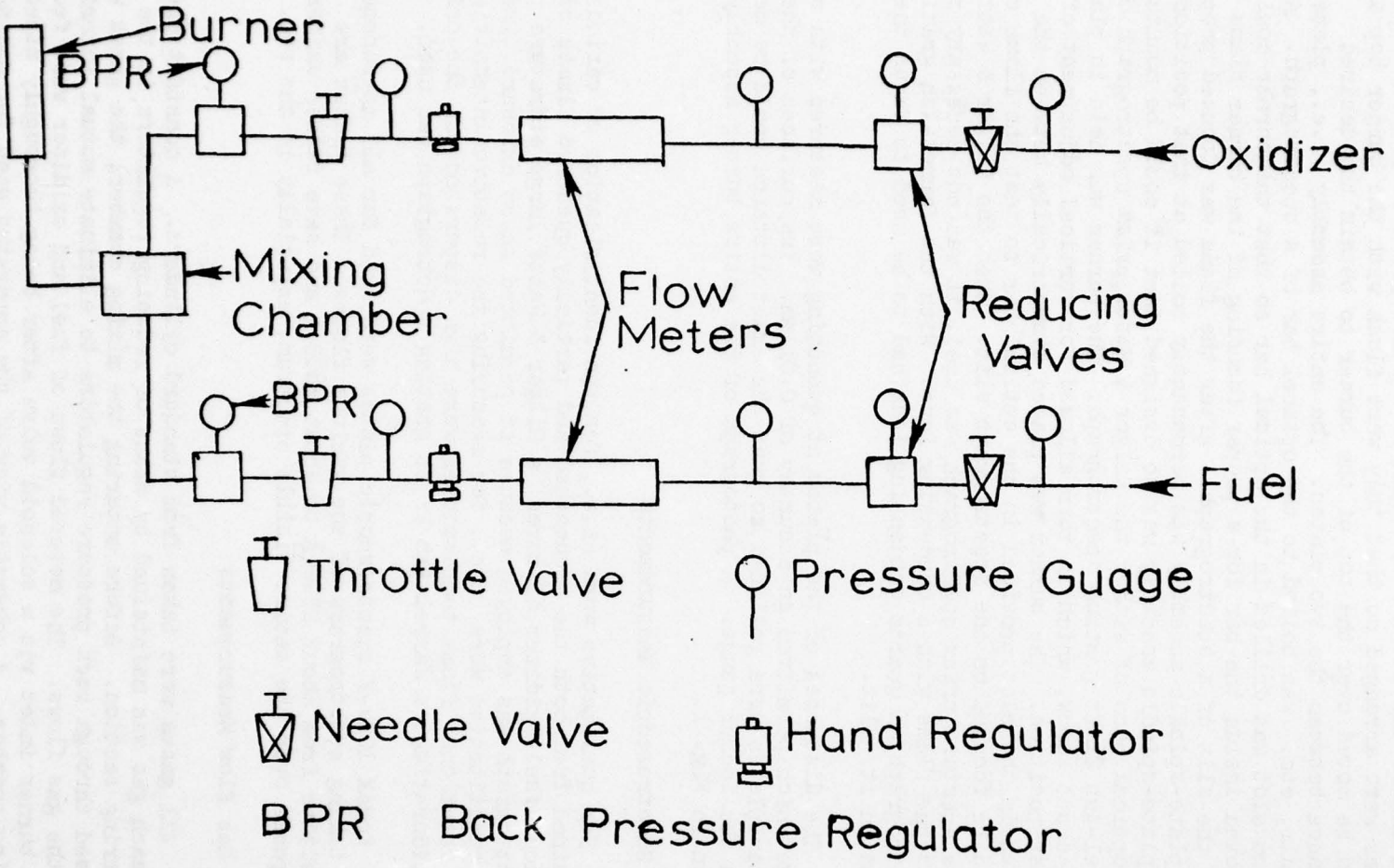

Fig. 4 Flow Diagram for Flame Quenching Studies

flows were calibrated with a vacuum type gas flow calibrator.[24] These calibrations were checked from time to time.

The chemical analyses of the various gases are given in Appendix A.

III. EXPERIMENTAL PROCEDURE

1. Determination of Flash-Back and Blow-Off Conditions

Before measurements of the quenching distances and spectrographic studies of the various flames could be undertaken, it was necessary to determine the stability of the flames of various fuel-air mixtures burning on rectangular burners. These measurements were necessary for the proper selection of fuel-air composition and flow rates so that neither flash-back nor blow-off would occur. These measurements were also made to compare the critical flow rates for flash-back and blow-off with those determined with circular burners. Flames of methane, acetylene, and hydrogen with air were always easy to stabilize. However, methane-oxygen flames showed considerable scatter in flash-back and blow-off because of the heating of the burner tip.

The procedure for measuring the critical flows for flash-back and blow-off was as follows:

In the methods of previous investigators first a diffusion flame of the fuel gas is started at the desired working pressure and the fuel flow is adjusted to predetermined value. Thereafter the air is added slowly without a change in fuel flow until flash-back of the flame takes place. In this way the condition of flash-back is approached on a path along which the mixture composition changes continuously. This was not desirable since the exact composition of the mixture in the burner tube at the moment of flash-back usually lies between the last and the preceding setting. In order to keep this error at a minimum, the gas flows were changed very slowly. Flash-back conditions for lean mixtures were established by increasing the fuel flow of lean flames until flash-back occurred. Such lean flames were obtained by using gas flows that were large enough to produce stable flames with any mixture ratio. Then both the oxidizer and fuel flow rates were reduced in succession until a lean flame resulted with a gas flow as low as possible.

Critical flow rates for blow-off were easier to obtain. First, a fuel-air flame was established for a certain composition of the gas mixture, well above the already measured critical flows for flash-back, then the amount of air was increased until blow-off occurred. After blow-off, the fuel flow rate was increased to a value more than in the previous case and then the air flow rate was increased until the blow-off occurred. In a similar fashion, blow-off was established for various fuel-air ratios of all gas mixtures considered.

The flow rates at flash-back and blow-off for acetylene-air mixtures obtained with a rectangular burner are shown in Fig. 5 and 6 together with the flow rates at flash-back and blow-off for circular tube burners.

2. Measurement of Quenching Distances

Quenching distance measurements were carried out for

1. Methane-Air Flames,
2. Methane-Oxygen Flames,
3. Acetylene-Air Flames, and
4. Hydrogen-Air Flames.

The experiments were started with diffusion flames (except in the case of acetylene-air flames; air was always mixed with the acetylene before starting the flame to avoid the formation of soot) at one atm pressure and the fuel flow was adjusted to a predetermined value. Thereafter the oxidizer was added slowly to obtain a flame at the predetermined mixture ratio. The flow of water through the cooling coils of the copper plates was then adjusted and plates were moved very slowly toward the flame. As soon as the plates touched the flame, the 14-channel temperature recorder was turned on to monitor the temperature of the plates as well as that of the cooling water at the inlet and outlet of the plates. The six copper-constantan thermocouples were used for this purpose. The plates were then moved very slowly and carefully into the flame until there was no visible flame radiation between the plates. Although there was a flame at the top of the plates, the flame between the plates was quenched. This process of flame quenching is illustrated in a sequence of photographs in Fig. 7 for a typical methane-air flame. As soon as the quenching was established, the flow of the gases was stopped by closing the solenoid switch. The quenching distance between the two plates was then measured with a feeler gauge. Upon completion of these measurements the plates were separated. Two measurements were made for each mixture ratio and flow rate. The average of the two values was used as the final value of the quenching distance. The plates were dried before each experiment. The quenching distances were measured at flow rates of 25, 50, and 100 cc/s to study the effect of gas speed and Reynolds number on the quenching distance. The copper plate temperature was maintained constant throughout the experiments. The results of these measurements for methane-air, methane-oxygen, acetylene-air, and hydrogen-air flames are given in Tables I-IV and in Fig. 8-11, together with the values given by Lewis and von Elbe[21] for comparison.

In order to determine the influence of the shape of the burner on the quenching distances, the quenching distances were measured with circular burners whose inner diameters were equal to the hydraulic diameter of the rectangular burners. These distances are also shown in Tables I-IV.

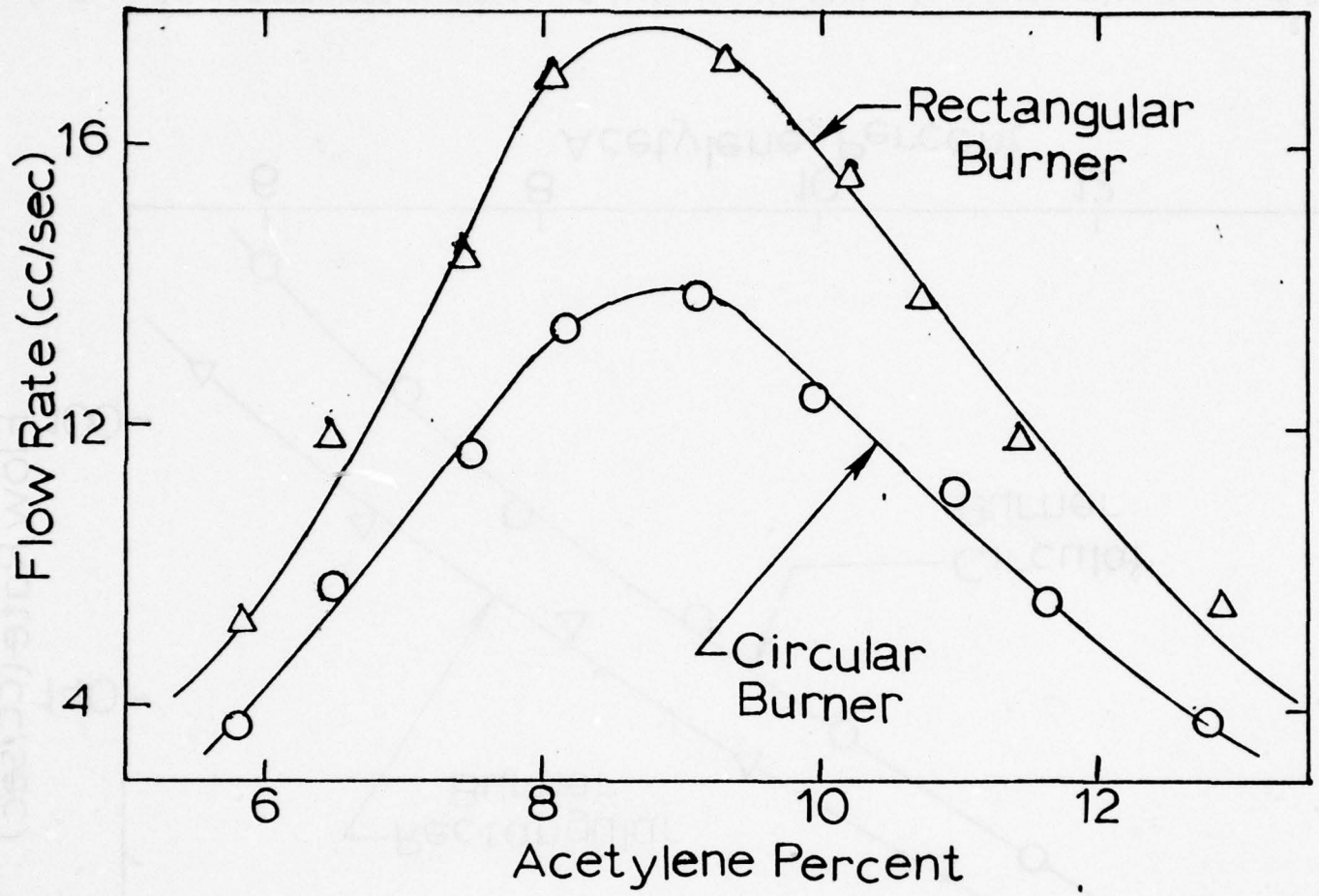

Fig. 5 Comparison of Flash-Back Conditions of Acetylene-Air Flames in a Rectangular Burner of Slot Width 0.17 cm with those of a Circular Burner with an inner diameter of 0.32 cm at room Temperature and 1 atm Pressure

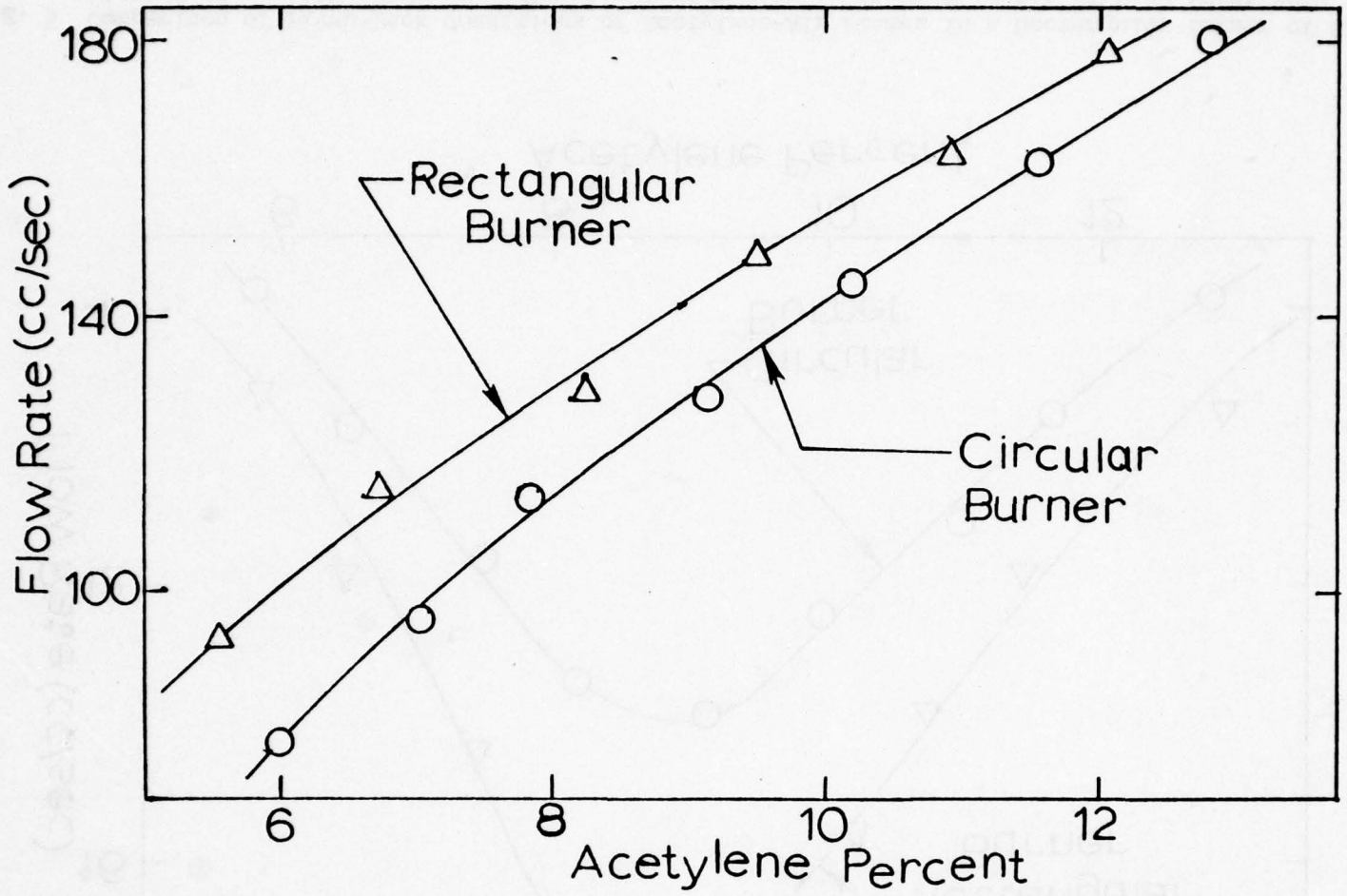

Fig. 6 Comparison of Blow-Off Conditions of Acetylene-Air Flames in a Rectangular Burner of Slot Width 0.17 cm with those of a Circular Burner with an inner diameter of 0.32 cm at room Temperature and 1 atm Pressure

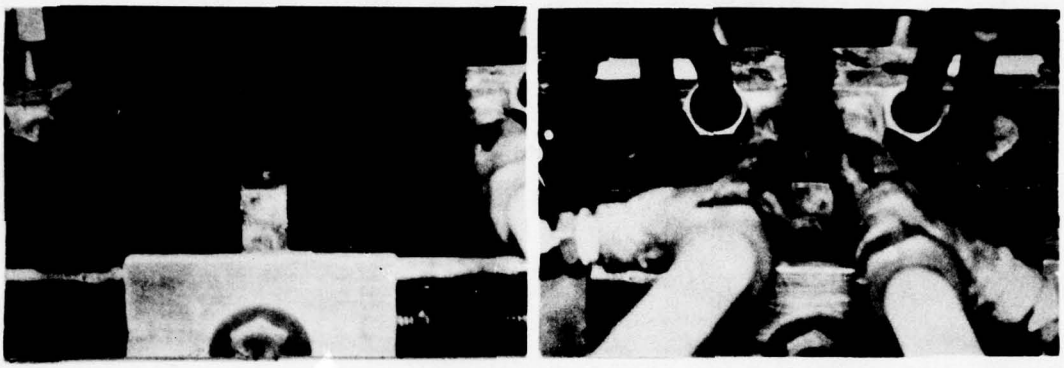

UNQUENCHED FLAME

PARTIALLY QUENCHED FLAME

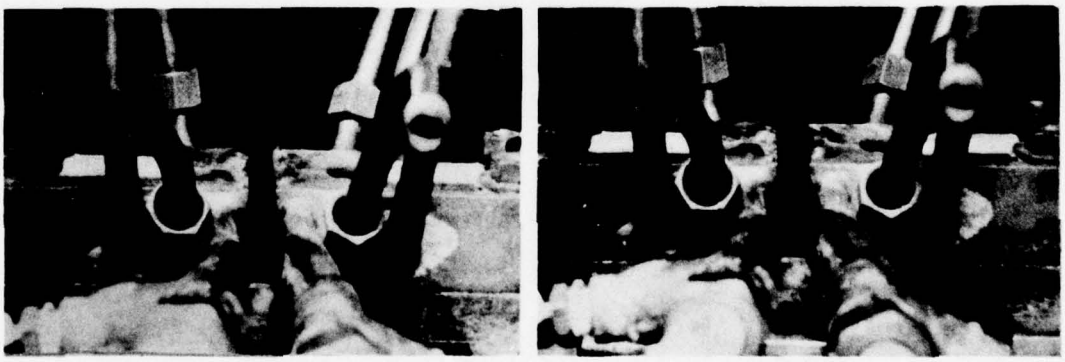

PARTIALLY QUENCHED FLAME

QUENCHED FLAME

Fig. 7 A series of Photographs Showing How the Quenching is Achieved for a Methane-Air Flame

Table I. Measured Quenching Distances of Methane-Air Flames for Different Gas Speeds and Reynolds Numbers

% CH_4 in air	Stoich. or M.E.R. Fraction	Average Gas Speed (m/s)			Reynolds Number			Quenching Distance with Copper Plates for a Rectangular Burner (mm)			Quenching Distance with Copper Plates for a Circular Burner (mm)		
		1	2	3	1	2	3	1	2	3	1	2	3
7.0	0.72	0.31	0.62	1.24	112.37	224.74	449.48	2.43	2.44	2.43	2.44	2.44	2.43
8.0	0.83	0.31	0.62	1.24	112.83	225.66	451.32	2.22	2.22	2.22	2.23	2.22	2.23
9.5	1.00	0.31	0.62	1.24	111.55	223.10	446.20	2.09	2.09	2.10	2.09	2.10	2.10
11.0	1.18	0.31	0.62	1.24	112.26	224.52	449.04	2.25	2.25	2.25	2.25	2.25	2.26
12.0	1.30	0.31	0.62	1.24	112.74	225.48	450.96	2.41	2.40	2.40	2.40	2.41	2.41

Table II. Measured Quenching Distances of Methane-Oxygen Flames for Different Gas Speeds and Reynolds Numbers

% CH_4 in O_2	Stoich. or M.E.R. Fraction	Average Gas Speed (m/s)			Reynolds Number			Quenching Distance with Copper Plates for a Rectangular Burner (mm)			Quenching Distance with Copper Plates for a Circular Burner (mm)		
		1	2	3	1	2	3	1	2	3	1	2	3
15.0	0.35	2.32	4.64	9.28	354.62	709.24	1418.48	0.76	0.76	0.77	0.76	0.77	0.77
25.0	0.67	2.32	4.64	9.28	397.16	794.32	1588.64	0.50	0.50	0.50	0.51	0.50	0.50
40.0	1.33	2.32	4.64	9.28	386.34	772.68	1545.36	0.61	0.62	0.61	0.62	0.62	0.61
45.0	1.64	2.32	4.64	9.28	392.67	785.34	1570.68	1.08	1.08	1.07	1.08	1.09	1.08
50.0	2.00	2.32	4.64	9.28	392.43	784.86	1569.72	1.83	1.83	1.85	1.84	1.84	1.85

Table III. Measured Quenching Distances of Acetylene-Air Flames for Different Gas Speeds and Reynolds Numbers

% C_2H_2 in air	Stoich. or M.E.R. Fraction	Average Gas Speed (m/s)			Reynolds Number			Quenching Distance with Copper Plates for a Rectangular Burner (mm)			Quenching Distance with Copper Plates for a Circular Burner (mm)		
		1	2	3	1	2	3	1	2	3	1	2	3
6.0	0.76	2.32	4.64	9.28	435.37	870.74	1741.48	0.74	0.78	0.78	0.76	0.78	0.79
7.0	0.90	2.32	4.64	9.28	428.70	857.40	1714.80	0.59	0.58	0.59	0.58	0.59	0.60
8.0	1.03	2.32	4.64	9.28	430.66	861.32	1722.64	0.55	0.58	0.58	0.56	0.58	0.58
9.0	1.18	2.32	4.64	9.28	432.65	865.30	1730.60	0.68	0.68	0.68	0.68	0.69	0.68
10.0	1.32	2.32	4.64	9.28	434.65	869.30	1738.60	0.83	0.83	0.83	0.84	0.83	0.84

Table IV. Measured Quenching Distances of Hydrogen-Air Flames for Different Gas Speeds and Reynolds Numbers

% H_2 in air	Stoich. or M.E.R. Fraction	Average Gas Speed (m/s)			Reynolds Number			Quenching Distance with Copper Plates for a Rectangular Burner (mm)			Quenching Distance with Copper Plates for a Circular Burner (mm)		
		1	2	3	1	2	3	1	2	3	1	2	3
20	0.59	2.32	4.64	9.28	364.52	729.04	1458.08	0.74	0.76	0.76	0.74	0.75	0.76
30	1.02	2.32	4.64	9.28	375.02	750.04	1500.08	0.59	0.58	0.58	0.58	0.60	0.60
40	1.59	2.32	4.64	9.28	348.10	696.20	1392.40	0.86	0.86	0.87	0.87	0.86	0.86
50	2.38	2.32	4.64	9.28	317.40	634.80	1269.60	1.76	1.76	1.75	1.77	1.76	1.76

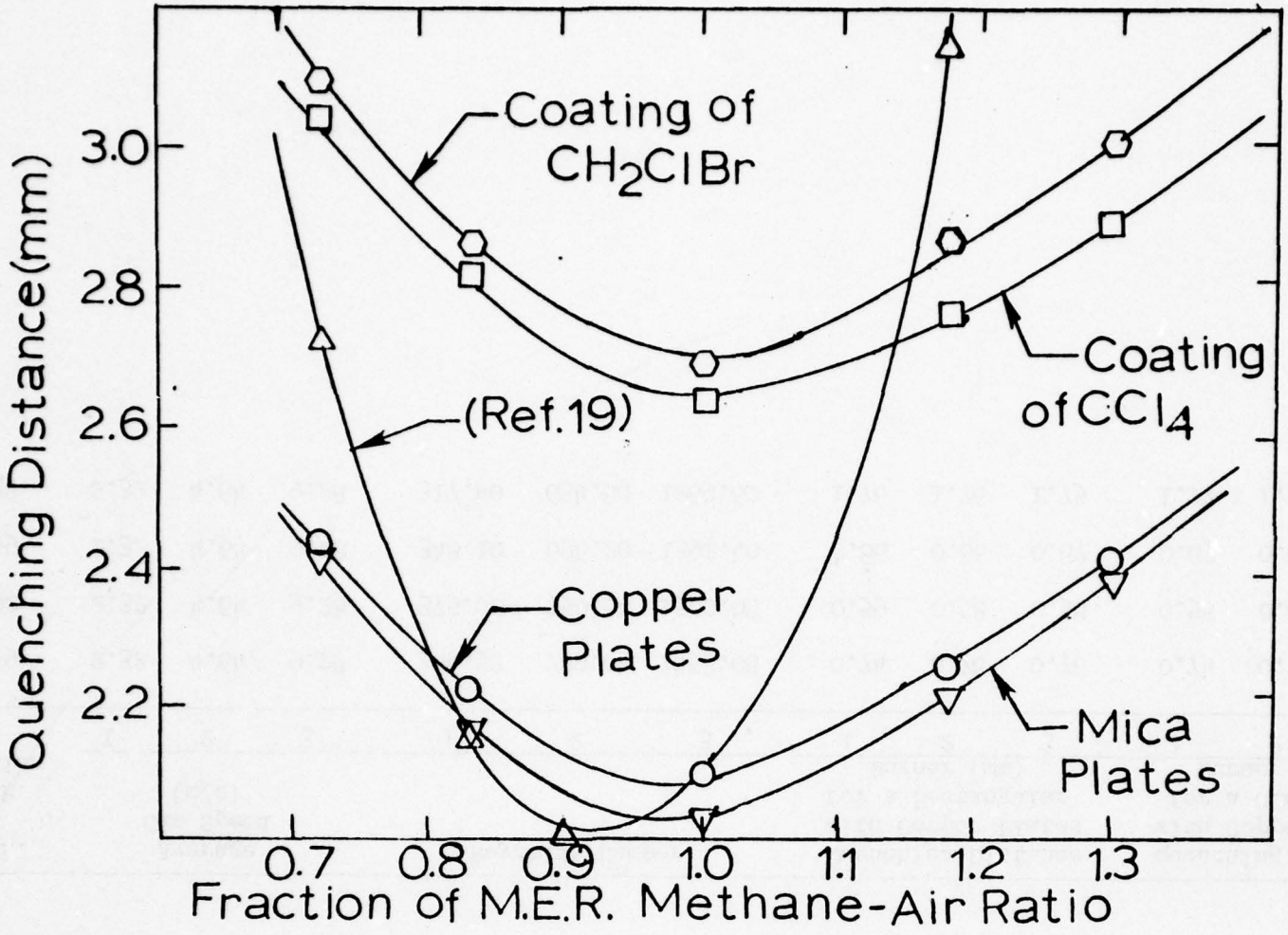

Fig. 8 Measured Quenching Distances of Methane-Air Flames for Different Plate Materials and Coatings at Room Temperature and 1 atm Pressure

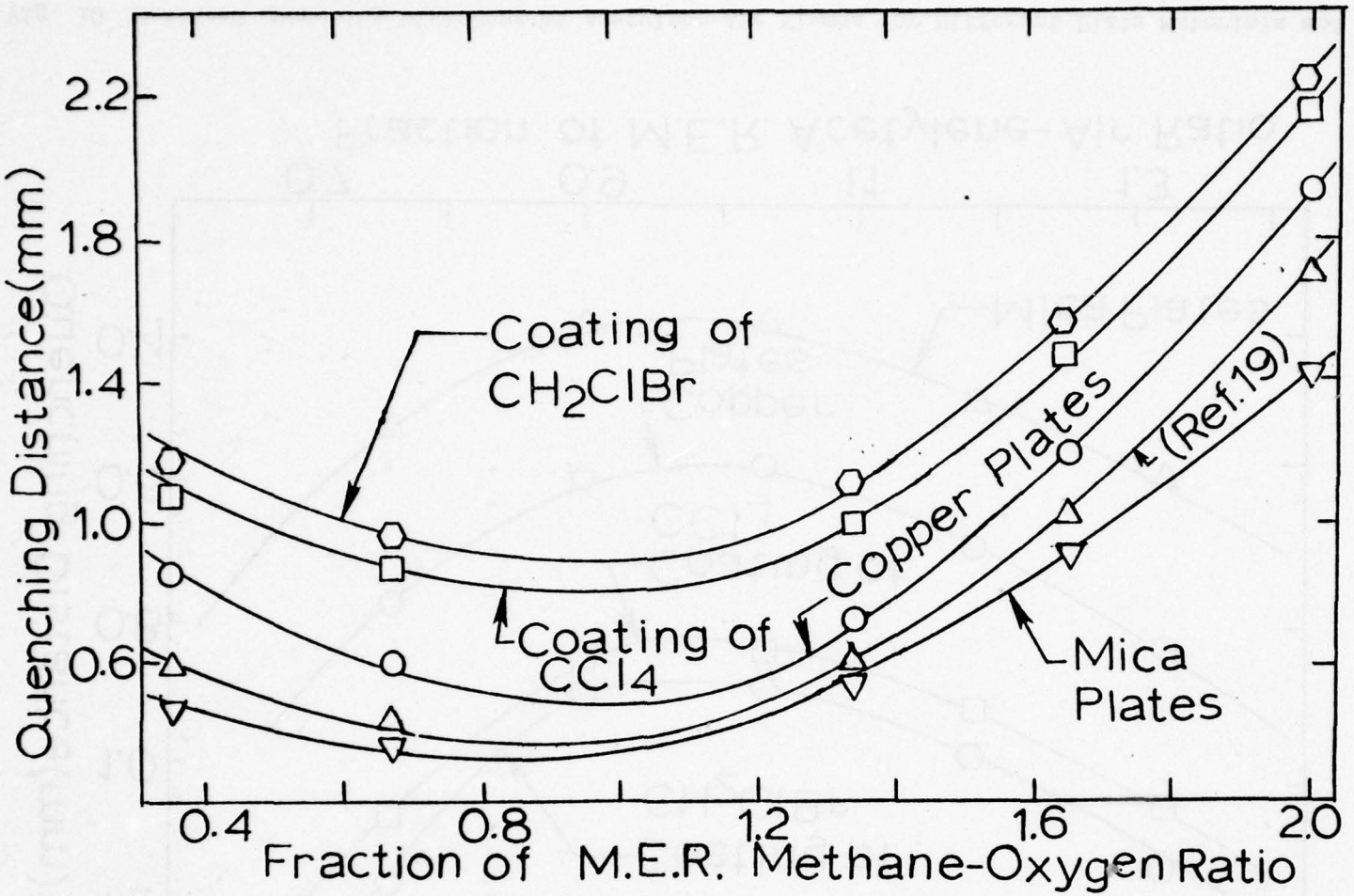

Fig. 9 Measured Quenching Distances of Methane-Oxygen Flames for Different Plate Materials and Coatings at Room Temperature and 1 atm Pressure

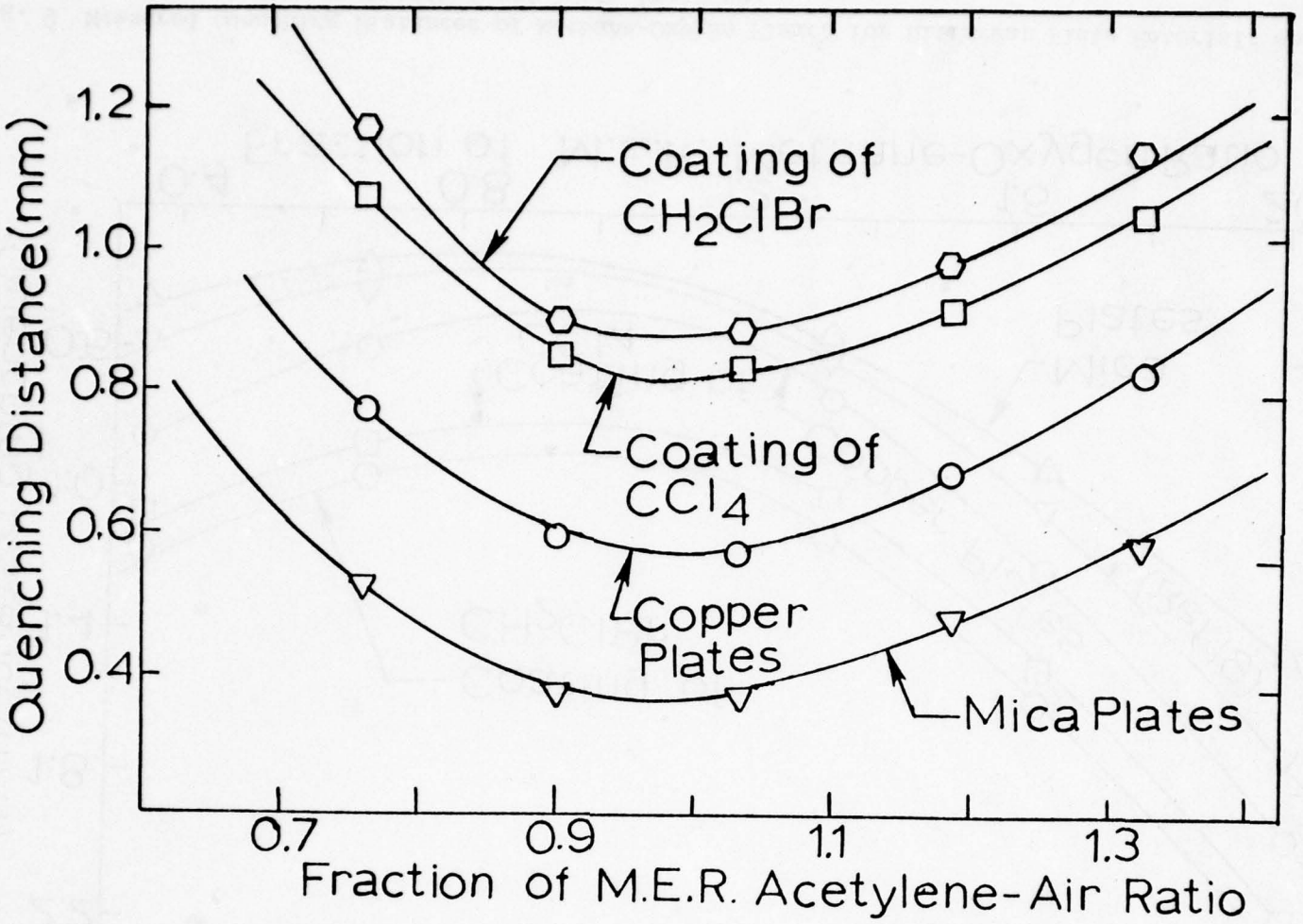

Fig. 10 Measured Quenching Distances of Acetylene-Air Flames for Different Plate Materials and Coatings at Room Temperature and 1 atm Pressure

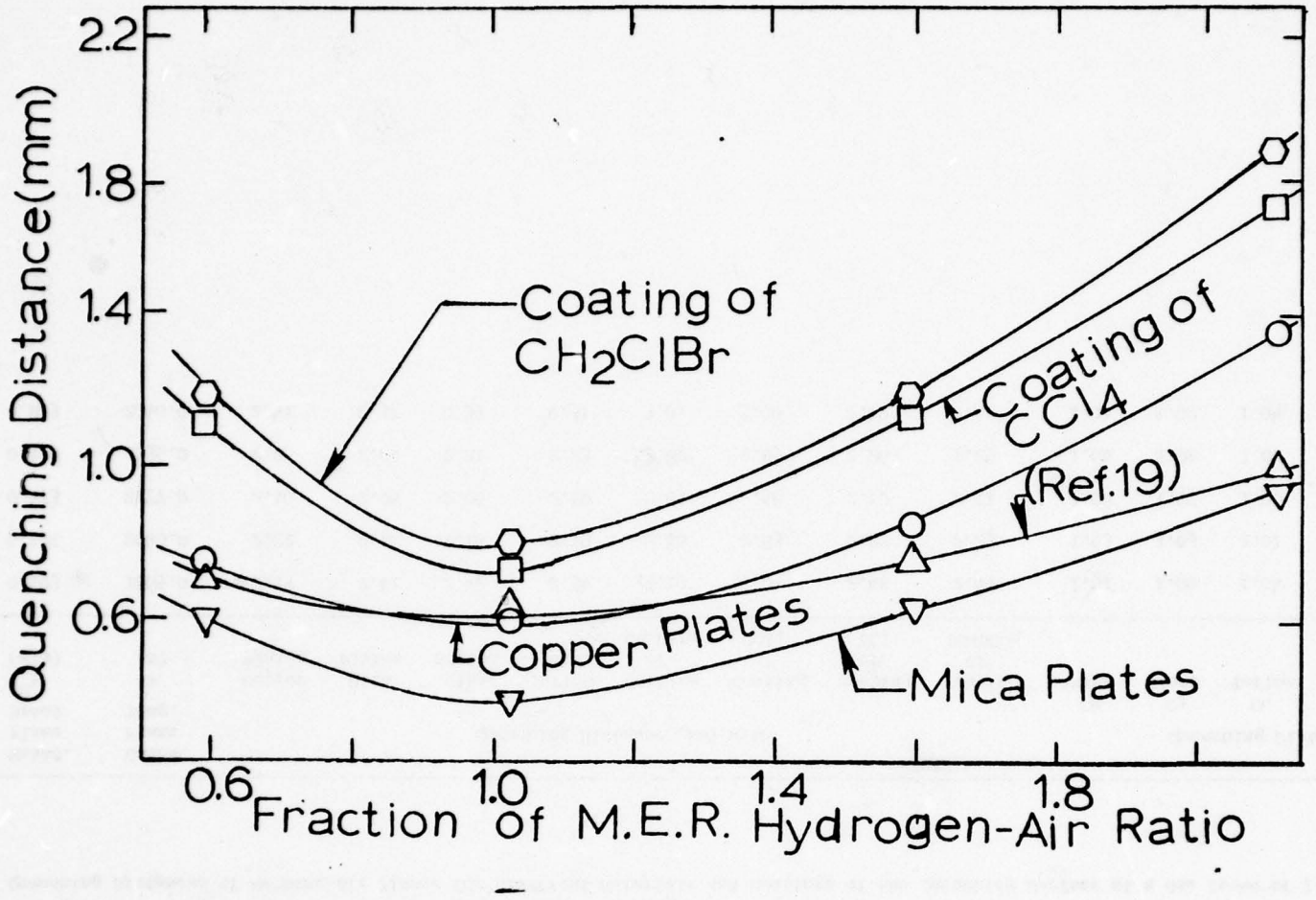

Fig. 11 Measured Quenching Distances of Hydrogen-Air Flames for Different Plate Materials and Coatings at Room Temperature and 1 atm Pressure

Table V. Measured Quenching Distances of Methane-Air Flames for Different Materials and Coatings of the Quenching Surface at a Gas Speed of 1.24 m/s

% CH_4 in air	Stoich. or M.E.R. Fract.	Measd. Flame Speed u_F (m/s)	Calcd. Flame Temp. T_F (K)	Quenching Distance (mm) with								Quenching Distance				
				Copper Plates	Mica Plates	Glass Strips	Teflon Plates	Coating of CH ClBr	Coating of CCl_4	Coating of KCl	Coating of $2NaHCO_3$	Cu Mica	Cu Glass	Cu Teflon	Cu CH ClBr	Cu CCl_4
7.0	0.72	0.193	1865.0	2.43	2.41	2.42	2.34	3.10	3.04	2.44	2.44	1.01	1.00	1.04	0.78	0.80
8.0	0.83	0.332	2040.0	2.22	2.16	2.16	2.19	2.86	2.83	2.22	2.23	1.03	1.03	1.01	0.78	0.78
9.5	1.0	0.473	2177.0	2.10	2.05	2.06	2.10	2.69	2.58	2.10	2.11	1.02	1.02	1.00	0.78	0.81
11.0	1.18	0.400	2135.0	2.25	2.20	2.21	2.23	2.87	2.85	2.26	2.25	1.02	1.02	1.01	0.78	0.79
12.0	1.30	0.223	2060.0	2.41	2.37	2.39	2.31	3.01	3.00	2.42	2.42	1.01	1.02	1.04	0.80	0.80

Table VI. Measured Quenching Distances of Methane-Oxygen Flames for Different Materials and Coatings of the Quenching Surface at a Gas Speed of 9.28 m/s

% CH_4 in air	Stoich. or M.E.R. Fract.	Measd. Flame Speed u_F (m/s)	Calc. Flame Temp. T_F (K)	Quenching Distance (mm) with							Quenching Distance			
				Copper Plates	Mica Plates	Glass Strips	Coating of CH ClBr	Coating of CCl_4	Coating of KCl	Coating of $2NaHCO_3$	Cu Mica	Cu Glass	Cu CH ClBr	Cu CCl_4
15.0	0.35	1.93	2600.0	0.77	0.56	0.57	1.08	0.98	0.77	0.78	1.38	1.35	0.71	0.79
25.0	0.67	3.34	2940.0	0.50	0.35	0.36	0.87	0.74	0.50	0.51	1.43	1.39	0.57	0.68
40.0	1.33	3.35	3000.0	0.61	0.47	0.50	0.99	0.88	0.62	0.62	1.30	1.22	0.62	0.69
45.0	1.67	2.68	2873.0	1.07	0.79	0.85	1.46	1.37	1.08	1.07	1.35	1.26	0.73	0.85
50.0	2.00	1.23	2578.5	1.85	1.30	1.39	2.15	2.05	1.85	1.85	1.42	1.33	0.86	0.90

Table VII. Measured Quenching Distances of Acetylene-Air Flames for Different Plate Materials and Coatings of the Quenching Surface at a Gas Speed of 9.28 m/s

% C_2H_2 in air	Stoich. or M.E.R. Fract.	Measd. Flame Speed u_F (m/s)	Calc. Flame Temp. T_F (K)	Quenching Distance (mm) with							Quenching Distance			
				Copper Plates	Mica Plates	Glass Strips	Coating of CH ClBr	Coating of CCl_4	Coating of KCl	Coating of $2NaHCO_3$	Cu Mica	Cu Glass	Cu CH ClBr	Cu CCl_4
6.0	0.76	1.66	2296.6	0.78	0.52	0.55	1.17	1.07	0.78	0.78	1.50	1.42	0.67	0.73
7.0	0.90	1.80	2448.8	0.59	0.37	0.37	0.90	0.85	0.59	0.60	1.59	1.59	0.66	0.69
8.0	1.03	1.88	2532.5	0.58	0.41	0.41	0.89	0.83	0.58	0.58	1.41	1.41	0.65	0.70
9.0	1.18	1.92	2588.3	0.68	0.52	0.52	0.98	0.91	0.68	0.69	1.39	1.31	0.69	0.75
10.0	1.32	1.32	2535.4	0.83	0.62	0.62	1.14	1.05	0.84	0.84	1.41	1.34	0.73	0.79

Table VIII. Measured Quenching Distances of Hydrogen-Air Flames for Different Plate Materials and Coatings of the Quenching Surface at a Gas Speed of 9.28 m/s

% H_2 in air	Stoich. or M.E.R. Fract.	Measd. Flame Speed u_F (m/s)	Calc. Flame Temp. T_F (K)	Quenching Distance (mm) with							Quenching Distance			
				Copper Plates	Mica Plates	Glass Strips	Coating of CH ClBr	Coating of CCl_4	Coating of KCl	Coating of $2NaHCO_3$	Cu Mica	Cu Glass	Cu CH ClBr	Cu CCl_4
20.0	0.59	1.10	1835.0	0.76	0.61	0.64	1.22	1.13	0.76	0.77	1.23	1.19	0.62	0.67
30.0	1.02	2.15	2390.0	0.58	0.37	0.38	0.81	0.74	0.59	0.58	1.58	1.53	0.72	0.78
40.0	1.59	2.91	2225.8	0.87	0.62	0.64	1.24	1.16	0.88	0.88	1.39	1.36	0.70	0.75
50.0	2.38	2.51	1880.0	1.75	1.16	1.17	2.28	2.01	1.74	1.75	1.51	1.50	0.77	0.87

The effect of quenching on flame pressure was determined by measuring the static pressure in the burner tube just below the tip of the burner. The flame pressure of the fuel-air flames was not changed by quenching; however, that of methane-oxygen flames increased by 2 mm of water or less. Therefore it was concluded that the measured quenching distances were not functions of the flame pressure.

To determine the effect of thermal conductivity of the material of the quenching plates, the quenching distances were also measured by using plates constructed of mica, copper with strips of glass glued to them, and teflon. Plates made of teflon could be used only with methane-air flames because the other fuel-oxidizer flames deform these plates. The results of these observations are given in Tables V-VIII and shown in Fig. 8-11.

In order to study the effect of salts and halogenated compounds on the quenching distances of flames, measurements were made with coated copper plate surfaces. Salts used were potassium chloride and sodium bicarbonate, and halogenated compounds included chlorobromomethane and carbon tetrachloride. Whereas the coatings of potassium chloride and sodium bicarbonate stayed on the copper plates during the duration of the measurements those of chlorobromomethane and carbon tetrachloride tended to disappear in a very short time. Therefore, these substances had to be applied several times during a single experiment. The results of these measurements are included in Tables V-VIII and Fig. 8-11.

3. Spectrographic Measurements

A Hilger & Watts prism spectrograph was used to obtain some qualitative information on the spectra of unquenched and partially quenched flames. The following procedure was adopted for obtaining the spectrograms:

After the flame was adjusted properly a spectrogram was taken. Then the quenching was started by moving in the copper plates. Spectrograms were taken at various positions of the plates until the flame was nearly extinguished. The exposure time was the same for all the flames. However, the last position of the plates was used for extended exposure times up to six times the normal value. The basic exposure time depended on the type of flame to be photographed. Whereas methane-air flames required an exposure time of 5 minutes, methane-oxygen and acetylene-air flames required only 15 seconds. As a reference the spectrum of mercury was recorded on each plate. A "U" shaped G.E. germicidal lamp was used as the source of the mercury spectrum. A reproduction of the spectrograms of an unquenched and a partially quenched flame of 12 percent methane in air is shown in Fig. 12. The individual bands are identified and tabulated in Table IX together with other related data. Identification of the bands was facilitated by consultation of handbooks on molecular spectra; e.g., Ref. (25).

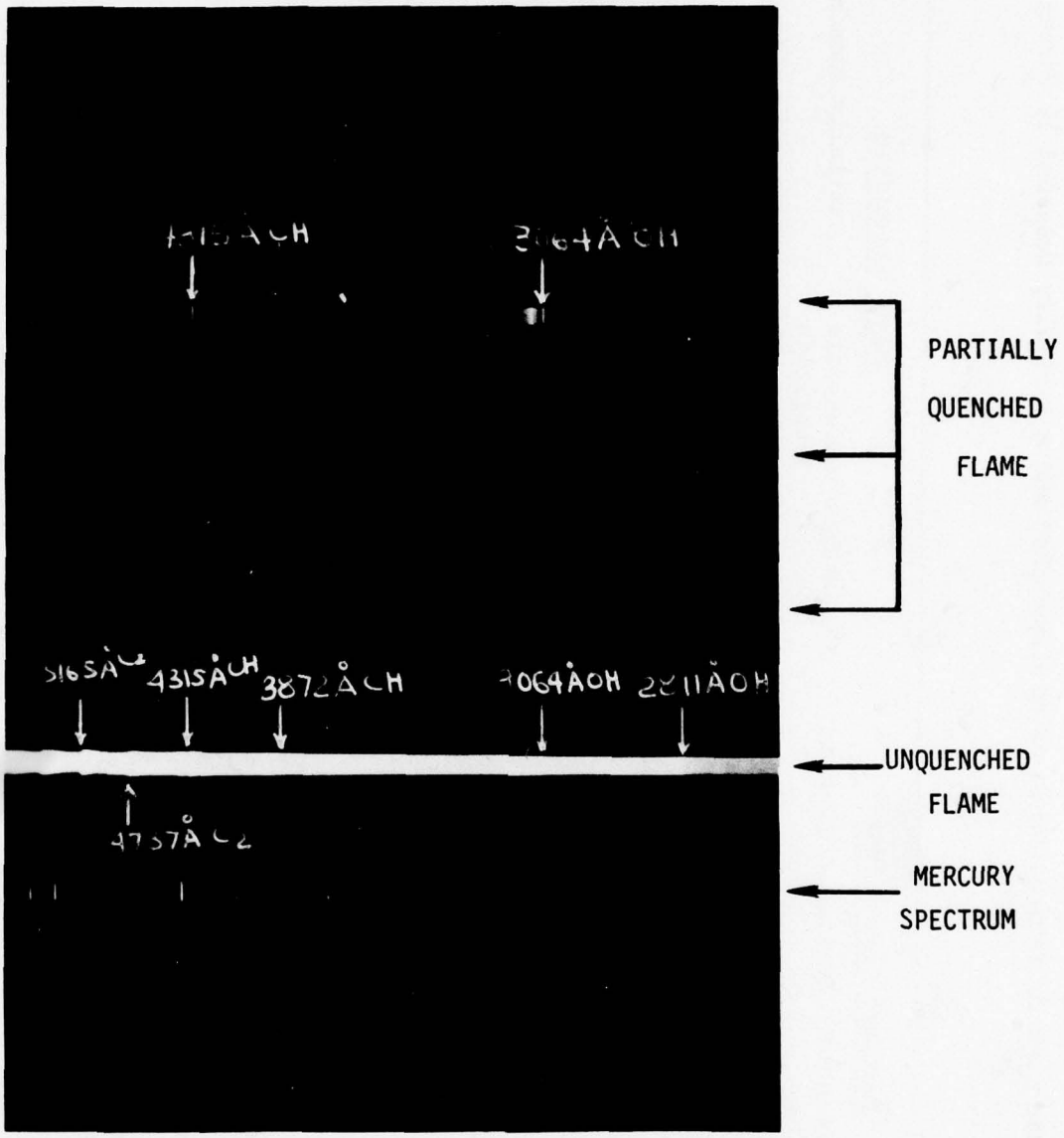

Fig. 12 Spectrum of an Unquenched and a Partially Quenched 12 Percent Methane in Air Flame Obtained with Hilger & Watts Prism Spectrograph; Comparison Mercury Spectrum is also shown

Table IX. Moderate Resolution Spectrograms of Various Bands of an Unquenched and a Partially Quenched 12 Percent Methane in Air Flame

Distance Between Copper Plates (mm)	Slit Setting		Exposure Time (min)				Bands Identified				
	Width or Opening (mm)	Height (mm)	Unquenched Flame	Partially Quenched Flame			Unquenched Flame	Electronic Transition	Partially Quenched Flame		
4.16	30 M	2 mm	5.0	5.0	10.0	30.0	2608 Å OH	$A^2\epsilon - x^2\pi$	3064 Å OH	3064 Å OH	3064 Å OH
							2811 Å OH	$A^2\epsilon - x^2\pi$	4315 Å CH	4315 Å OH	4315 Å OH
							3064 Å OH	$A^2\epsilon - x^2\pi$			
							3872 Å CH	$B^2\epsilon - x^2\pi$			
							4315 Å CH	$A^2\Delta - x^2\pi$			
							4737 Å CC	$A^3\pi - x^3\pi$			
							5165 Å CC	$A^3\pi - x^3\pi$			
							5635 Å CC	$A^3\pi - x^3\pi$			
							6059 Å CC	$A^3\pi - x^3\pi$			

For a quantitative evaluation of the spectra emitted by the flames a Jarrel-Ash 21 ft. grating spectrograph was used. To obtain the shortest exposure time possible a quartz lens was used to project an image of the flame on the spectrograph slit. Spectrograms were obtained over as wide a range of wavelengths as possible and at various stages of the quenching process. The exposure times were increased when the intensity of the radiation was reduced considerably by the quenching plates. Again a mercury spectrum was recorded on each plate as a reference.

The spectrograms obtained for 40 percent methane and 60 percent oxygen flame and for a 40 percent hydrogen and 60 percent air flame are shown in Fig. 13. The individual bands are identified in Table X together with the wavelengths of the band head and other pertinent information.

4. Determination of the Rotational Temperature of the Combustion Gases

As pointed by Dieke and Crosswhite,[26] the bands of the OH radical are usually best suited for determining the temperature of a flame. Because the rotational structure of the OH bands is simple and the isointensity method does not require a great amount of sophisticated equipment. Furthermore, the necessary spectroscopic data needed for the calculations are readily available. Unfortunately, the OH bands in even the unquenched flames of acetylene-air, methane-oxygen, and hydrogen-air mixtures are much too weak and practically nonexistent in methane-air flames, with exposure times ranging up to 4 hours.

Since the CH bands at 3870 and 4315 Å are very prominent in these flames, they were selected for the determination of the rotational temperature of these flames. The 4315 Å CH band is the most intense and very easily observed in all flames containing carbon and hydrogen (both quenched and partially quenched). On the other hand the structure of the 3870 Å CH band is simpler and, therefore, more amenable to rotational temperature measurements. However, this band is not as strong as the 4315 Å CH band, which is very easily observed even in very weak flames. Therefore both the 3870 Å CH and the 4315 Å CH bands were used, wherever possible, for the determination of the rotational flame temperature. In the 4315 Å CH band, only the short wavelength region was selected. The measurements were made on two flames, one containing 40 percent methane and 60 percent oxygen and the other containing 10 percent acetylene and 90 percent air. The relative intensities of the various lines in the band were determined with a microdensitometer. With these values the rotational temperature was derived by the following formula:

$$\ln I_{n'n''} - \ln A^{*}_{n'n''} = \ln F - E_{n'}/kT_{rot} \qquad (3)$$

where

$E_{n'}$ = rotational energy of the upper state for a fixed vibrational transition,

Table X. High-Resolution Spectrograms of Various Bands of an Unquenched and a Partially Quenched 40 Percent Methane in Oxygen Flame

Distance Between Plates (mm)	Slit Setting		Exposure Time (min)				Bands Identified					
	Width or Opening (μm)	Height (mm)	Unquenched Flame		Partially Quenched Flame		Unquenched Flame				Partially Quenched Flame	
							Band	Electronic Transition	Band	Electronic Transition	Case I	Case II
2.03 (Case I)[a]	20	2	30	60	30	60	3143Å CH	$C^2\Sigma - X^2\Pi$	5470Å CC	$A^3\Pi - X^3\Pi$	3872Å CH	
							3064Å OH	$A^2\Sigma - X^2\Pi$	5502Å CC	$A^3\Pi - X^3\Pi$	4315Å CH	4315Å CH
1.19 (Case II)[b]							3872Å CH	$B^2\Sigma - X^2\Pi$	5541Å CC	$A^3\Pi - X^3\Pi$	4678Å CC	and none else
							4315Å CH	$A^2\Delta - X^2\Pi$	5585Å CC	$A^3\Pi - X^3\Pi$	4685Å CC	
							4678Å CC	$A^3\Pi - X^3\Pi$	5635Å CC	$A^3\Pi - X^3\Pi$	4698Å CC	
							4685Å CC	$A^3\Pi - X^3\Pi$	5959Å CC	$A^3\Pi - X^3\Pi$	4715Å CC	
							4698Å CC	$A^3\Pi - X^3\Pi$	6005Å CC	$A^3\Pi - X^3\Pi$	4737Å CC	
							4715Å CC	$A^3\Pi - X^3\Pi$	6060Å CC	$A^3\Pi - X^3\Pi$	5129Å CC	
							4737Å CC	$A^3\Pi - X^3\Pi$	6122Å CC	$A^3\Pi - X^3\Pi$	5165Å CC	
							5129Å CC	$A^3\Pi - X^3\Pi$	6191Å CC	$A^3\Pi - X^3\Pi$	5502Å CC	
							5165Å CC	$A^3\Pi - X^3\Pi$			5541Å CC	
											5585Å CC	
											5635Å CC	
											6122Å CC	
											6191Å CC	

a Case I corresponds to the distance between the plates of 2.03 mm and an exposure time of 30 minutes for the partially quenched flame.

b Case II corresponds to the distance between the plates of 1.19 mm and an exposure time of 60 minutes for the partially quenched flame.

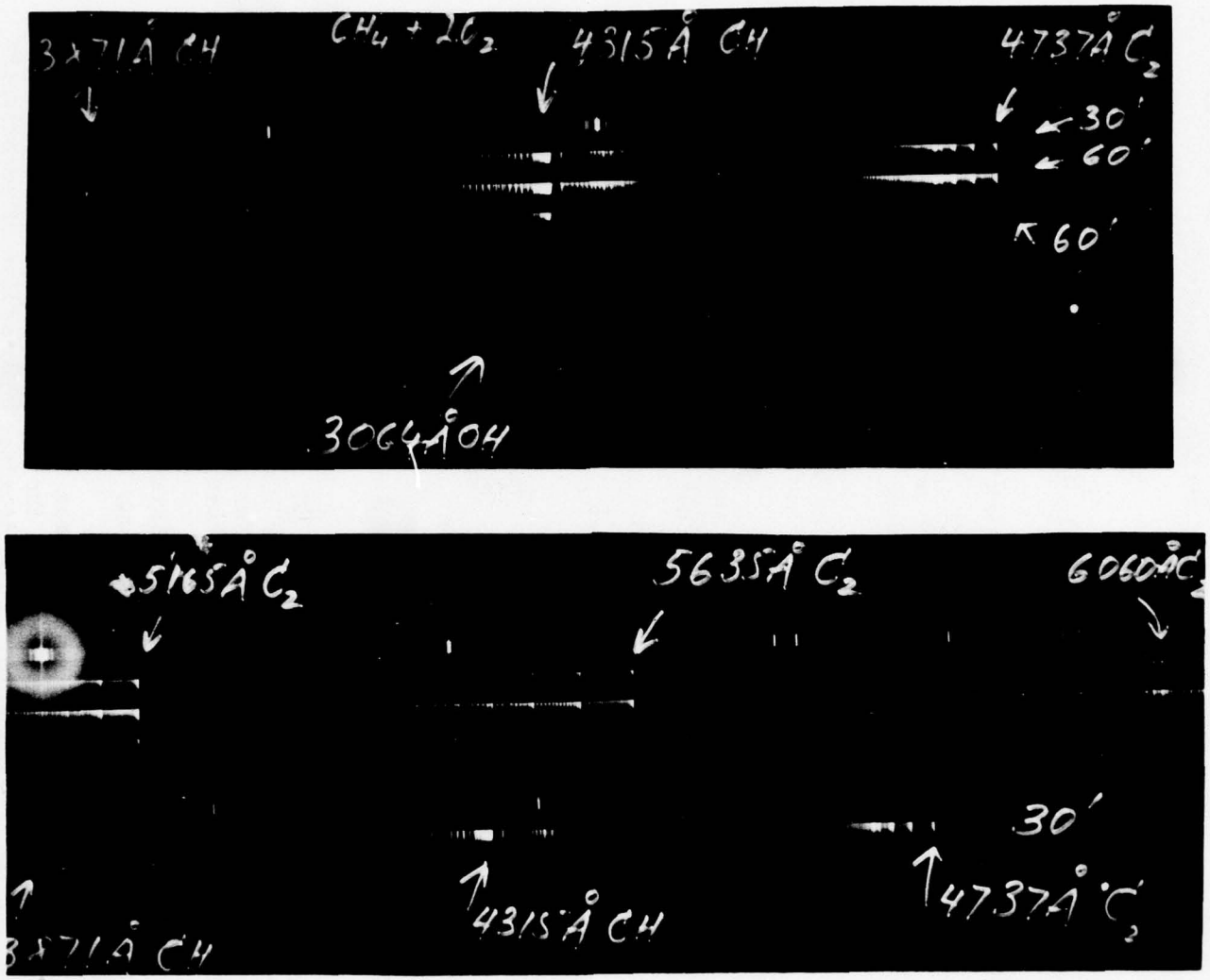

Fig. 13 Spectrum of Unquenched and a Partially Quenched 40 Percent Methane-in-Oxygen and 40 Percent Hydrogen-in-Air Flames Obtained with Jarrel-Ash Grating Spectrograph (a) Lower Wavelength Side; (b) Higher Wavelength Side. Comparison Mercury Spectrum is Also Shown

$I_{n'n''}$ = relative intensity of a rotational transition,

n', n'' = quantum numbers of the rotational levels in the upper and lower electronic states, respectively,

$A^*_{n'n''} = A_{n'n''}\ \nu_{n'n''}$,

$A_{n'n''}$ = transition probability including the statistical weight,

$\nu_{n'n''}$ = wave number of the line,

F = constant depending on electronic transition and instrument factors but independent of $E_{n'}$,

T_{rot} = rotational temperature of interest, and

k = Boltzmann's constant.

According to Eq. (3) a graph of $\ell n\,(I_{n'n''}/A^*_{n'n''})$ vs $E_{n'}$ gives a straight line whose slope is $-1.44/T_{rot}$, when $E_{n'}$, is expressed in wave number units (i.e., cm^{-1}) and the rotational temperature in Kelvin.

The values of $A_{n'n''}$ and $E_{n'}$ for the 3870Å CH band have been determined by Dieke[27] and those of the 4315Å CH band by Broida.[28]

In Eq. (3) everything but the rotational temperature is known. Thus the rotational temperature is given by the slope of the $\ell n\,(I_{n'n''}/A^*_{n'n''})$ vs $E_{n'}$ curve.

For the 40 percent methane and 60 percent oxygen, and for the 10 percent acetylene and 90 percent air flames, the rotational flame temperatures were determined, both for the unquenched and partially quenched flames. The results are shown in Fig. 14-17.

5. Measurements of the Quenching Distances of Flames of Hydrogen-Oxygen Mixtures Containing Various Inert Gases

The quenching distances of flames of hydrogen-oxygen-inert gas mixtures were measured to determine the effect of inert gases such as helium, argon, nitrogen and carbon dioxide. Two series of experiments were performed, i.e., one with 68.2 percent inert gas and the other with 55.6 percent inert gas in the mixture. The procedure for measuring the quenching distances was the same as used for other fuel-oxidizer

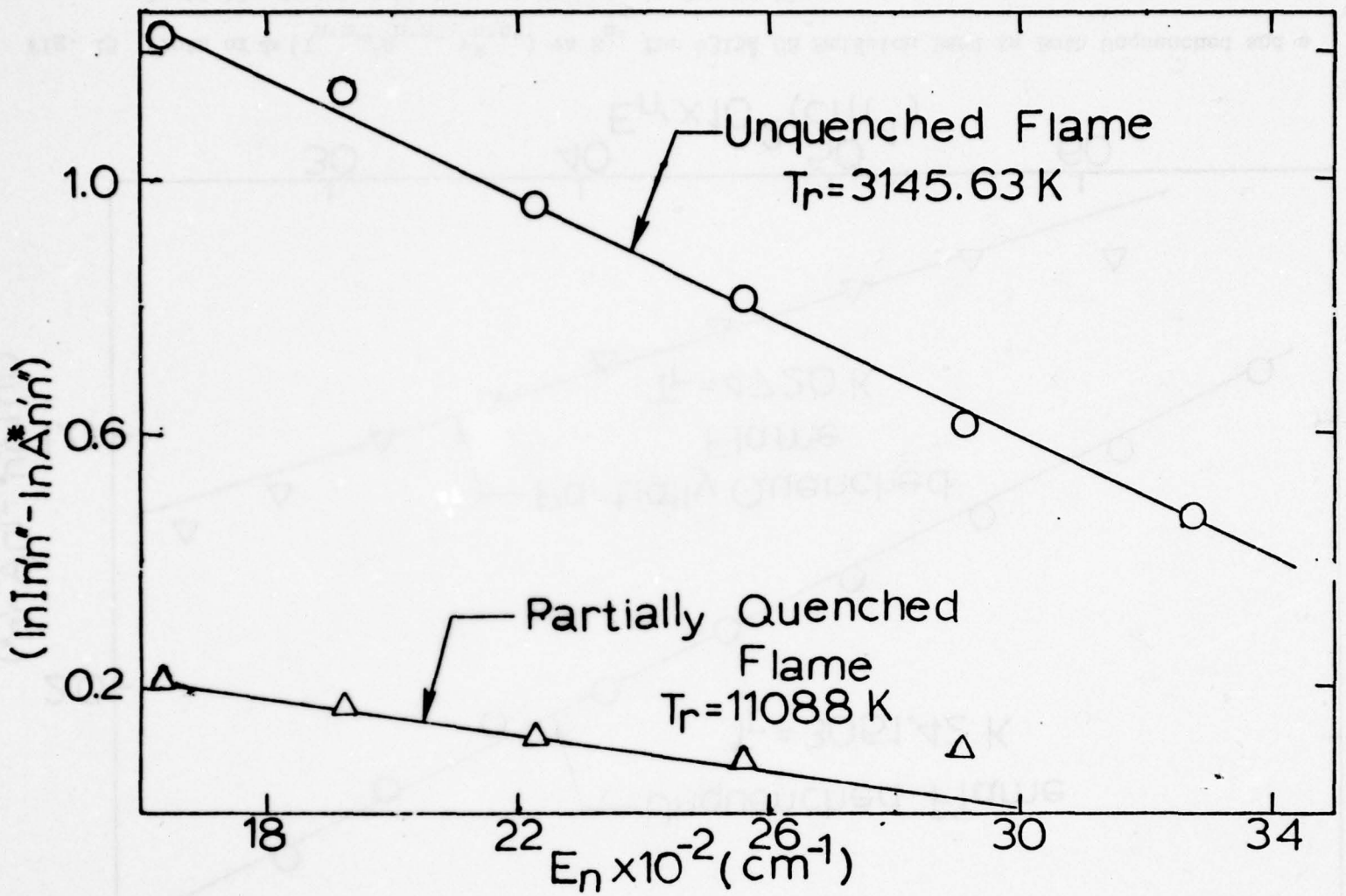

Fig. 14 Plots of $\ell n\, I_{n'n''}/A_{n'n''}\, \nu^4_{n'n''}$ vs $E_{n'}$ for 3870Å CH Emission Band in Both Unquenched and a Partially Quenched 40 Percent Methane in Oxygen Flame.

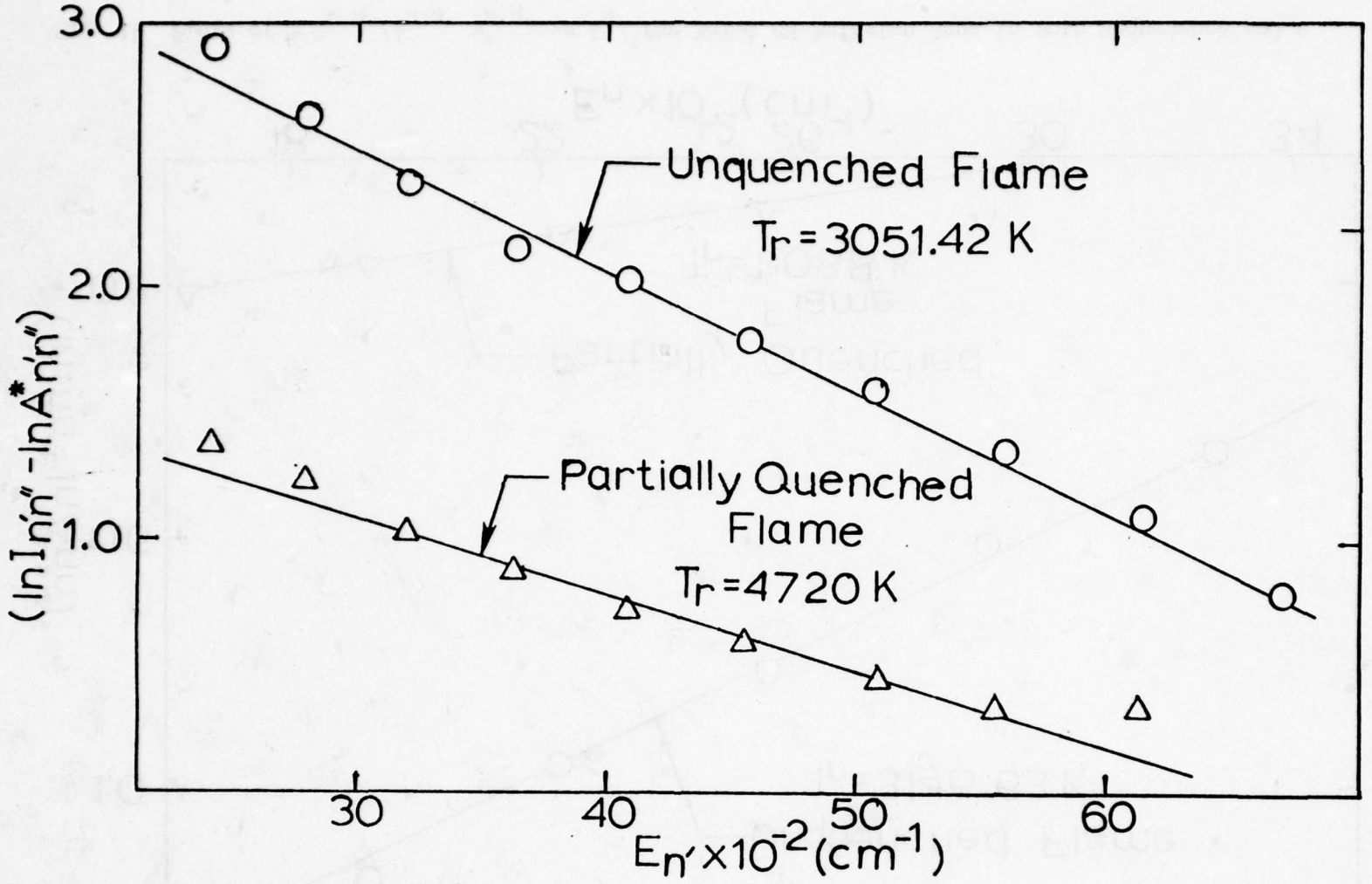

Fig. 15 Plots of $\ell n\,(I_{n'n''}/A_{n'n''}\ \nu^4_{n'n''})$ vs $E_{n'}$ for 4315Å CH Emission Band in Both Unquenched and a Partially Quenched 40 Percent Methane in Oxygen Flame.

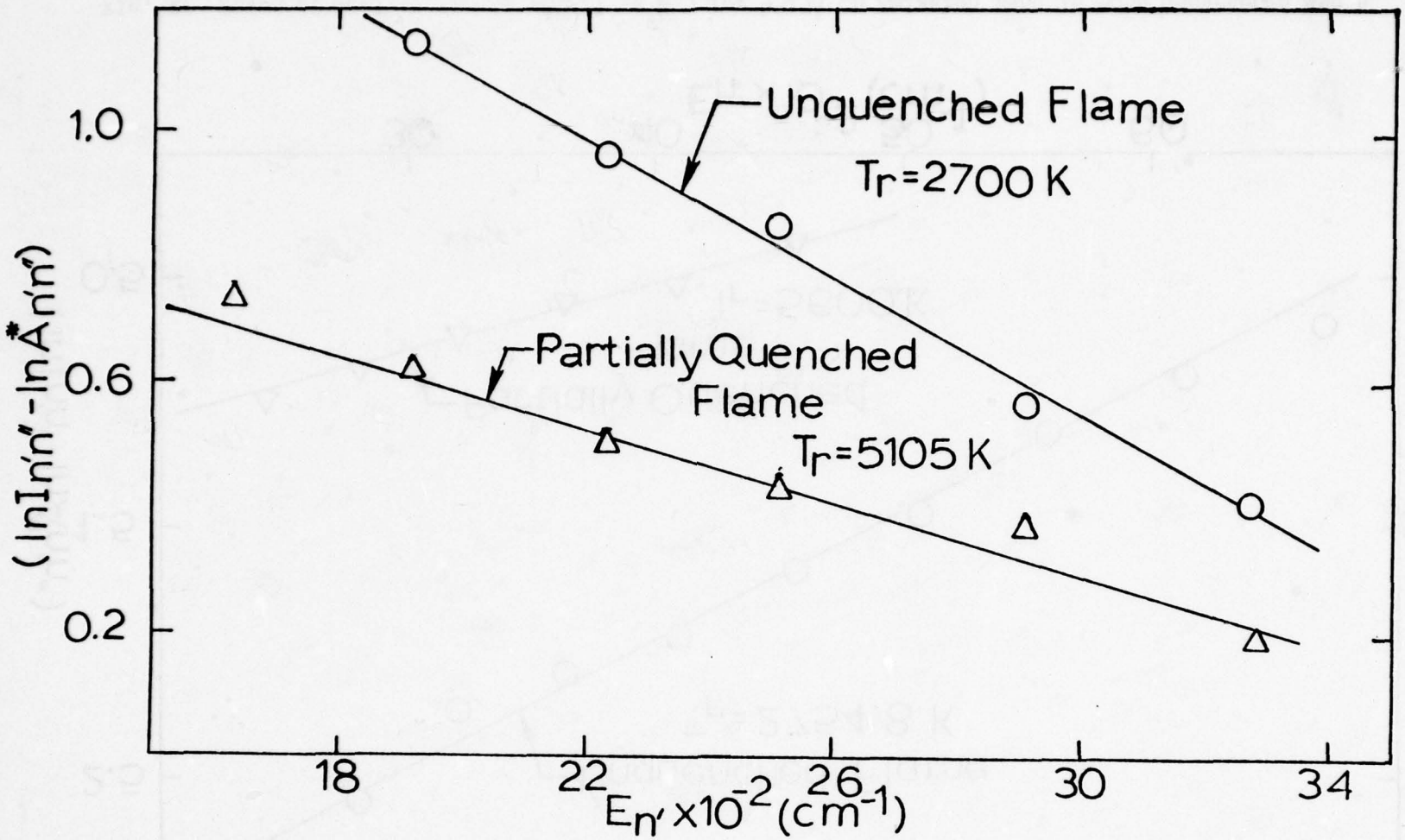

Fig. 16 Plots of $\ell n\,(I_{n'n''}/A_{n'n''}\ \nu^{4}_{n'n''})$ vs $E_{n'}$ for 3870Å CH Emission Band in Both Unquenched and a Partially Quenched 10 Percent Acetylene in Air Flame.

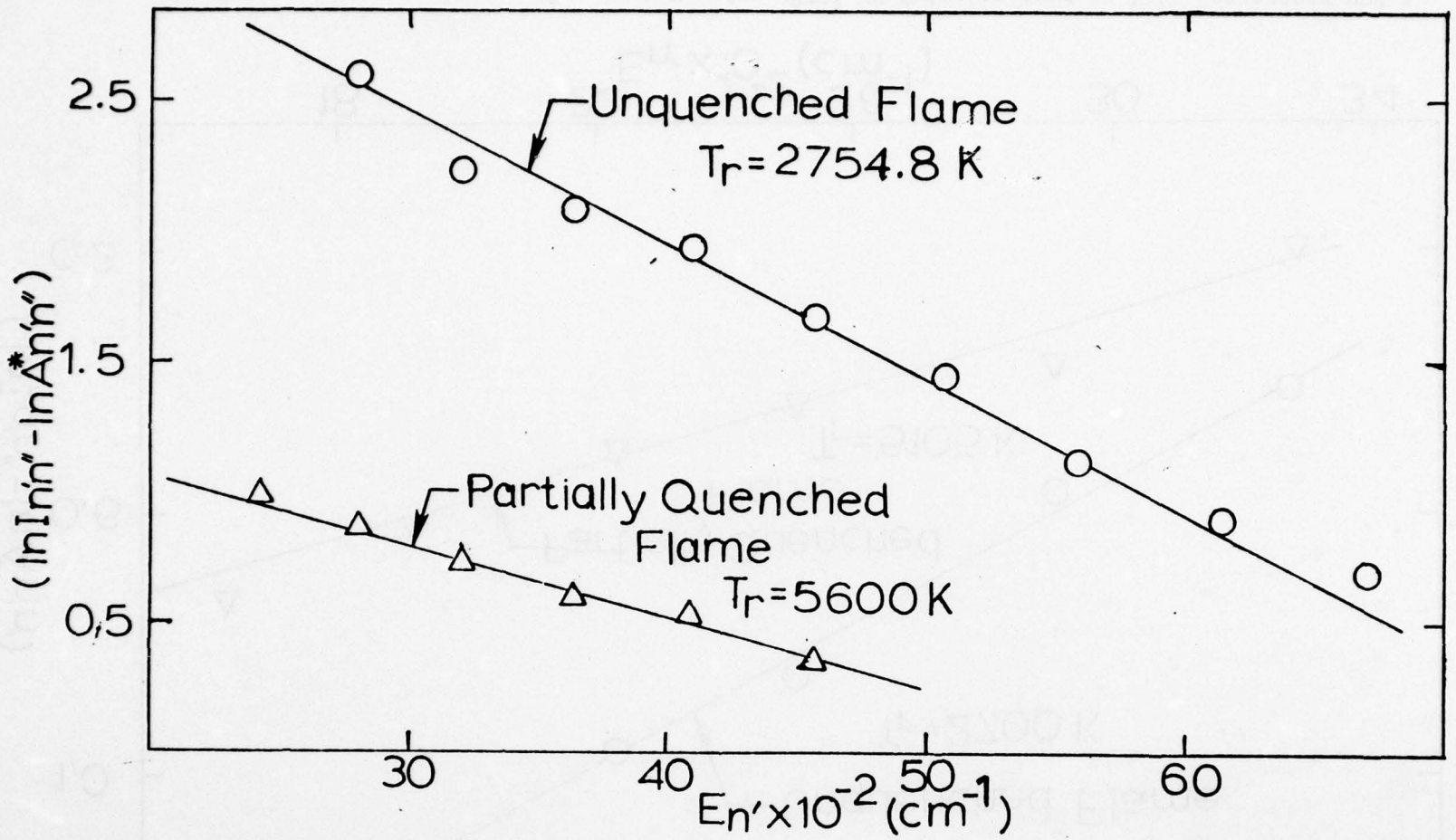

Fig. 17 Plots of $\ell n\,(I_{n'n''}/A_{n'n''}\ \nu^4_{n'n''})$ vs $E_{n'}$ for 4315Å CH Emission Band in Both Unquenched and a Partially Quenched 10 Percent Acetylene in Air Flame.

mixture flames. In this case the quenching distances were measured only for a volume flow rate of 100 cc/s. However, the relative proportions of hydrogen and oxygen in the mixture were varied. The results of these measurements are given in Fig. 18 and 19.

6. Experimental Determination of Flame Speeds

In order to study the relationship between flame speed and quenching distance, the flame speeds of various fuel-oxidizer mixtures had to be determined experimentally. Since only relative values are needed the flame cone method was used for these measurements because this method is quite easy and fairly reliable; the results are shown in Fig. 20-22.

7. Calculation of Flame Temperature

Because of the relationship between flame temperature and quenching distance, the flame temperature and quenching distance, the flame temperatures of various fuel-oxidizer mixtures were calculated for the case that the combustion gas is in complete thermodynamic and chemical equilibrium. The method given by Edse[29] was used for calculating the flame temperatures and the values of equilibrium constants and enthalpies, etc., were taken from JANNAF Tables.[30] The results of these calculations, including the equilibrium compositions of the combustion gases, are given in Tables XI-XX.

IV. DISCUSSION OF RESULTS

Tables I-IV show the measured quenching distances of methane-air, methane-oxygen, acetylene-air, and hydrogen-air flames for different gas speeds and Reynolds numbers. The last three columns in these tables show the measured quenching distances for a circular burner. From the results shown in these tables, it appears that the quenching distances are independent of the shape of the burner and also of the gas speed and Reynolds number for a given gas mixture of the various fuel-oxidizer flames considered. Quenching distance measurements of the previous investigators did not include the effect of gas speed and Reynolds number.

The observation that the quenching distance does not depend on the geometry of the burner is in contradiction to the findings of Berlad and Potter.[20] They used three burners of different shapes and showed that all three burners lead to different quenching distances. These results may be attributed to the different technique used by them which involved an adjustable slot burner in contrast to the arrangement used in the present investigation.

Tables V-VIII show the quenching distances for methane-air, methane-oxygen, acetylene-air, and hydrogen-air flames as measured with different plate materials and coatings. These results are also shown graphically in Fig. 8-11. The quenching distances reported by Lewis and von Elbe[21] for methane-air, methane-oxygen, and hydrogen-air flames are included for

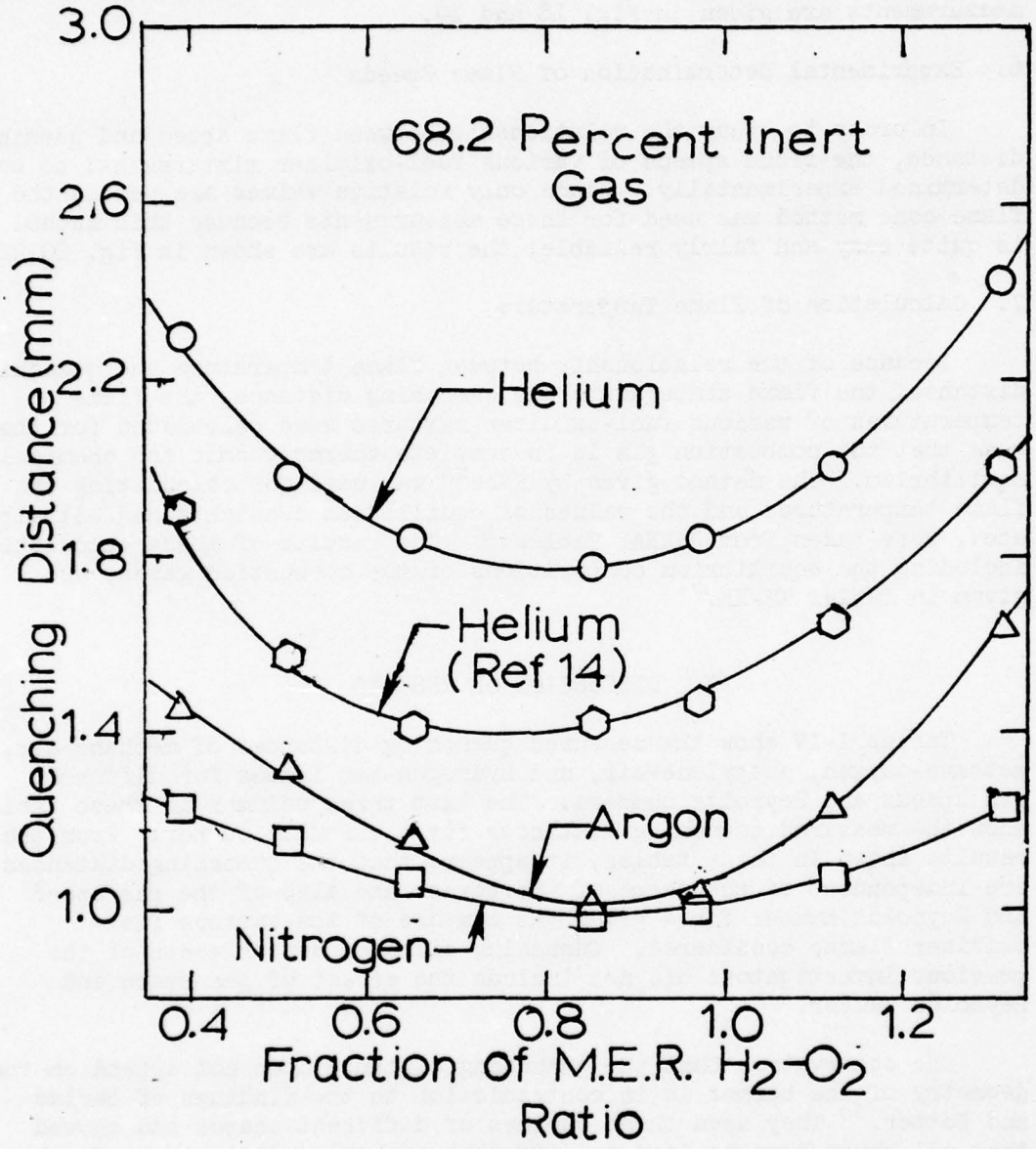

Fig. 18 Measured Quenching Distances of Hydrogen-Oxygen Flames with Various Inert Gas Additives (for 68.2 Percent Inert Gas) at Room Temperature and 1 atm Pressure

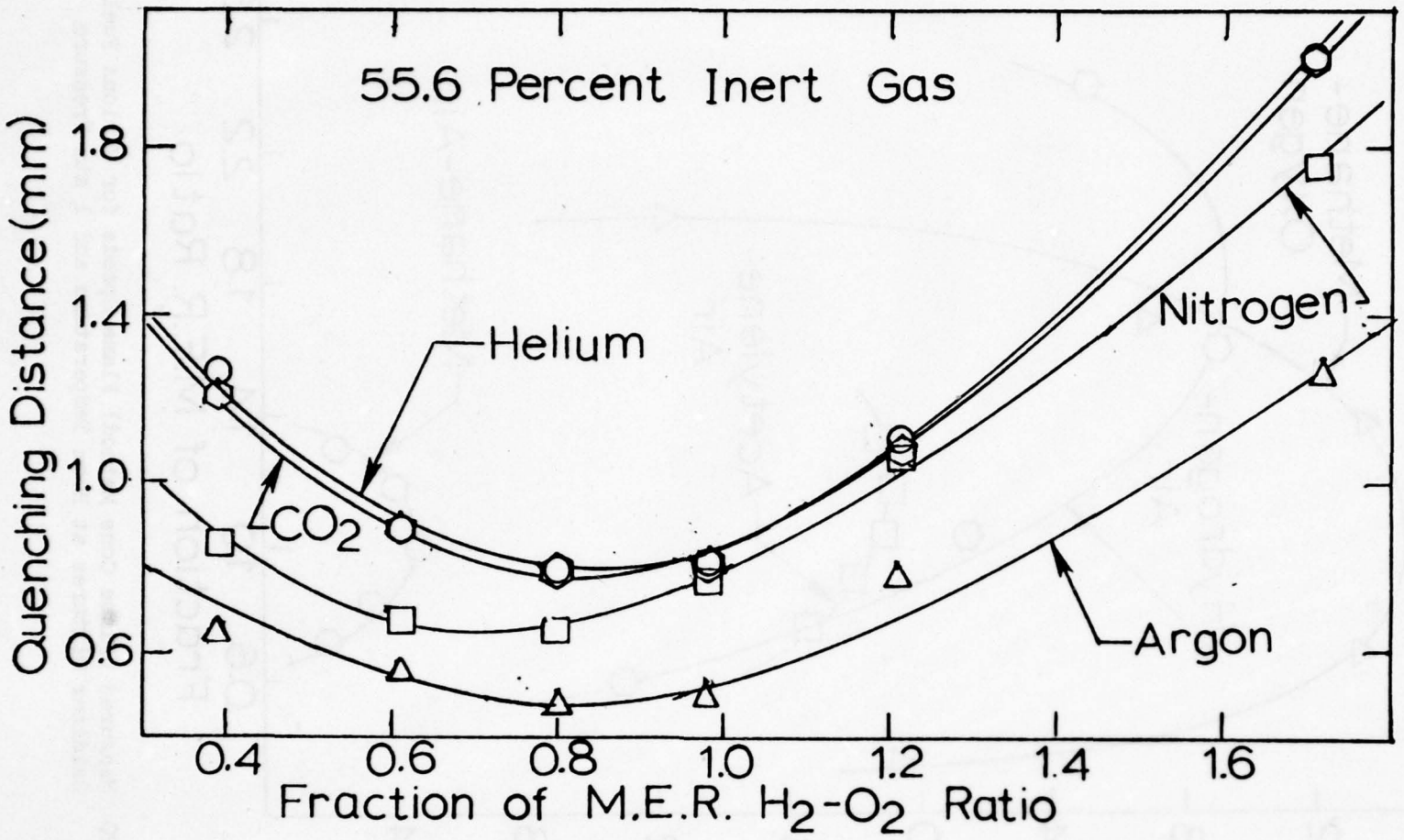

Fig. 19 Measured Quenching Distances of Hydrogen-Oxygen Flames with Various Inert Gas Additives (for 55.6 Percent Inert Gas) at Room Temperature and 1 atm Pressure

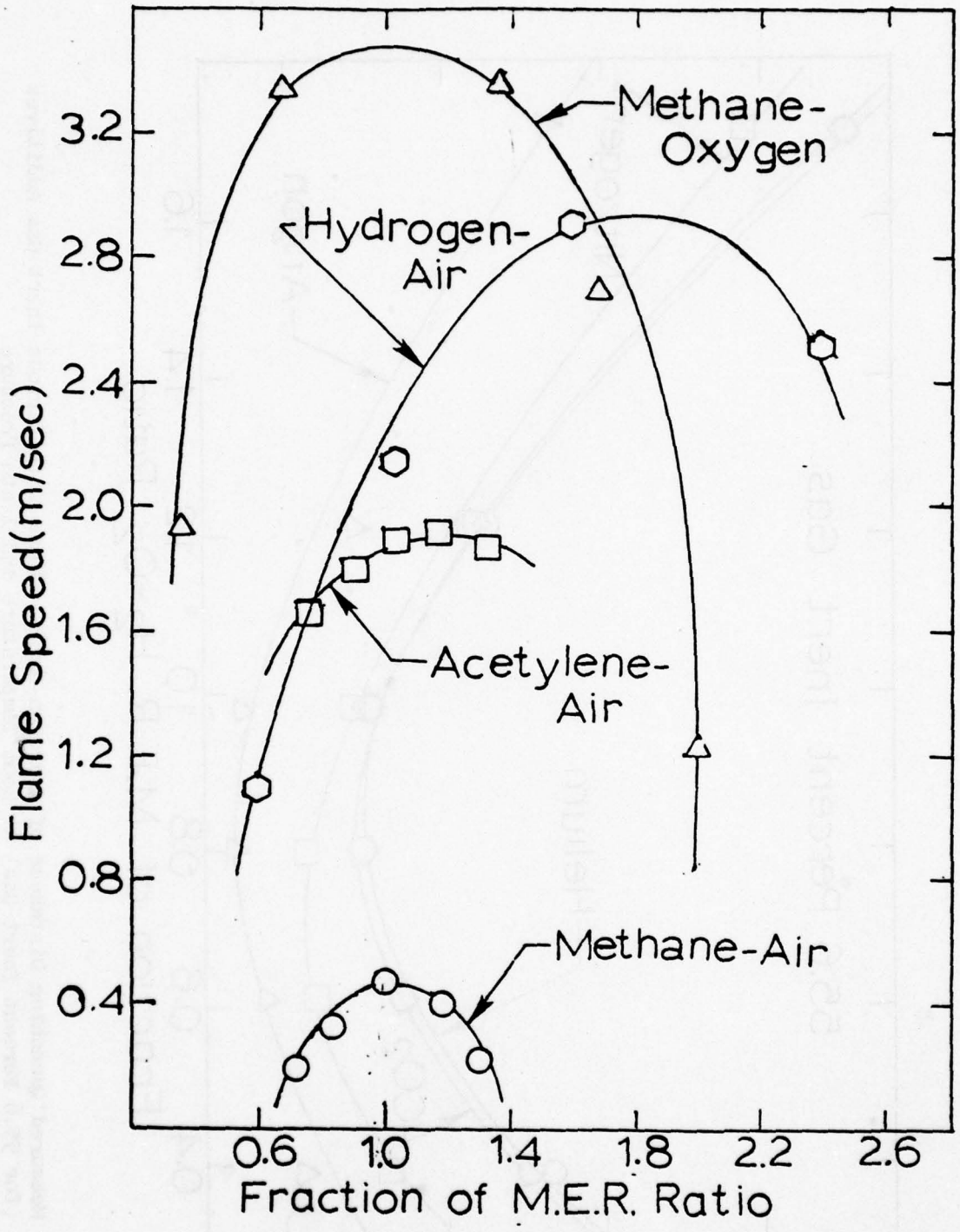

Fig. 20 Measured (Flame Cone Method) Flame Speeds for Various Fuel-Oxidizer Mixtures at Room Temperature and 1 atm Pressure

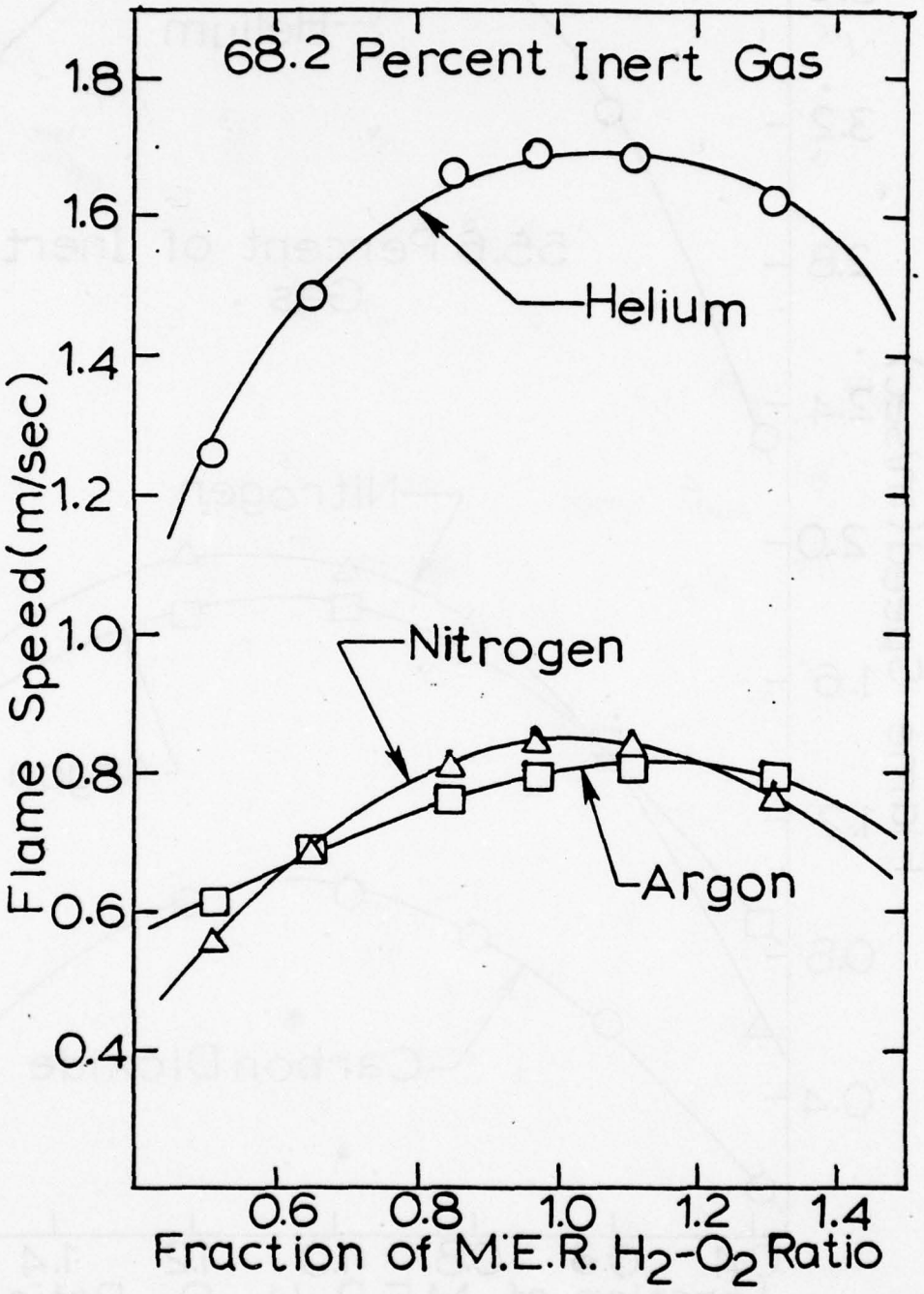

Fig. 21 Measured (Flame Cone Method) Flame Speeds for Hydrogen-Oxygen Mixtures with Various Inert Gas Additives (for 68.2 Percent Inert Gas) at Room Temperature and 1 atm Pressure

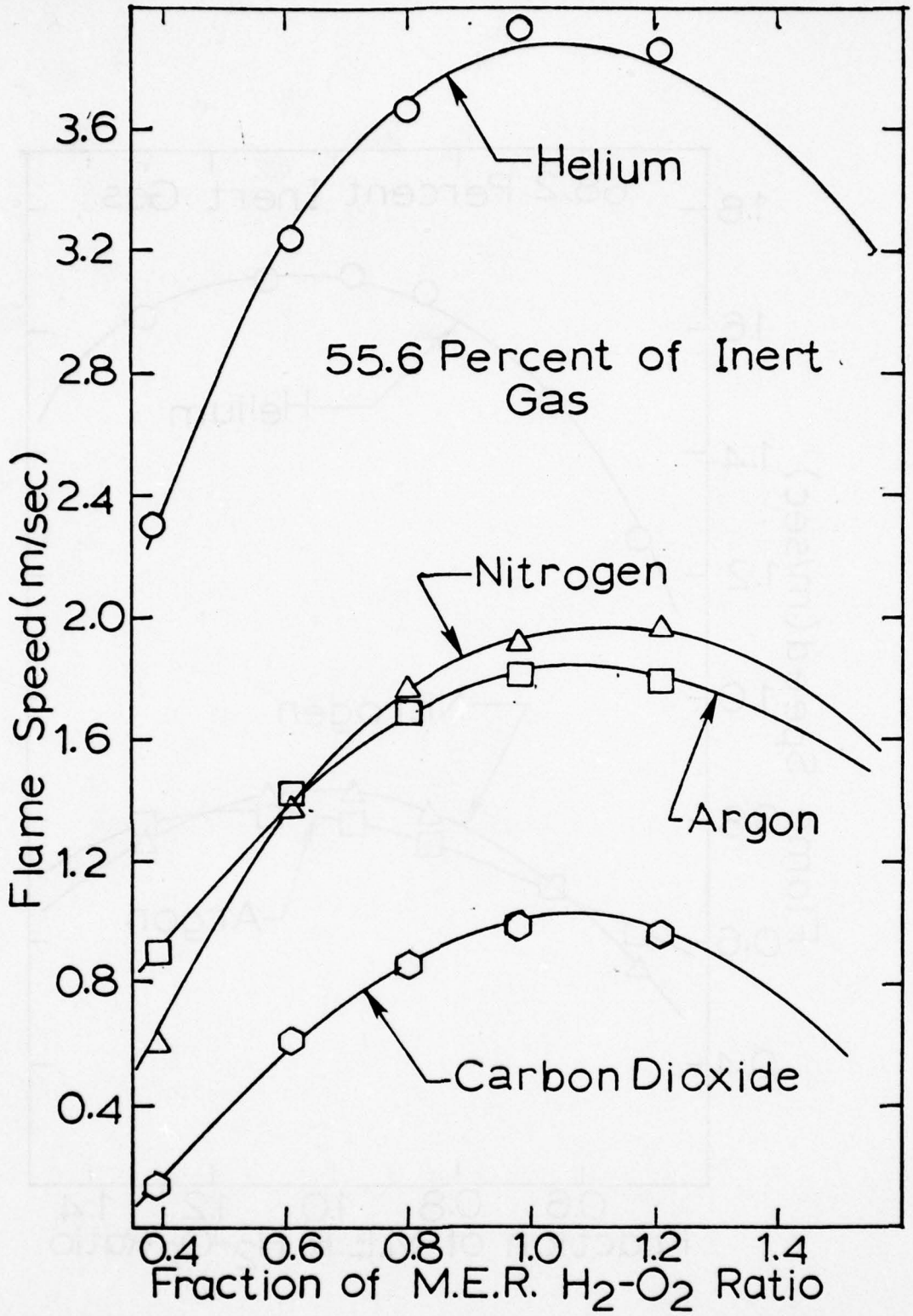

Fig. 22 Measured (Flame Cone Method) Flame Speeds for Hydrogen-Oxygen Mixtures with Various Inert Gas Additives (for 55.6 Percent Inert Gas) at Room Temperature and 1 atm Pressure

Table XI. Calculated Adiabatic Flame Temperatures and Composition of the Combustion Gas of Methane-Air Flames, at 300 K and 1 atm pressure.

Gas Composition %		Stoich. or M.E.R.	Flame Temp.	Composition of Product (Burned) Gases									
CH_4	Air	Fraction	(K)	H_2	H	O_2	O	OH	H_2O	NO	CO	CO_2	N_2
6.0	94.0	0.61	1680	7.017-6	3.209-7	7.645-2	9.896-6	2.788-4	1.198-1	1.689-3	1.146-5	6.000-2	7.416-1
7.0	93.0	0.72	1865	6.057-5	4.888-6	5.370-2	5.291-5	8.988-4	1.394-1	2.719-3	1.215-4	6.986-2	7.330-1
8.0	92.0	0.83	2040	3.726-4	4.360-5	3.140-2	1.711-4	2.097-3	1.584-1	3.445-3	8.667-4	7.904-2	7.241-1
9.0	91.0	0.94	2162	1.649-3	2.033-4	1.155-2	2.538-4	3.041-3	1.760-1	2.849-3	4.096-3	8.556-2	7.146-1
10.0	90.0	1.06	2174	1.395-2	5.580-4	1.500-4	2.711-5	9.988-4	1.810-1	3.130-4	2.750-2	7.364-2	6.955-1
11.0	89.0	1.18	2135	2.491-2	6.255-4	3.400-5	1.059-5	6.181-4	1.869-1	1.374-4	4.303-2	6.317-2	6.786-1
12.0	88.0	1.30	2060	4.386-2	5.047-4	3.500-6	1.943-6	2.428-4	1.832-1	3.560-5	6.189-2	5.352-2	6.586-1

READ 7.017-6 as 7.017×10^{-6} and so on

Table XII. Calculated Adiabatic Flame Temperatures and Composition of the Combustion Gas of Methane-Oxygen Flames, at 300 K and 1 atm pressure.

Gas Composition %		Stoich. or M.E.R. Fraction	Flame Temp. (K)	Composition of Product (Burned) Gases							
CH_4	O_2			H_2	H	O_2	O	OH	H_2O	CO	CO_2
10.0	90.0	0.20	2252.4	4.073-4	1.602-4	6.920-1	3.275-3	1.248-2	1.922-1	3.652-3	9.581-2
20.0	80.0	0.50	2870.0	-------	-------	-------	-------	-------	-------	-------	-------
30.0	70.0	0.86	2995.4	4.785-2	3.477-2	1.410-1	4.246-2	9.764-2	3.862-1	1.507-1	9.945-2
40.0	60.0	1.33	3000.0	1.316-1	5.766-2	2.100-2	1.639-2	6.250-2	4.100-1	2.398-1	6.108-2
50.0	50.0	2.00	2578.5	3.652-1	2.134-2	4.550-5	1.422-4	3.866-3	2.803-1	2.967-1	3.240-2

READ 4.073-4 as 4.073×10^{-4} and so on

Table XIII. Calculated Adiabatic Flame Temperatures and Composition of the Combustion Gas of Acetylene-Air Flames, at 300 K and 1 atm pressure.

Gas Composition %		Stoich. or M.E.R. Fraction	Flame Temp. (K)	Composition of Product (Burned) Gases									
C_2H_2	Air			H_2	H	O_2	O	OH	H_2O	NO	N_2	CO	CO_2
5.0	95.0	0.63	2060.0	8.407-5	2.218-5	7.360-2	2.815-4	1.545-3	5.036-2	5.588-3	7.660-1	9.718-4	1.015-1
6.0	94.0	0.76	2296.6	5.688-4	2.312-4	4.730-2	1.076-3	4.021-3	5.881-2	7.725-3	7.572-1	7.518-3	1.155-1
7.0	93.0	0.90	2448.8	1.866-3	8.666-4	2.805-2	1.879-3	6.269-3	6.590-2	7.847-3	7.446-1	2.525-2	1.174-1
8.0	92.0	1.03	2532.5	4.354-3	1.969-3	1.450-2	2.108-3	7.369-3	7.164-2	6.525-3	7.294-1	5.107-2	1.103-1
9.0	91.0	1.18	2588.3	8.756-3	3.444-3	6.300-3	1.753-3	7.089-3	7.504-2	4.639-3	7.126-1	8.102-2	9.803-2
10.0	90.0	1.32	2595.0	1.522-2	4.730-3	2.400-3	1.133-3	5.805-3	7.736-2	2.872-3	6.941-1	1.149-1	8.079-2
12.0	88.0	1.62	2535.4	3.746-2	5.775-3	1.950-4	2.444-4	2.507-3	7.148-2	7.169-4	6.546-1	1.809-1	4.529-2

READ 8.407-5 as 8.407×10^{-5} and so on.

Table XIV. Calculated Adiabatic Flame Temperatures and Composition of Combustion Gas of Hydrogen-Air Flames, at 300 K and 1 atm pressure.

Gas Composition %		Stoich. or M.E.R. Fraction	Flame Temp. (K)	Composition of Product (Burned) Gases							
H_2	Air			H_2	H	O_2	O	OH	H_2O	NO	N_2
10.0	90.0	0.24	1065.0	-------	-------	-------	-------	-------	-------	-------	-------
20.0	80.0	0.59	1835.0	5.858-5	3.504-6	7.200-2	4.281-5	9.729-4	2.216-1	2.714-3	7.006-1
30.0	70.0	1.02	2390.0	2.311-2	2.416-3	2.500-3	4.306-4	6.357-3	3.202-1	1.977-3	6.396-1
40.0	60.0	1.59	2225.8	1.684-1	2.721-3	5.500-6	7.604-6	7.023-4	2.868-1	6.041-5	5.413-1
50.0	50.0	2.38	1880.0	3.324-1	3.906-4	5.500-9	1.848-8	2.153-5	2.231-1	6.936-7	4.389-1

READ 5.858-5 as 5.858×10^{-5} and so on

Table XV. Calculated Adiabatic Flame Temperatures and Composition of Combustion Gas of Hydrogen-Oxygen and 68.2 Percent Helium or Argon Flames, at 300 K and 1 atm pressure.

Gas Composition %			Stoich. or M.E.R.	Flame Temp.	Composition of Product (Burned) Gases					
H_2	O_2	He or Ar	Fraction	(K)	H_2	H	O_2	OH	H_2O	He or Ar
16.0	15.8	68.2	0.51	1924.1	9.220-5	8.800-6	8.430-2	1.475-3	1.730-1	7.410-1
17.0	14.8	68.2	0.57	2018.6	2.238-4	2.610-5	6.810-2	2.287-3	1.843-1	7.449-1
18.0	13.8	68.2	0.65	2110.0	5.528-4	7.800-5	5.190-2	3.502-3	1.952-1	7.484-1
19.0	12.8	68.2	0.74	2195.5	1.266-3	1.993-4	3.550-2	4.739-3	2.058-1	7.520-1
20.0	11.8	68.2	0.85	2274.2	2.710-3	4.307-4	1.970-2	5.522-3	2.158-1	7.553-1
21.0	10.8	68.2	0.97	2331.6	7.378-3	9.717-4	5.700-3	5.156-3	2.228-1	7.575-1
22.0	9.8	68.2	1.12	2271.3	2.762-2	1.375-3	1.870-4	1.718-3	2.143-1	7.547-1
23.0	8.8	68.2	1.31	2103.9	5.865-2	8.036-4	4.500-6	3.358-4	1.928-1	7.474-1

READ 9.220-5 as 9.220×10^{-5} and so on.

Table XVI. Calculated Adiabatic Flame Temperatures and Composition of the Combustion Gas of Hydrogen-Oxygen and 55.6 Percent Helium or Argon Flames, at 300 K and 1 atm pressure.

Gas Composition %			Stoich. or M.E.R. Fraction	Flame Temp. (K)	Composition of Product (Burned) Gases						
H_2	O_2	He or Ar			H_2	H	O_2	O	OH	H_2O	He or Ar
19.4	25.0	55.6	0.39	2115.0	3.570-4	6.670-5	1.677-1	6.480-4	5.109-3	2.115-1	6.146-1
22.4	22.0	55.6	0.51	2333.2	1.769-3	4.758-4	1.181-1	2.022-3	1.148-2	2.432-1	6.229-1
24.4	20.0	55.6	0.61	2454.5	4.273-3	1.311-3	8.470-2	3.265-3	1.649-2	2.623-1	6.277-1
26.4	18.0	55.6	0.73	2584.4	1.346-2	4.158-3	3.766-2	4.140-3	2.143-2	2.858-1	6.333-1
27.4	17.0	55.6	0.80	2634.2	2.932-2	7.536-3	1.326-2	3.088-3	1.938-2	2.928-1	6.346-1
29.4	15.0	55.6	0.98	2722.0	-------	-------	-------	-------	-------	-------	-------
31.4	13.0	55.6	1.21	2584.2	6.526-2	9.155-3	1.560-3	8.425-4	9.605-3	2.820-1	6.316-1

READ 3.570-4 as 3.570×10^{-4} and so on

Table XVII. Calculated Adiabatic Flame Temperatures and Composition of the Combustion Gas of Hydrogen-Oxygen and 68.2 Percent Nitrogen Flames, at 300 K and 1 atm pressure.

Gas Composition %			Stoich. or M.E.R. Fraction	Flame Temp. (K)	Composition of Product (Burned) Gases							
H_2	O_2	N_2			H_2	H	O_2	O	OH	H_2O	NO	N_2
16.0	15.8	68.2	0.51	1542.0	2.160-6	4.600-8	8.420-2	2.250-6	1.300-4	1.738-1	1.028-3	7.408-1
17.0	14.8	68.2	0.57	1620.0	5.930-6	1.620-7	6.800-2	4.750-6	2.192-4	1.857-1	1.255-3	7.447-1
18.0	13.8	68.2	0.65	1690.0	1.563-5	5.270-7	5.180-2	9.076-6	3.479-4	1.976-1	1.452-3	7.487-1
19.0	12.8	68.2	0.74	1767.5	4.510-5	1.852-6	3.540-2	1.704-5	5.495-4	2.096-1	1.607-3	7.527-1
20.0	11.8	68.2	0.85	1837.5	1.137-4	4.870-6	1.900-2	2.401-5	7.366-4	2.217-1	1.494-3	7.568-1
21.0	10.8	68.2	0.97	1910.0	6.025-4	2.092-5	3.000-3	1.763-5	7.043-4	2.335-1	7.401-4	7.613-1

READ 2.160-6 as 2.160×10^{-6} and so on.

Table XVIII. Calculated Adiabatic Flame Temperatures and Composition of the Combustion Gas of Hydrogen-Oxygen and 55.6 Percent Nitrogen Flames, at 300 K and 1 atm pressure.

Gas Composition %			Stoich. or M.E.R. Fraction	Flame Temp. (K)	Composition of Product (Burned) Gases							
H_2	O_2	N_2			H_2	H	O_2	O	OH	H_2O	NO	N_2
19.4	25.0	55.6	0.39	1779.1	2.116-5	1.269-6	1.678-1	3.709-5	8.200-4	2.144-1	3.160-3	6.140-1
22.4	22.0	55.6	0.51	1983.8	1.947-4	2.108-5	1.183-1	2.113-4	2.756-3	2.504-1	5.282-3	6.229-1
24.4	20.0	55.6	0.61	2114.5	6.000-4	8.088-5	8.430-2	4.296-4	4.638-3	2.745-1	6.122-3	6.291-1
26.4	18.0	55.6	0.73	2237.5	1.931-3	3.079-4	5.060-2	7.753-4	7.272-3	2.974-1	6.423-3	6.352-1
27.4	17.0	55.6	0.80	2295.5	3.464-3	5.673-4	3.420-2	9.120-4	8.430-3	3.080-1	6.005-3	6.382-1
29.4	15.0	55.6	0.98	2381.4	1.311-3	1.648-3	6.400-3	6.184-4	7.556-3	3.235-1	3.061-3	6.438-1

READ 2.116-5 as 2.116×10^{-5} and so on.

Table XIX. Calculated Adiabatic Flame Temperatures and Composition of the Combustion Gas of Hydrogen-Oxygen and 68.2 Percent Carbon Dioxide Flames, at 300 K and 1 atm pressure.

Gas Composition %			Stoich. or M.E.R. Fraction	Flame Temp. (K)	Composition of Product (Burned) Gases							
H_2	O_2	CO_2			H_2	H	O_2	O	OH	H_2O	CO	CO_2
16.0	15.8	68.2	0.51	------	-------	--------	-------	-------	-------	-------	-------	-------
17.0	14.8	68.2	0.57	1248.0	2.745-8	8.129-11	6.900-2	1.859-8	6.493-6	1.858-1	2.612-6	7.454-1
18.0	13.8	68.2	0.65	1300.0	8.233-8	3.210-10	5.260-2	4.127-8	1.131-5	1.978-1	4.912-6	7.494-1
19.0	12.8	68.2	0.74	1350.0	2.481-7	1.217-9	3.660-2	8.145-8	1.891-5	2.099-1	1.667-5	7.536-1
20.0	11.8	68.2	0.85	1406.0	8.991-7	5.395-9	1.980-2	1.562-7	3.052-5	2.222-1	3.868-5	7.578-1
21.0	10.8	68.2	0.97	1450.0	4.188-6	1.945-8	3.400-3	1.176-7	2.941-5	2.346-1	2.160-4	7.617-1

READ 2.745-8 as 2.745×10^{-8} and so on.

Table XX. Calculated Adiabatic Flame Temperatures and Composition of the Combustion Gas of Hydrogen-Oxygen and 55.6 Percent Carbon Dioxide Flames, at 300 K and 1 atm pressure.

Gas Composition %			Stoich. or M.E.R. Fraction	Flame Temp. (K)	Composition of Product (Burned) Gas							
H_2	O_2	CO_2			H_2	H	O_2	O	OH	H_2O	CO	CO_2
19.4	25.0	55.6	0.39	1530.0	1.466-6	3.042-8	1.486-1	2.331-6	1.356-4	1.885-1	5.368-5	6.627-1
22.4	22.0	55.6	0.51	1650.0	8.358-6	2.650-7	1.066-1	8.470-6	3.424-4	2.207-1	2.324-4	6.722-1
24.4	20.0	55.6	0.61	1730.0	2.514-5	9.828-7	7.780-2	1.707-5	5.700-4	2.426-1	6.542-4	6.783-1
26.4	18.0	55.6	0.73	1800.0	6.778-5	2.964-6	4.900-2	2.703-5	8.286-4	2.648-1	1.757-3	6.836-1
27.4	17.0	55.6	0.80	1836.0	1.208-4	5.485-6	3.420-2	3.265-5	9.751-4	2.760-1	2.683-3	6.858-1
29.4	15.0	55.6	0.98	1910.0	5.583-4	2.010-5	5.750-3	2.442-5	9.366-4	2.982-1	5.801-3	6.884-1
31.4	13.0	55.6	1.21	1750.0	5.553-3	1.734-5	3.500-6	1.389-7	5.914-5	3.096-1	4.894-2	6.357-1

READ 1.466-6 as 1.466×10^{-6} and so on.

a comparison. The results showing the effects of various inert gases (helium, argon, nitrogen, and carbon dioxide) on the quenching distances of hydrogen-oxygen flames with 68.2 percent and 55.6 percent of the inert gas addition to the combustible mixtures are shown in Fig. 18 and 19. In Fig. 18, the measured quenching distances of Friedman[15] for hydrogen-oxygen flames with 68.2 percent helium are included for comparison. From these data, it can be concluded that the quenching distance is dependent on the fuel-oxidizer ratio of a given gas mixture and has its smallest value near the optimum (M.E.R.) fuel-to-oxidizer ratio. This observation is in agreement with those of the previous investigators.

From Fig. 8, 9, and 11 it can be seen that the measured quenching distances in the present investigation agree well with those published by Lewis and von Elbe except for fuel-rich flames of methane and air. According to values reported by Lewis and von Elbe (Fig. 8) it appears that at an equivalent ratio of approximately 1.15 for methane-air the quenching distance becomes infinitely large, which means that a mixture containing approximately 10.93 percent methane and 89.07 percent air should not support a stable flame on a cold burner rim. On the other hand it is known[21] that the flammability limit for methane-air mixtures occurs at 13.34 percent methane. In view of this observation a flame of 12 percent methane and 88 percent air mixture should have a finite quenching distance. This conclusion was confirmed by the measurements of the present investigation (see Fig. 8).

One of the most important observations of the present study is the discovery of the effect of the quenching surface material on the quenching distance. Previous investigators[13-16] reported that the quenching distance is independent of the quenching material and also independent of the quenching surface. The results shown in Fig. 8-11 indicate clearly that there is a surface effect. The quenching distances are much lower for plates of mica and copper covered with glass than with plain copper plates. The quenching distances are increased substantially when copper plates are coated with chlorobromomethane or carbon tetrachloride. This observation indicates that copper plates are much more effective in quenching a flame than plates made of mica or glass and that compounds such as chlorobromomethane and carbon tetrachloride are very effective in flame quenching.

The reason the different quenching plate materials give widely different quenching distances is attributed to the different heat transfer coefficients[31] of these materials. As expected the greater the thermal conductivity of the material the greater the flame quenching distance; i.e., the greater the flame quenching capability of the material. According to these considerations, copper, because of its higher heat transfer coefficient is much more effective in flame quenching than mica, glass, or teflon.

According to data shown in the last two columns of Tables V-VIII the quenching distances of methane-air, methane-oxygen, acetylene-air, and hydrogen-air flames are not affected by coatings of potassium

chloride and sodium bicarbonate salts, although these salts are known to be strong flame inhibitors when admixed to the combustible mixtures in powdered form.[7,8] That the coatings of halogenated compounds produce a significant increase in the quenching distances of these combustible mixtures is attributed to volatility of these compounds. These compounds, being very volatile even at room temperature, diffuse into the flame at the time of coating and thus inhibit the growth of active chain carriers in the flame. On the other hand the salts do not evaporate when coated with the plate surfaces since the melting points of these salts are of the order of 900 K[32] and these temperatures were never reached by the water cooled copper plate surfaces, indicating that no chemical reaction of the salts with the flame can take place. These results indicate that the surface as a catalyst plays actually a minor role in the quenching process.

According to the data presented in Fig. 8-11 chlorobromomethane is more effective than carbon tetrachloride. These results are in agreement with the criteria, for the efficiency of these compounds as flame suppressors, reported by Belles and O'Neal[2] and by Rosser et al.[3] According to Belles and O'Neal,[2] a halogenated extinguishing agent which increases the overall reaction rate of the fuel-air mixture is, in general, more effective. Based on this criterion and using a special technique to calculate the overall rates, they were able to show that chlorobromomethane is a better flame quenching agent than carbon tetrachloride. Rosser et al.[3] measured flame speeds of methane-air mixtures with the addition of various halogenated flame inhibitors. They concluded that those halogenated compounds which produce lower flame speeds of the fuel-air-agent mixtures are the more effective ones. Based on this criterion it was also found that chlorobromomethane is more effective in flame inhibition than carbon tetrachloride.

As expected the quenching distances of hydrogen-oxygen flames are increased when inert gases are added (Fig. 18 and 19) and they increase as the amount of inert gas is increased.

The effect of flame speed on the quenching distance is shown in Fig. 20 and Tables V-VIII. According to these results, mixtures having high flame speeds have small quenching distances, which means that it is more difficult to quench a rapidly burning flame. On the other hand, for hydrogen-oxygen mixtures to which various inert gases have been added (Fig. 18 and 19) this simple relationship does not exist. In this case a flame having a higher speed is not always more difficult to quench. Thus hydrogen-oxygen-helium mixtures which have much higher flame speeds (Fig. 21 and 22) than mixtures containing either argon, nitrogen, or carbon dioxide, have quenching distances (Fig. 18 and 19) which are significantly greater than those of the latter. A similar argument holds for flame temperatures of these mixtures; i.e., a flame burning with higher flame temperature is not always more difficult to quench (Tables XV-XX and Fig. 18 and 19).

Summarizing these observations it cannot be stated flatly that all flames having higher flame speeds and temperatures will necessarily have a lower quenching distance; i.e., they are more difficult to

quench. Therefore it appears that quenching distance is also dependent on the thermal conductivity, heat capacity, diffusion coefficients, etc., of the gas mixture.

To study the effect of thermal conductivity, heat capacity, and diffusion of chain carriers, the coefficients of thermal conductivity, heat capacities, and diffusion coefficients of H, O, and OH were calculated at 293.15 K (taken approximately as the room temperature) and at 1500 K for the various gas mixtures. The temperature of 1500 K was selected arbitrarily to represent approximately the average temperature of the combustion gases during quenching. A rather low value of room temperature (293.15 K) was taken since experimental values of thermal conductivities and heat capacities for some gases were available at this temperature.[32] The procedures employed for calculating the coefficients of thermal conductivity, heat capacities, and diffusion coefficients of the various gas mixtures are given in Appendix B and numerical values of these parameters are given in Tables XXI-XXVI. According to the data for hydrogen-oxygen-inert gas mixtures (Tables XXII-XXVI), those gas mixtures having a higher thermal conductivity, a lower specific heat at constant pressure, and a higher diffusion coefficient have greater quenching distances. Thus mixtures of hydrogen-oxygen to which helium has been added have flames which are easier to quench than those mixtures containing either argon, nitrogen, or carbon dioxide. The comparison is based upon the same amount of inert gas (by volume). Evidently these properties exert a greater influence on the quenching distance than the flame speeds and flame temperatures.

The finding that gas mixtures in which diffusion is very rapid have higher quenching distances is in agreement with the observation that in flames of hydrogen-oxygen-helium dissipation of energy by diffusion to the solid copper plates is enhanced by the low molecular mass of helium.

According to the data of Tables XXII-XXVI on methane-air, methane-oxygen, acetylene-air, and hydrogen-air gas mixtures, the coefficients of thermal conductivity, heat capacities, and diffusion coefficients differ very slightly. Therefore nothing can be said on relationship between quenching distance and thermal conductivity, heat capacity, and diffusion rates of the mixture. It appears that quenching distances are primarily determined by the flame speed and flame temperature of the combustible gas mixture.

The results of the spectroscopic measurements (Fig. 12 and 13, Tables IX and X) show that the relative intensity of some bands in partially quenched flames is very low when compared to the unquenched flames for the same exposure times and some of the bands do not show at all, even when the exposure times have been more than doubled. Figure 12 and Table IX show a comparison of the spectrograms of unquenched and partially quenched flames of 12 percent methane and 88 percent air for different exposure times of the partially quenched flames. Even for an exposure time of six times (30 min) that of the unquenched flame (5 min) the only bands present in the partially

Table XXI. Calculated Thermal Conductivities of Pure Gases

Gas	Temperature (K)	A	ϵ/k (K)	$\Omega(\frac{2}{1},2)^*$	Calculated Thermal Conductivity cal/cm s(K) (10^{-5})
Helium	293.15 1500.0	2.576	10.22	0.7061 0.5619	36.36 103.35
Argon	293.15 1500.0	3.418	124.00	1.1160 0.8072	4.13 12.93
Hydrogen	293.15 1500.0	2.968	33.30	0.8410 0.6611	40.65 127.31
Oxygen	293.15 1500.0	3.433	113.00	1.0820 0.7978	6.04 22.13
Nitrogen	293.15 1500.0	3.681	91.50	1.0220 0.7724	6.05 19.99
Carbon Dioxide	293.15 1500.0	3.996	190.00	1.5750 0.8558	3.40 18.81
Methane	293.15 1500.0	3.882	137.00	1.1510 0.8165	7.25 48.37
Acetylene	293.15 1500.0	4.221	185.00	1.2830 0.8490	5.02 26.92
Air	293.15 1500.0	3.617	97.00	1.0380 0.7831	5.90 19.55

Table XXII. Calculated Thermal Conductivities of Gas Mixtures

Gas Mixture	Temp. (K)	1	2	3	λ_1	λ_2	λ_3	λ_x^{mix}
					cal/cm·s (K) (10^5)			
CH_4+	293	0.10	0.90	----	7.92	6.00	----	6.16
Air	1500				48.37	20.19	----	22.35
CH_4+	293	0.40	0.60	----	7.92	6.20	----	6.81
O_2	1500				48.37	22.13	----	30.91
C_2H_2	293	0.08	0.92	----	5.00	6.00	----	5.91
+ Air	1500				26.92	20.19	----	20.63
H_2+	293	0.30	0.70	----	44.46	6.00	----	13.34
Air	1500				127.31	20.19	----	41.19
H_2+	293	0.294	0.15	0.556	44.46	6.20	36.11	22.42
O_2+He	1500				127.31	22.13	103.35	64.43
H_2+	293	0.294	0.15	0.556	44.46	6.20	4.20	9.19
O_2+Ar	1500				127.31	22.13	12.93	26.94
H_2+	293	0.294	0.15	0.556	44.46	6.20	6.02	9.94
O_2+N_2	1500				127.31	22.13	19.99	29.87
H_2+O_2	293	0.294	0.15	0.556	44.46	6.20	3.47	8.89
+CO_2	1500				127.31	22.13	18.81	29.38

Table XXIII. Calculated Heat Capacities for the Various Gas Mixtures

Gas Mixture	Temp. (K)	1	2	3	c_{p1}	c_{p2} (cal/g(K)	c_{p3}	c_{pmix}
CH_4+	293	0.10	0.90	----	0.5333	0.2400	------	0.2693
Air	1500				1.2860	0.2883	------	0.3881
CH_4+	293	0.40	0.60	----	0.5333	0.2198	------	0.3452
O_2	1500				1.2860	0.2726	------	0.6780
C_2H_2	293	0.08	0.92	----	0.3969	0.2400	------	0.2526
+Air	1500				0.6768	0.2883	------	0.3194
H_2+	293	0.03	0.70	----	3.3949	0.2400	------	1.1865
Air	1500				3.8198	0.2883	------	1.3478
H_2+	293	0.294	0.150	.556	3.3949	0.2198	1.2500	1.7261
O_2+He	1500				3.8198	0.2726	1.2500	1.8589
H_2+	293	0.294	0.150	.556	3.3949	0.2198	0.1250	1.1006
O_2+Ar	1500				3.8198	0.2726	0.1250	1.2334
H_2+	293	0.294	0.150	.556	3.3949	0.2198	0.2518	1.1711
O_2+N_2	1500				3.8198	0.2726	0.3087	1.3355
H_2+	293	0.294	0.150	.556	3.3949	0.2198	0.1978	1.1410
O_2+CO_2	1500				3.8198	0.2726	0.3146	1.3388

Table XXIV. Calculated Diffusion Coefficients of atomic hydrogen in Various Gas Mixtures

Gas Mixture	Temp. (K)	B	C	D	D_{AB}	D_{AC} (cm^2/s)	D_{AD}	D_H(mix)
CH_4+	293	0.10	0.90	----	0.951	1.015	------	1.008
Air	1500				11.005	11.747	------	11.668
CH_4+	293	0.40	0.60	----	0.951	1.085	------	1.027
O_2	1500				11.005	12.560	------	11.888
C_2H_2+	293	0.08	0.93	----	0.838	1.015	------	0.998
Air	1500				9.695	11.747	------	11.551
H_2+	293	0.30	0.70	----	1.672	1.015	------	1.151
Air	1500				19.347	11.747	------	13.316
H_2+	293	0.294	0.15	0.556	1.672	1.085	1.641	1.532
O_2+He	1500				19.347	12.560	18.999	17.729
H_2+	293	0.294	0.15	0.556	1.672	1.085	1.106	1.224
O_2+Ar	1500				19.347	12.560	12.806	14.173
H_2+	293	0.294	0.15	0.556	1.672	1.085	1.106	0.996
O_2+N_2	1500				19.347	12.560	11.533	13.272
H_2+	293	0.294	0.15	0.556	1.672	12.560	0.952	1.113
O_2+CO_2	1500				19.347	12.560	11.024	12.891

Table XXV. Calculated Diffusion Coefficients of Atomic Oxygen in Various Gas Mixtures

Gas Mixture	Temp. (K)	B	C	D	D_{AB}	D_{AC}	D_{AD}	D_O(mix)
					(cm^2/s)			
CH_4+	293	0.10	0.90	----	0.241	0.227	-----	0.228
Air	1500				2.786	2.628	-----	2.643
CH_4+	293	0.40	0.60	----	0.241	0.237	-----	0.239
O_2	1500				2.786	2.737	-----	2.756
C_2H_2+	293	0.08	0.92	----	0.196	0.227	-----	0.224
Air	1500				2.267	2.628	-----	2.595
H_2+	293	0.30	0.70	----	0.713	0.227	-----	0.285
Air	1500				8.248	2.628	-----	3.303
H_2+	293	0.294	0.15	0.556	0.713	0.237	0.564	0.492
O_2+He	1500				8.248	2.737	6.523	5.692
H_2+	293	0.294	0.15	0.556	0.713	0.237	0.233	0.291
O_2+Ar	1500				8.248	2.737	2.696	3.371
H_2+	293	0.294	0.15	0.556	0.713	0.237	0.225	0.284
O_2+N_2	1500				8.248	2.737	2.600	3.286
H_2+	293	0.294	0.15	0.556	0.713	0.237	0.202	0.263
O_2+CO_2	1500				8.248	2.737	2.343	3.051

Table XXVI. Calculated Diffusion Coefficients of OH in Various Gas Mixtures

Gas Mixture	Temp. (K)	B	C	D	D_{AB}	D_{AC}	D_{AD}	D_{OH_2}(mix)
					(cm^2/s)			
CH_4+	293	0.10	0.90	-----	0.221	0.207	-----	0.208
Air	1500				2.553	2.392	-----	2.407
CH_4+	293	0.40	0.60	-----	0.221	0.215	-----	0.217
O_2	1500				2.553	2.484	-----	2.511
C_2H_2+	293	0.08	0.92	-----	0.177	0.207	-----	0.204
Air	1500				2.048	2.392	-----	2.360
H_2+	293	0.30	0.70	-----	0.650	0.207	-----	0.260
Air	1500				7.524	2.392	-----	3.007
H_2+	293	0.294	0.15	0.556	0.650	0.215	0.513	0.448
O_2+He	1500				7.524	2.484	5.941	5.180
H_2+	293	0.294	0.15	0.556	0.650	0.215	0.211	0.264
O_2+ Air	1500				7.524	2.484	2.441	3.056
H_2+	293	0.294	0.15	0.556	0.650	0.215	0.205	0.259
O_2+N_2	1500				7.524	2.484	2.368	2.992
H_2+	293	0.294	0.15	0.556	0.650	0.215	0.184	0.240
O_2+CO_2	1500				7.524	2.484	2.130	2.774

quenched flame are the 3064Å OH, and 4315Å CH, whereas the 2608Å OH, 2811Å OH, 3872Å CH, 4737Å CC, 5165Å CC, 5635Å CC, and 6059Å CC, show very clearly in the unquenched flame but do not show at all in the partially quenched flame. The intensity of the various bands in the partially quenched flame depends very much on the distance between the two copper plates. The absence of some bands in the partially quenched flame most likely is due to a change of the reaction mechanism in the partially quenched flame. The absence, or at least the drastic reduction in the intensity, of these radiating molecules may be caused either by loss of energy due to heat transfer or by diffusion out of the combustion gas to the cold quenching surface. The diffusion of active species to the quenching surface reduces the overall reaction rate and thus lowers the flame temperature, which is in agreement with the temperature measurements made by means of a platinum-platinum rhodium thermocouple. Temperatures of no more than 1600 K were observed for the partially quenched flame. At these temperatures the concentration of atoms and free radicals is very small and, therefore, at this point diffusion becomes less important.

To obtain more information on the state of the reaction zone of the unquenched and partially quenched flame, the relative intensities of the two bands (3870Å CH and 4315Å CH were determined and used for calculating the rotational temperature of the CH radical. The results of these calculations are shown in Fig. 14-17. According to these data the experimentally determined rotational flame temperatures for the unquenched flames of a 40 percent methane - - 60 percent oxygen and a 10 percent acetylene - - 90 percent air mixture are in good agreement with the theoretically calculated flame temperatures (Tables XII and XIII). Hence it may be assumed that thermodynamic and chemical equilibrium prevails in the unquenched flames. The experimentally determined rotational temperatures of partially quenched flames were found to range from 5,000 to 11,000 K. Since these temperatures exceed the theoretical values by a factor of 3 to 6 it must be concluded that the quenching process prevents the CH molecules from reaching thermodynamic equilibrium. This conclusion is further supported by the observation that, for an unquenched flame of the same fuel-oxidizer mixture, the difference between the experimentally determined rotational flame temperatures of 3870Å CH and that of 4315Å CH is small (Fig. 14-17), whereas for the partially quenched flame the difference is too much to reconcile. This further indicates the lack of general thermodynamic equilibrium for the unquenched flame.

V. THEORETICAL ANALYSIS OF QUENCHING PROCESS

Because the complexity of the quenching process precludes any rigorous analysis a number of simplifying assumptions must be made to develop a model of this process which can be treated theoretically.

First, only laminar flames are considered in this analysis as well as in the experimental phase of this investigation. It is assumed that the flow of unburned gas is steady and one-dimensional and that the

unquenched combustion process is adiabatic and that the very small change in pressure (less than 3 mm H_2O) across the combustion wave (usually refered to as flame front) can be disregarded. In the experimental phase only flames burning at a pressure of one atmosphere were employed.

The theoretical analysis is based on the fundamental concepts developed by Williams[33] who states that a combustion wave initiated by some source (e.g., spark) of energy introduced into the combustion gas will propagate and will form a self-supporting wave only when there is sufficient transfer of energy to heat a zone of gas, whose thickness is that of the flame front, to the ignition temperature of the combustible gas mixture.

The theoretical analysis of flame quenching will be based on this ignition criterion and effects of both thermal conduction and diffusion will be considered. Although the reaction mechanism should be included in a complete analysis, the influence of the quenching process on the chemistry of the combustion process will be disregarded because of its complexity. When a flame burning at the tip of a rectangular burner tube whose exit port has length a and width b (see Fig. 23) is surrounded by two plates parallel to the long side of the burner port a, the total amount of heat introduced per unit time into the space between the quenching plates can be expressed by the following equation

$$H_{gen} = c_p abu_F(T_F - T_O) \quad J/s \ , \quad (4)$$

Fig. 23 Burner Port

where

c_p = average specific heat of the gas mixture per unit volume in J/m^3 K,

a = length of burner port in m,

b = width of burner port in m,

u_F = flame speed in m/s,

T_F = adiabatic flame temperature in K, and

T_O = temperature of the initial gas mixture in K.

Width of the burner port, b, is 0.0032 m for methane-air flame and 0.0017 m for the other flames.

To develop an expression for the heat transfer to the quenching wall, $\dot{H}_{wall}$, the simplified model of the quenching process shown in Fig. 24 is used. When the quenching plates are not in contact with the flame the distance, x, between the flame zone and the plate wall is considered to be sufficiently large so that there is no transfer of heat from the flame to the plates. As the distance, x, between the flame reaction zone and the plate surface is decreased heat transfer from the flame to the wall will begin and at a certain distance, d_Q, between the quenching plates, a large amount of heat of the flame contained in the space between the plates is transferred to the plates. When complete

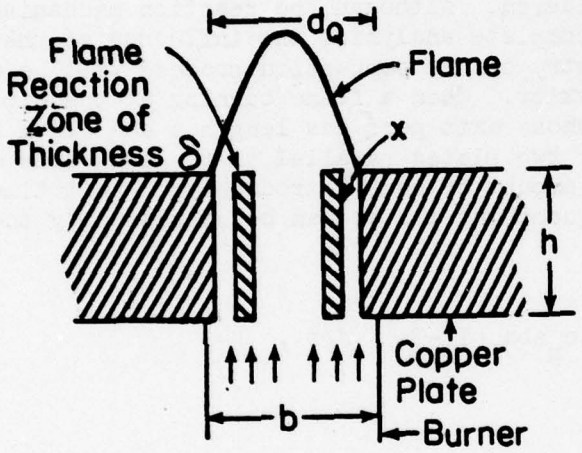

Fig. 24 Rectangular Burner with Quenching Plates (not to scale)

quenching has occurred the flame will burn at the top of the quenching plates, as shown in Fig. 24. Prior to the appearance of the flame on top of the quenching plates (that is, just at the verge of quenching) the amount of heat transferred from the flame to one of the two quenching surfaces can be expressed as follows:

$$\dot{H}_{wall} = \frac{\lambda ah(T_F - T_{wall})}{\alpha(d_Q\sqrt{2}-\delta)} \quad J/s, \tag{5}$$

where

λ = thermal conductivity of the gas mixture in J/s.m.K,

h = height of the quenching plate in m (in the present case it is equal to 0.0254 m),

T_{wall} = wall surface temperature in K, which is taken to be equal to the gas temperature of the unburned gas, T_o,

δ = laminar flame thickness in m,

d_Q = flame quenching distance in m,

α = a dimensionless factor of the order of unity to account for heat conduction process in a gas; the term $(T_F - T_{wall}/\alpha(d_Q/2 - \delta)$ represents the temperature gradient between the centerline and the quenching wall.

If it is assumed that at the time of quenching all of the heat released in the combustion wave is transferred to the quenching plates, we can write

$$\dot{H}_{gen}/2 = \dot{H}_{wall} \text{ for one quenching plate surface.}$$

Using the expressions given in Eq. (4) and (5) and solving for d_Q we arrive at

$$d_Q = \frac{4 \lambda h + 2\delta c_p b u_F}{\alpha c_p b u_F} \text{ m.} \qquad (6)$$

Actually this procedure is rather approximate because the burned gas leaving the burner port formed by the top of the quenching surfaces is still fairly hot and definitely contains a moderately large amount of excess thermal energy. For a given gas speed this amount of energy may be considered to be constant and accounted for by the empirical coefficient α.

Since it is quite difficult to measure the laminar flame thickness, δ, it is eliminated by using one of the following empirical relationships for δ:

(1) According to Williams[33] we have

$$\delta \simeq \lambda / c_p u_F,$$

where all the quantities have been previously defined. This relationship is based on the thermal theory of flame propagation and follows from the conservation of energy and mass. When this relationship is substituted into Eq. (6) we obtain an expression for the quenching distance, d_Q, which is based on the thermal theory of flame propagation.

(2) Another relationship for the thickness of the combustion zone has been proposed by Bechert[34] who stated that

$$\delta \simeq D_{mix}/u_F,$$

where

D_{mix} = average diffusion coefficient of the atomic species H, O, and the radical OH in the combustion gas.

Bechert obtained this expression by considering both diffusion and thermal conductivity as the primary factors in the mechanism of flame propagation. When this relation is used to eliminate the laminar flame thickness from Eq. (6), an expression for the quenching distance is obtained which takes into consideration the effects of thermal conductivity and diffusion. However, it must be pointed out that in the quenching process heat transfer is that from the flame to a cold wall and not from a flame zone to a unburned gas and also diffusion is to a cold wall.

(3) A third, well known, relationship for the flame zone thickness has been formulated by Mallard and Le Chatelier.[35]

$$u_F \simeq \frac{\lambda}{c_p} (T_F - T_{ig}/T_{ig} - T_0) \frac{1}{\delta},$$

where

T_{ig} = ignition temperature of the gas mixture in K.

The derivation of this relation, like relation (1), also takes only thermal conductivity into consideration. When this reaction is used to eliminate δ from Eq. (6), the resulting expression for the quenching distance, d_Q, is expressed in terms of the ignition temperature, T_{ig}, of the gas mixture. This relation was used by Friedman[15] to obtain a theoretical expression for the quenching distance.

Because of the lack of reliable values for the ignition temperature, only relations (1) and (2) will be used for the theoretical calculation of quenching distances. However relation (3) will be used to calculate ignition temperatures by means of measured quenching distances. Thus when relation (1) is substituted in Eq. (6) we obtain

$$d_Q = \frac{2\lambda}{c_p b u_F} \left(\frac{2h + b}{\alpha}\right) \quad m, \tag{7}$$

and when relation (2) is used in Eq. (6) to eliminate δ, the resulting expression for the quenching distance becomes

$$d_Q = \frac{4\lambda h + 2D_{mix} c_p b}{c_p b u_F \alpha} \quad m. \tag{8}$$

Now if relation (3) is also used to eliminate δ from Eq. (6), we get

$$d_Q = \frac{4 \lambda h + 2 \lambda b(T_F - T_{ig}/T_{ig} - T_O)}{c_p b u_F \alpha} ,$$

which, after rearrangement, gives an expression for the ignition temperature, T_{ig}, of the combustible gas mixture.

Thus

$$T_{ig} = \frac{T_O l - T_O m + T_F n}{l - m + n} \quad K, \tag{9}$$

where

$$l = d_Q \alpha c_p b u_F ,$$

$$m = 4 \lambda h , \text{ and}$$

$$n = 2 \lambda b .$$

Since the expressions for the quenching distance contain the empirical factor α, it is necessary to examine its role and magnitude before actual calculations of the quenching distance or ignition temperature can be undertaken.

If the flow of energetic molecules from the combustion gas to the cold wall of the quenching plate is increased either by diffusion (such as in the case of hydrogen-oxygen-helium gas mixture) or by heat transfer (such as in the case of copper quenching plates), for a fixed wall temperature, T_{wall}, the value of α will have to be reduced to account for the resulting increase in the quenching distance [Eq. (7) and (8)]. Thus lower values of α should be selected for hydrogen-oxygen-helium and hydrogen-rich hydrogen-air gas mixtures, and also for the copper quenching plates. Rather higher values of α will have to be selected for the remaining gas mixtures and also for the case when quenching plates are made of mica or glass to account for the resulting decrease in the quenching distance.

Jakob[36] has pointed out, while discussing the theory of thermal conductivity of different gases, that the value of a similar coefficient ϵ lies between 1 and 2.5 for individual gases and no value has been reported for gas mixtures.

For a comparison of the experimentally determined quenching distances with those predicted by the theory developed here, the theoretical quenching distances of the various fuel-oxidizer mixtures were calculated, for three different compositions of each gas mixture, from Eq. (7) and (8). The results are given in Tables XXVII-XXX. As pointed out earlier, Eq. (9) was used to calculate the ignition temperatures of the various gas mixtures with the experimentally determined values of the quenching distances. These results are also shown in Tables XXVII-XXX.

From Tables XXVII and XXVIII it can be concluded that Eq. (8) can be used to predict the order of magnitude of the quenching distance of a flame if a reliable method can be established to calculate the value of the coefficient α. Although α has been selected somewhat arbitrarily, it can be seen that it is rather constant, at least for a given combustible mixture. From Table XXVII we see that only one value of α is needed to predict the quenching distances of all the gas mixtures and in Table XXVIII also only one value of α is necessary to yield the order of magnitude of the quenching distance for all the hydrogen-oxygen-inert gas mixtures (except for hydrogen-oxygen-helium where a lower value of α has been used to account for the increase in diffusion rates). We also see from Table XXVII that a higher value of α is to be selected if mica plates are used for measuring the quenching distance to account for the decreased heat transfer from the hot gas to the cold wall. It can also be seen from Tables XXVII and XXVIII that the same value of α, as used in Eq. (8), can be used to yield the right order of magnitude of the measured ignition temperatures of the various gas mixtures. The fact that a higher value of the coefficient α is desired for copper plates than for mica plates, shows that thermal conductivity contributes more than indicated by the temperature gradient. The same reasoning applies for diffusion.

Equation (8), which represents the experimentally observed quenching distance values of the various fuel-oxidizer mixtures fairly well and also the right order of magnitude of their ignition temperatures, takes both thermal conductivity and diffusion into consideration. When Eq. (7) is used, with the same value of α, agreement between theory and experiment is not satisfactory (see Tables XXVII and XXVIII). This result is not surprising since Eq. (7) does not include the effect of diffusion on the quenching mechanism. However by a suitable selection of α values, this equation can also yield the correct value of the quenching distance and even the right order of magnitude of the ignition temperatures. Results obtained with such values of α are tabulated in Tables XXIX and XXX. A careful inspection of these tables reveals, however, that Eq. (7) is not consistent. An increase of the diffusion rate in a gas mixture does not necessarily entail a reduction of α (e.g., for hydrogen-oxygen-helium gas mixtures); the value of α is 2 whereas for hydrogen-oxygen-argon gas mixtures it is 1.5, which signifies an increase of the quenching distance of hydrogen-oxygen-argon mixtures. According to experimental observations the opposite is true. When a constant value of α is chosen to represent the measured quenching distances, the right order of magnitude of the measured quenching distances are obtained. However,

Table XXVII. Comparison of Measured Quenching Distances of Various Fuel-Oxidizer Mixtures with Those Predicted by Thermal-Diffusion Model

Gas Mixture	Quench. Plate Material	Value of α Taken	Quench. Dist.* (mm)	Quench. Dist.** (mm)	Ignit. Temp.*** (K)	Measd. Ignit. Temp. (K)	Measd. Quench. Dist. (mm)
8% CH_4	Copper	4.0	1.26	3.78	416.3	969 (35)	2.22
in Air	Mica						2.16
9% CH_4	Copper	4.0	0.87	2.63	369.0	978 (35)	2.15
in Air	Mica						2.12
11% CH_4	Copper	4.0	0.98	3.01	376.4		2.25
in Air	Mica						2.20
25% CH_4	Copper	4.0	0.20	0.45	351.6		0.50
in O_2	Mica	6.0	0.13	0.30	347.8		0.35
40% CH_4	Copper	4.0	0.19	0.43	336.6		0.61
in O_2	Mica	6.0	0.12	0.29	330.0		0.47
50% CH_4	Copper	4.0	0.51	1.16	326.6		1.85
in O_2	Mica	6.0	0.34	0.78	324.8		1.30
6% C_2H_2	Copper	4.0	0.49	0.98	393.4		0.78
in Air	Mica	6.0	0.33	0.65	393.4		0.52
8% C_2H_2	Copper	4.0	0.43	0.84	456.6	578 (35)	0.58
in Air	Mica	6.0	0.29	0.56	432.4		0.41
10% C_2H_2	Copper	4.0	0.40	0.84	368.6		0.83
in Air	Mica	6.0	0.27	0.56	361.0		0.59
30% H_2	Copper	4.0	0.24	0.68	344.6	844 (35)	0.58
in Air	Mica	6.0	0.16	0.46	347.9		0.37
40% H_2	Copper	4.0	0.19	0.54	333.7		0.87
in Air	Mica	6.0	0.13	0.36	331.1		0.62
50% H_2	Copper	4.0	0.26	0.68	308.6		1.75
in Air	Mica	6.0	0.17	0.46	308.5		1.16

* From Eq. (7)
** From Eq. (8)
*** From Eq. (9)

Table XXVIII. Comparison of Measured Quenching Distances of Hydrogen-Oxygen-Inert Gas Mixtures with Those Predicted by Thermal-Diffusion Model

Gas Mixture	Quench. Plate Material	Value of α Taken	Quench. Dist.* (mm)	Quench. Dist** (mm)	Ignit. Temp.*** (K)	Measd. Ignit. Temp. (K)	Measd. Quench. Dist. (mm)
55.6% He 24.4% H_2 +20% O_2+	Copper	4.0	0.42	0.83	359.9		0.88
55.6% He 29.4% H_2 +15% O_2+	Copper	4.0	0.40	0.75	373.9		0.80
55.6% He 31.4% H_2 +13% O_2+	Copper	4.0	0.44	0.80	346.6		1.11
55.6% He 24.4% H_2 +20% O_2+	Copper	6.0	0.12	0.59	319.1		0.55
55.6% Ar 29.4% H_2 +20% O_2+	Copper	6.0	0.10	0.48	320.1	746 (36)	0.49
55.6% Ar 31.4% H_2 +13% O_2+	Copper	6.0	0.11	0.49	311.4		0.78
55.6% Ar 24.4% H_2 +20% O_2+	Copper	6.0	0.16	0.62	318.9		0.67
55.6% N_2 29.4% H_2 +15% O_2+	Copper	6.0	0.13	0.47	313.6	740 (36)	0.76
55.6% N_2 31.4% H_2 +13% O_2+	Copper	6.0	0.13	0.46			0.89
55.6% N_2 24.4% H_2 +20% O_2+	Copper	6.0	0.26	1.25	318.4		0.90
55.6% CO_2 29.4% H_2 +15% O_2+	Copper	6.0	0.17	0.80	313.9	783 (36)	0.81
55.6% CO_2 31.4% H_2 +13% O_2+	Copper	6.0	0.18	0.83	310.9		0.95

* From Eq. (7)

** From Eq. (8)

*** From Eq. (9)

Table XXIX. Comparison of Measured Quenching Distances of Various Fuel-Oxidizer Mixtures with Those Predicted by Thermal Model

Gas Mixture	Quench. Plate Material	Value of α Taken	Quench. Dist.* (mm)	Quench. Dist.** (mm)	Ignit. Temp.*** (K)	Measd. Ignit. Temp. (K)	Measd. Quench. Dist. (mm)
8% CH_4	Copper	2.0	2.56	7.56	415	969 (35)	2.22
in Air	Mica						2.16
9% CH_4	Copper	2.0	1.74	5.26	610.8	978 (35)	2.15
in Air	Mica						2.12
11% CH_4	Copper	2.0	1.96	6.02	701.7		2.25
in Air	Mica						2.20
25% CH_4	Copper	2.0	0.40	0.90	537.0		0.50
in O_2	Mica	3.0	0.27	0.60	500.9		0.35
40% CH_4	Copper	2.0	0.38	0.86	429.2		0.61
in O_2	Mica	3.0	0.25	0.58	395.2		0.47
50% CH_4	Copper	2.0	1.02	2.32	381.1		1.85
in O_2	Mica	3.0	0.68	1.56	373.1		1.30
6% C_2H_2	Copper	2.0	0.98	1.96	Neg.		0.78
in Air	Mica	3.0	0.66	1.30	Ignit. Temp.		0.52
8% C_2H_2	Copper	2.0	0.86	1.68	Neg.	578 (35)	0.58
in Air	Mica	3.0	0.58	1.12	Ignit. Temp.		0.41
10% C_2H_2	Copper	2.0	0.80	1.68	1498.6		0.83
in Air	Mica	3.0	0.54	1.12	873.2		0.59
30% H_2	Copper	2.0	0.48	1.38	532.3	844	0.58
in Air	Mica	3.0	0.32	0.92	583.8	(35)	0.37
40% H_2	Copper	2.0	0.38	1.08	345.7		0.87
in Air	Mica	3.0	0.26	0.72	340.9		0.62
50% H_2	Copper	2.0	0.52	1.36	319.9		1.75
in Air	Mica	3.0	0.34	0.92	320.1		1.16

* From Eq. (7)

** From Eq. (8)

*** From Eq. (9)

Table XXX. Comparison of Measured Quenching Distances of Hydrogen-Oxygen-Inert Gas Mixtures with Those Predicted by Thermal Model

Gas Mixture	Quench. Plate Material	Value of α Taken	Quench. Dist.* (mm)	Quench. Dist.** (mm)	Ignit. Temp.*** (K)	Measd. Ignit. Temp. (K)	Measd. Quench. Dist. (mm)
55.6% He 24.4% H_2 +20% O_2+	Copper	2.0	0.84	1.66	909.6		0.88
55.6% He 29.4% H_2 +15% O_2+	Copper	2.0	0.80	1.50	1546.7		0.80
55.6% He 31.4% H_2 +13% O_2+	Copper	2.0	0.88	1.60	527.2		1.11
55.6% He 24.4% H_2 +20% O_2+	Copper	1.5	0.48	2.36	629.6		0.55
55.6% Ar 29.4% H_2 +15% O_2+	Copper	1.5	0.40	1.92	587.3	746 (36)	0.49
55.6% Ar 31.4% H_2 +13% O_2+	Copper	1.5	0.44	1.96	380.6		0.78
55.6% Ar 24.4% H_2 +20% O_2+	Copper	1.5	0.64	2.48	1071.9		0.67
55.6% N_2 29.4% H_2 +15% O_2+	Copper	1.5	0.52	1.88	424.7	740 (36)	0.76
55.6% N_2 31.4% H_2 +13% O_2+	Copper	1.5	0.52	1.84	-----		0.89
55.6% N_2 24.4% H_2 +20% O_2+	Copper	1.5	1.04	5.00	Neg. Ignit. Temp.		0.90
55.6% CO_2 29.4% H_2 +15% O_2+	Copper	1.5	0.68	3.20	520.8	783 (36)	0.81
55.6% CO_2 31.4% H_2 +13% O_2+	Copper	1.5	0.72	3.32	426.8		0.95

* From Eq. (7)

** From Eq. (8)

**** From Eq. (9)

for certain gas mixtures not even the order of magnitude of the ignition temperatures is obtained. According to Tables XXIX and XXX, some ignition temperatures are even negative; e.g., those of acetylene-air and hydrogen-oxygen-carbon dioxide mixtures. Actually the ignition temperature of a gas mixture does not vary appreciably with composition[37]; however the theoretical values fluctuate as much as 1000 K.

To rule out the possibility that the measured quenching distances are in error, the quenching distances for various fuel-oxidizer mixtures measured with cooled copper plates were used to calculate the minimum ignition energy for these mixtures by means of an equation developed by Williams[33];

$$H_{min} = d_Q^2 \lambda (T_F - T_O)/u_F \quad \text{cal}, \tag{10}$$

where

H_{min} = minimum ignition energy in cal,

λ = thermal conductivity of the gas mixture at room temperature in cal/s cm K,

T_F = flame temperature in K,

T_O = temperature of unburned gas in K,

u_F = measured flame speed in cm/s, and

d_Q = quenching distance as measured with cooled copper plates in cm.

The results of these calculations are given in Table XXXI. The measured minimum ignition energies have been taken from Lewis and von Elbe.[21]

A comparison of the calculated minimum ignition energies derived from Eq. (10) with quenching distances measured in this investigation for the various fuel-oxidizer mixtures and those measured directly by Lewis and von Elbe is shown in Table XXXI. According to this table, measured minimum ignition energies agree fairly well with calculated values. In view of the fact that Eq. (10) does not include diffusion effects, this agreement must be considered as satisfactory. Hence it is concluded that the experimental quenching distances reported in this investigation are quite accurate and that the theoretical expression for the quenching distance, including the effects of thermal conductivity and diffusion [Eq. (8)], predicts at least the order of magnitude of the actual quenching distances of any combustible gas mixture.

Table XXXI. Comparison of Calculated and Measured Minimum Ignition Energies of Various Fuel-Oxidizer Mixtures

Gas Mixture	Quenching Distance (mm)	Calculated Minimum Ignition Energy (cal)	Measured Minimum Ignition Energy[21] (cal)
10% Methane in Air	2.15	1.161×10^{-4}	0.72×10^{-4}
40% Methane in Oxygen	0.61	2.042×10^{-6}	4.30×10^{-6}
8% Acetylene in Air	0.58	2.361×10^{-6}	----------
30% Hydrogen in Air	0.58	4.362×10^{-6}	4.50×10^{-6}
29.4% Hydrogen + 15% Oxygen + 55.6% Helium	0.80	8.843×10^{-6}	10.52×10^{-6}
29.4% Hydrogen + 15% Oxygen + 55.6% Argon	0.49	2.969×10^{-6}	2.15×10^{-6}
29.4% Hydrogen + 15% Oxygen + 55.6% Nitrogen	0.76	6.096×10^{-6}	4.35×10^{-6}
29.4 % Hydrogen + 15% Oxygen + 55.6% Carbon Dioxide	0.81	9.582×10^{-6}	9.20×10^{-6}

Although in a rigorous derivation of expressions for the rate of flame propagation and quenching distances not only diffusion and heat transfer but also the chemical reaction rates and the mechanism should be included, it appears that under many conditions one of these three processes is predominant so that an equation based on this process alone will produce results which agree with experimentally obtained data. Thus Simon et al.[18] and Berlad[19] derived equations which were based on radical diffusion alone and were successful in predicting the correct quenching distances of fuel-oxidizer mixtures burning at subatmospheric pressures. Strauss et al.[38] have measured the burning velocities of many fuel-oxidizer mixtures at very high pressures. They observed that flame speeds of fuel-oxygen mixtures increased significantly with increases in pressure, whereas those of fuel-air mixtures decreased slightly when pressure was increased. They concluded that heat transfer is primarily responsible for the increase and diffusion becomes predominant when pressure neither affects the degree of dissociation nor the temperature gradient in the flame zone.

Thermal conductivity and diffusion coefficients depend on temperature and gas composition in a very complicated manner (Appendix B and Ref. 39). For this reason it is very difficult to write down explicit algebraic equations for principal equations of change for flame propagation.

Although this study has shed some light on the mechanism of flame attenuation and quenching much work still remains to be done to develop criteria which can be used successfully for the design of flame quenching devices. Specifically, more detailed and quantitative spectroscopic studies are needed to elucidate the effect of quenching on the reaction mechanism. Also, the analysis of the flame gas by means of mass spectrometry should be included in an effort to determine the chemical reaction rates and the role of diffusion.

V. CONCLUSIONS

From the present experimental as well as theoretical work on flame quenching the following conclusions can be drawn:

1. Flame quenching distances of laminar flames of various fuel-oxidizer mixtures were found to be independent of the speed and Reynolds number of the unburned gas and also unaffected by the geometry of the burner.

2. Flame quenching distances depend on thermal conductivity, diffusion coefficient, heat capacity, flame temperature, gas composition, and flame speed of the combustible gas mixture.

3. Flame quenching distances also depend on the nature of material of the quenching surface.

4. Spectroscopic studies of flame quenching have shown that some of the radicals present in the unquenched flame may not exist at all or at least appear only at extremely low concentrations in the partially quenched flames. This observation is an indication that the reaction mechanism of the unquenched flame is modified by the destruction of certain radicals by the quenching process.

5. Measurements of rotational flame temperatures of both unquenched and partially quenched flames have shown that flame quenching leads to nonequilibrium conditions in the flame zone.

6. A theoretical expression for the quenching distance based on a simplified mathematical model of the flame has been developed. Both thermal conduction and mass diffusion have been taken into consideration. The quenching distances predicted by this theory are in satisfactory agreement with the experimentally determined values.

TRANSITION FROM DEFLAGRATION TO DETONATION AT VERY LOW TEMPERATURES

Although it has been established very clearly that flames propagating into explosive gas mixtures, which are cooled to cryogenic temperatures, form detonation waves after extremely short distances of travel, the reason for this phenomenon is not well understood. Since the normal flame speed is greatly reduced as the temperature of the unburned gas is lowered, the drastic reduction in the measured induction distance must be caused by gas dynamic effects. Since the speed of sound in the cold gas mixtures is lower than at room temperature, the initial compression wavelets may coalesce to form a shock wave preceding the combustion zone at a closer distance from the flame front. However, the speed of sound is proportional only to the square root of the gas temperature, whereas the normal rate of flame propagation was found to be directly proportional to the temperature of the unburned gas. Since all experiments in the low temperature range were carried out at atmospheric pressure, the initial density of the unburned gas increased with decreasing temperature. Therefore, it was assumed that this increase in the gas density is responsible for the decrease in detonation induction distance. However, a few experiments carried out with fuel-air mixtures in which the nitrogen was replaced by both high molecular mass (e.g., argon) and low molecular mass (helium) gases produced results which appear to be at variance with the theory that initial density has a direct effect on the detonation-induction distance. Since any combustion process, started in a pre-mixed explosive gas mixture, in principle can occur at constant pressure (Bunsen flame with $\Delta p \sim 2$ to 4 cm H_2O), or at constant volume (weak detonation), it may be expected that a flame propagating from the point of ignition into a large volume of combustible gas initially must start out at conditions between these two extreme cases. According to our observations, the pressure behind the flame front rises very rapidly to the value of the stable detonation wave when the initial gas temperature of the combustible gas mixture is low, whereas it remains unchanged for a long distance when the initial gas temperature is raised to room temperature or above. We concluded from this fact that the induction distance is indeed a simple function of the initial gas density. To obtain a quantitative relationship between the conditions of the initial gas and the induction distances a series of experiments has been started with various fuel-oxygen-inert gas mixtures at various initial temperatures and pressures.

THE EFFECT OF TURBULENCE ON THE RATE FORMATION OF DETONATION WAVES

Previous experiments carried out in closed tubes equipped with a fan near the ignitor to create an initial turbulence in the gas prior to ignition did not reveal any effect of this turbulence on the induction distance. It was concluded that the turbulent motion of the unburned gas ceased before the flame propagated into the gas. Therefore, a new detonation tube has been constructed for the study of the effect of initial turbulence in the unburned gas mixture on the induction distance. This tube has an open end so that the gas can be passed through the tube at various speeds prior to ignition. A special device will be used to generate different turbulence levels in the flow and the gas will be ignited at various distances from the closed end of the tube where the combustible mixture is introduced.

AD-A062 291 OHIO STATE UNIV COLUMBUS DEPT OF AERONAUTICAL AND AS--ETC F/G 7/4
IGNITION, COMBUSTION, DETONATION, AND QUENCHING OF REACTIVE MIX--ETC(U)
JUN 78 R EDSE, O P DHIMAN AFOSR-73-2511

UNCLASSIFIED AFOSR-TR-78-1483 NL

2 OF 2
ADA
062291

END
DATE FILMED
3-79
DDC

REFERENCES

1. Burdon, M.C., Burgoyne, J.A., and Weinberg, J.F.; Effect of Methyl Bromide on Combustion of Some Fuel-Air Mixtures: Fifth Symposium (International) on Combustion, 647, The Combustion Institute, Pittsburgh (1955)

2. Belles, F.E., and O'Neal, C. Jr.; Effect of Halogenated Extinguishing Agents on Flame Quenching and Chemical Interpretation of their Action: Sixth Symposium (International) on Combustion, 806, Reinhold, London (1957)

3. Rosser, W.A., Wise, H., and Miller, J.; Mechanism of Combustion Inhibition by Compounds Containing Halogen: Seventh Symposium (International) on Combustion, 175, Butterworths, London (1959)

4. Wilson, W.E. Jr., O'Donovan, J.T., and Fristrom, R.M.; Flame Inhibition by Halogen Compounds: Twelfth Sumposium (International) on Combustion, 929, The Combustion Institute, Pittsburgh (1969)

5. Larsen, E.R.; Halogenated Fire Extinguishants: Flame Suppression by a Physical Mechanism?: American Chemical Society Symposium Series, V. 1975, No. 16 (1975)

6. Dolan, J.E.; The Suppression of Methane/Air Ignitions by Powders: Sixth Symposium (International) on Combustion, 787, Reinhold, London (1957)

7. Laffitte, P., and Bouchet, R.; Suppression of Explosion Waves in Gaseous Mixtures by means of Fine Powders: Seventh Symposium (International) on Combustion, 504, Butterworths, London (1959)

8. Iya, S.K., Wollowitz, S., and Kasken, W.E.; The Mechanism of Flame Inhibition by Sodium Salts: Fifteen Symposium (International) on Combustion, 329, The Combustion Institute, Pittsburgh (1975)

9. McHale, E.T.; Flame Inhibition by Potassium Compounds: Combustion and Flame 1, V. 24, No. 2, 277 (1975)

10. Egerton, A.C., Everett, A.J., and Moore, N.P.W.; Sintered Metals as Flame Traps: Fourth Symposium (International) on Combustion, 689, The Williams and Wilkins Co., Baltimore (1953)

11. Palmer, K.N.; The Quenching of Flames by Wire Gauzes: Seventh Symposium (International) on Combustion, 497, Butterworths, London (1959)

12. Dixon, T.; Gross Voided Flame Arrestors for Fuel Tank Explosion Protection: Technical Report AFAPL-TR-73-124, Wright Patterson Air Force Base, Ohio (1974)

13. Blanc, M.V., Guest, P.G., von Elbe, G., and Lewis, B.; Ignition of Explosive Gas Mixtures by Electric Sparks: The Journal of Chemical Physics, V. 15, No 11, 798, (1947)

14. Blanc, M.V., Guest, P.G., von Elbe, G., and Lewis, B.; Minimum Ignition Energies and Quenching Distances of Mixtures of Hydrocarbons and Ether with Oxygen and Inert Gases: Third Symposium on Combustion, Flame, and Explosion Phenomena, 40, Williams and Wilkins, Baltimore (1949)

15. Friedman, R.; The Quenching of Laminar Oxyhydrogen Flames by Solid Surfaces: Third Symposium on Combustion, Flame and Explosion Phenomena, 110, Williams and Wilkins, Baltimore (1949)

16. Friedman, R., and Johnston, W.C.; The Wall Quenching of Laminar Propane Flames as a Function of Pressure, Temperature, and Air-Fuel Ratio: J. Appl. Phys. 21, 791 (1950)

17. Nair, M.R.S., and Gupta, M.C.; Measurement of Flame Quenching Distances in Constant Volume Combustion Vessels: Combustion and Flame, 21, 321 (1973)

18. Simon, D.M., Belles, E.F., ans Spakowski, A.E.; Investigation and Interpretation of the Flammability Region for Some Lean Hydrogen-Air Mixtures: Fourth Symposium (International) on Combustion, 126, Williams and Wilkins Co., Baltimore (1953)

19. Berlad, A.L.; Flame Quenching by a Variable-Width Rectangular-Channel Burner as a Function of Pressure for Various Propane-Oxygen-Nitrogen Mixtures: J. Phys. Chem., 58, 1023 (1954)

20. Berlad, A.L., and Potter, A.E.; Prediction of the Quenching Effect of Various Surface Geometries: Fifth Symposium (International) on Combustion, 728, Reinhold Publishing Corporation, New York (1955)

21. Lewis, B., and von Elbe, G.; Combustion, Flames, and Explosions of Gases, second edition, Academic Press Inc., New York (1961)

22. Gaydon, A.G.; The Spectroscopy of Flames, second edition, Chapman and Hall Ltd., London (1974)

23. Gaydon, A.G., and Wolfhard, H.G.; Flames, Their Structure, Radiation and Temperature, Chapman and Hall Ltd., London (1970)

24. Strauss, W.A. and Edse, R.; Vacuum Type Gas Flow Calibrator: Review of Scientific Instruments, V. 30, No. 4, 258 (1959)

25. Pearse, R.W.B., and Gaydon, A.G.; The Identification of Molecular Spectra: second edition, Chapman and Hall Ltd., London (1950)

26. Dieke, G.H., and Crosswhite, H.M.; The Ultraviolet Bands of OH, Fundamental Data: Journal of Quantitative Spectroscopy and Radiative Transfer, 2, 97 (1962)

27. Dieke, G.H.; Physical Measurements in Gas Dynamics and Combustion: Princeton Series on High Speed Aerodynamics and Jet Propulsion, V. 9, 514 (1954)

28. Broida, H.P.; Rotational and Vibrational Temperatures of CH in Flames at Atmospheric Pressure: The Journal of Chemical Physics, V. 21, No. 2, 340 (1953)

29. Edse, R.; Aerothermochemistry: to be published

30. JANNAF Thermochemical Tables: NSRDS-NBS-37, U.S. Department of Commerce Publication, second edition, (1971)

31. Kuzman, Raznjevic; Handbook of Thermochemical Tables and Charts, McGraw Hill Book Co., New York (1976)

32. Perry, J.H., Perry, R.H., Chilton, C.H., and Kirkpatrick, S.D.; Chemical Engineers Handbook: McGraw Hill Book Co., New York (1963)

33. Williams, F.A.; Combustion Theory: Addison-Wesley Publishing Company, Inc., Reading, Massachusetts, 187, (1965)

34. Bechert, K.; Ann. Phys., Leipzig, 4, 191 (1949) and 5, 349 and 7, 113 (1950)

35. Mallard and Le Chatelier; Ann. Mines, (8), 4, 274 (1883)

36. Jakob, M.; Heat Transfer: Vol. 1, John Wiley and Sons, Inc., New York, 71 (1949)

37. Jost, W.; Explosion and Combustion Processes in Gases: McGraw Hill Book Company, Inc., New York, 32 (1946)

38. Strauss, W.A., Pliickebaum, J.W., and Edse, R.; Combustion Phenomena as a Function of Pressure: ARL 61, Aeronautical Research Laboratory, Office of Aerospace Research, United States Air Force, Wright Patterson Air Force Base, Ohio (1961)

39. Hirschfelder, J.O., Curtiss, C.F., and Bird, R.B.; Molecular Theory of Gases and Liquids: John Wiley & Sons, Inc., New York, 514 (1954)

40. Penner, S.S.; Chemistry Problems in Jet Propulsion: Pregamon Press, New York, 242, (1957)

APPENDIX A

GAS ANALYSIS

The gases used for studying the attenuation and quenching of flames were either commercial or technical grades. Compressed air was supplied by this laboratory. Conventional techniques were applied to dry and purify the air which then was stored in large tanks. The analysis of the commercial gases was furnished by the supplier as typical analyses of sample lots. The composition of the various gases and the manufacturer's name are listed below:

Methane:	Technical Grade	Matheson Company
	methane	93.63%
	nitrogen	3.1%
	propane	2.5%
	carbon dioxide	0.6%

The remaining impurities consist of butane, pentane, hexane, heptane, and sulphur

Hydrogen:	Regular Grade	Air Reduction Corporation
	hydrogen	99.3% - 99.6%
	oxygen	0.5%

moisture comprises remaining impurity.

Oxygen:	Commercial Grade	Burdette Company
	oxygen	99.5% (minimum)
	moisture	8 grains per $ft.^3$
Helium:	Grade A	Matheson Company
	argon	99.995%

containing traces of hydrogen, methane, oxygen, moisture, neon, nitrogen, argon, and carbon dioxide.

Argon:	Grade A	Matheson Company
	argon	99.995%

containing traces of oxygen, hydrogen, nitrogen, and carbon dioxide.

Nitrogen:	Commercial Grade	Matheson Company
	nitrogen	99.948%

containing traces of oxygen, moisture, carbon dioxide, and argon.

Carbon Dioxide:	Commercial Grade	Matheson Company

containing traces of nitrogen, moisture, and oxygen.

APPENDIX B

CALCULATION OF THERMAL CONDUCTIVITY OF PURE GASES AND GAS MIXTURES USED FOR FLAME QUENCHING EXPERIMENTS

PURE MONO AND POLYATOMIC GASES

For thermal conductivity values at room temperature for monoatomic and polyatomic gases, the experimental values given in Ref. (31) were taken and for calculations at 1500 K the procedure given by Penner[40] was used. When experimental values of the coefficients of thermal conductivity were available, they were used. For a pure monoatomic gas, i, the coefficient of thermal conductivity, λ_i, to a first approximation is given by the following equation reported by Penner[40]:

$$\lambda_i = 1.99 \times 10^{-4} \frac{\sqrt{T_i/\mathcal{M}_i}}{\sigma_i^2 \ \Omega_i^{(2,2)*}} \quad \text{cal/cm s K,} \tag{11}$$

where

T_i = temperature of gas i in degrees K,

$\mathcal{M}$ = molecular mass of gas i in g/mole,

σ_i = collision diameter for the gas i in Å, and

$\Omega_i^{(2,2)*}$ = collision integral which depends on the parameter, $T^* = kT_i/\epsilon$,

where

k = Boltzmann's constant

and

ϵ = energy of a molecule.

For a pure polyatomic gas the coefficient of thermal conductivity is given by the following approximate relation as suggested by Penner[40]:

$$\lambda_i = 1.99 \times 10^{-4} \frac{\sqrt{T_i/m_i}}{\sigma_i^2 \, \Omega_i^{(2,2)*}} \left(\frac{4}{15} \frac{Cvi}{\mathcal{R}} + \frac{3}{5} \right) \quad \text{in cal/cm s K,} \tag{12}$$

where

c_{v_i} = molar heat capacity at constant volume for species i.

The factor $\left(\frac{4}{15} \frac{Cvi}{\mathcal{R}} + \frac{3}{5} \right)$ is known as Eucken approximation which takes into account the transfer of energy between the translational and internal energy modes. The values of σ_i, $\Omega_i^{(2,2)*}$, and ϵ/k are tabulated by Hirschfelder *et al.*[39] for all gases used in this investigation.

The results of these calculations are tabulated in Table XXI at 293.15 K and 1500 K. Temperature of 1500 K was considered to be representative of all flames studied.

COEFFICIENTS OF THERMAL CONDUCTIVITY OF VARIOUS GAS MIXTURES

Methods for calculating the coefficients of thermal conductivity of mixtures of monatomic and polyatomic molecules are available.[39] These calculations are laborious and usually not very reliable because of the uncertain energy transfer between translational and internal degrees of freedom.[40] For this reason the coefficients of thermal conductivity of gas mixtures will be estimated by use of empirical relations.[40]

For two-component mixtures, with large difference in thermal conductivity between the two components, the following formula, given by Penner,[40] yields useful approximations:

$$\lambda_{mix} = \tfrac{1}{2} \left[(\lambda_1 \eta_1 + \lambda_2 \eta_2) + \frac{\lambda_1 \lambda_2}{\left(\eta_1 \sqrt{\lambda_2} + \eta_2 \sqrt{\lambda_1} \right)^2} \right] \quad ; \tag{13}$$

and for binary mixtures, with similar thermal conductivities for two chemical species, the formula is[40]

$$\frac{1}{\sqrt{\lambda_{mix}}} = \frac{\eta_1}{\sqrt{\lambda_1}} + \frac{\eta_2}{\sqrt{\lambda_2}} \quad , \tag{14}$$

where

λ_{mix} = coefficient of thermal conductivity of mixture of gases in cal/cm s K,

λ_1 = coefficient of thermal conductivity of the lighter constituent in cal/cm s K,

λ_2 = coefficient of thermal conductivity of the heavier constituent in cal/cm s K, and

η_1, η_2 = mole fractions of species 1 and 2, respectively.

The results of these calculations are given in Table XXII. For ternary gas mixtures the thermal conductivities were calculated by the method given by Friedman.[15] Only one composition of each fuel-oxidizer system has been tabulated.

HEAT CAPACITIES OF VARIOUS GAS MIXTURES

The heat capacities, $c_{p_{mix}}$, of the various gas mixtures were calculated by assuming that they are simple linear combinations of those of the constituents as given by the following formula:

$$c_{p_{mix}} = \eta_1 c_{p_1} + \eta_2 c_{p_2} + \eta_3 c_{p_3} + \text{----}$$

$$= \sum_i \eta_i c_{p_i} \quad , \tag{15}$$

where c_{p_i} denotes the specific heat at constant pressure of the species i at the desired temperature. The calculated values of $c_{p_{mix}}$ for the various gas mixtures are given in Table XXIII.

CALCULATION OF COEFFICIENTS OF DIFFUSION OF HYDROGEN ATOMS, OXYGEN ATOMS, AND HYDROXYL RADICAL IN MIXTURES OF VARIOUS GASES AT ROOM TEMPERATURE AND 1500 K

According to Chemical Engineers' Handbook,[32] the effectiveness of a diffusing species A in a mixture of gases is given by

$$D_{A'} = \frac{1 - \eta_A}{\left(\eta_B/D_{AB}\right) + \left(\eta_c/D_{AC}\right) + \left(\eta_D/D_{AD}\right)} \quad \text{----} \,, \tag{16}$$

where

η_A, η_B, η_C, and η_D are the mole fractions of the species A, B, C, and D, respectively, and

D_{AB}, D_{AC}, D_{AD} are the binary diffusion coefficients of species A with species B, C, and D, respectively.

To calculate binary diffusion coefficients, an approximate method developed by Gilliland[32] may be used. This method gives uncertainty of 20% in the experimentally computed values at the most.

According to Gilliland we have

$$D_{AB} = 0.0043 \frac{T^{3/2}}{p\left(V_A^{1/3} + V_B^{1/3}\right)^2} \sqrt{\frac{1}{m_A} + \frac{1}{m_B}} \quad \text{cm}^2/\text{s} \,, \tag{17}$$

where

T = temperature in K,

p = pressure in atm,

m_A, m_B = molecular masses of species A and B, respectively, in g/mole, and

V_A, V_B = molal volume (atomic volume) of liquid at normal boiling point in cc/g mole (cc/g atom), respectively, of the species A and B.

The results of these calculations are shown in Tables XXIV-XXVI.